



VNIVERSITAT
DE VALÈNCIA

Analysis of new methodologies for the measurement of optometric parameters in natural vision conditions

Memòria presentada per
Vicent Sanchis i Jurado
per optar al grau de
Doctor en Optometria i
Ciències de la Visió.

Universitat de València, 2017
Director Álvaro Pons Moreno

En Álvaro Pons i Moreno, professor titular del Departament d'Òptica, Optometria i Ciències de la Visió de la Universitat de València, certifica que el treball "*Analysis of new methodologies for the measurement of optometric parameters in natural viewing conditions*" ha estat realitzat sota la seva direcció per En Vicent Sanchis i Jurado per optar al grau de Doctor en Optometria i Ciències de la Visió.

A handwritten signature in black ink, appearing to read 'Álvaro Pons Moreno', with a stylized flourish at the end.

Signat Álvaro Pons Moreno

Burjassot, Maig 2017

Esta tesi ha sigut finançada per la Conselleria d'Educació, Investigació, Cultura i Esport de la Generalitat Valenciana mitjançant les ajudes ACIF/2014/142 i BEFPI 2016

Vull agrair la col·laboració de totes aquelles persones i institucions que han fet possible la realització d'aquesta tesi.

En primer lloc al Dr. Álvaro Pons per tot l'esforç, dedicació i paciència que ha suposat dirigir el present treball.

A la Dra. Sophie Triantaphillidou per la seva ajuda, supervisió i per haver-me animat i orientat en la programació de GUIs.

A tots i cadascun dels membres del Grup d'Investigació en Optometria.

Durant aquest temps he tingut l'ocasió de conèixer a gent meravellosa de diferents llocs del món, a tots vosaltres, gràcies de tot cor!



A la meva família, i a la persona que més estime

Listen!

(Navi, The Legend of Zelda: Ocarina of Time)

And if I fly, or if I fall

Least I can say I gave it all

(RuPaul Andre Charles)

Dong!

(Error, Matlab)

Index

Index.....	1
Index of figures.....	6
Index of tables.....	11
Resumen	13
Summary	33
Chapter 1	41
Introduction and objective	41
1.1. Anatomy and physiology of the human eye	41
1.1.1. Retina.....	42
1.1.2. Photoreceptors	43
1.1.3. Ganglion cells	44
1.1.4. Optic nerve.....	46
1.1.5. Lateral geniculate nucleus.....	47
1.1.6. Visual cortex	48
1.2. Visual Acuity.....	49
1.2.1. Introduction.....	49
1.2.2. Factors affecting the VA	50
1.2.3. Methods of measurement of the VA.....	58

1.2.4. Standard values	60
1.3. Contrast Sensitivity Function.....	62
1.3.1. Introduction.....	62
1.3.2. Relationship between the VA and the CSF.....	67
1.3.3. Factors influencing the CSF	67
1.3.4. Measuring methods	77
1.3.5. Temporal CSF	81
1.3.6. Spatial channels.....	83
1.3.7. Clinical application	84
1.3.8. Limitations	86
1.4. Objectives	87
Chapter 2	89
Objective measurement of the fixation disparity under natural viewing conditions	89
2.1. Justification.....	89
2.2. Experimental development.....	94
2.2.1. Mathematical development.....	94
2.2.2. Participants.....	96
2.2.3. Stimuli	97
2.2.4. Apparatus.....	97

2.2.5. Procedure	98
2.3. Results	99
2.3.1. Black symbols on white background	99
2.3.2. White symbols on black background.....	103
2.3.3. Differences between both designs.....	106
2.4. Comparison with other systems.....	107
2.5. Conclusions and future work.....	109
Chapter 3	111
Measurement of the suprathreshold sensitivity with common displays.....	111
3.1. Justification.....	111
3.2. Experimental development.....	113
3.2.1 Display.....	113
3.2.2. Stimuli	113
3.2.3. Test	114
3.2.4. Participants.....	115
3.3. Results	115
3.4. Comparison with other studies	117
3.5. Conclusions and future work	120
Chapter 4	123
Peripheral contrast sensitivity under natural binocular viewing.....	123

4.1. Justification.....	123
4.2. Experimental development.....	125
4.3. Results	129
4.3.1 Effect of fixation target.....	129
4.3.2. Peripheral sensitivity	133
4.4. Comparison with other systems.....	135
4.5. Conclusions and future work.....	136
Chapter 5	139
Objective measurement of the pupil size variation over time under different viewing conditions.....	139
5.1. Justification.....	139
5.2. Experimental development.....	140
5.3. Results	143
5.4. Comparison with other systems.....	149
5.5. Conclusions and future work.....	154
Annex I.....	159
Bit stealing.....	159
Annex II	163
Web Cam Eye Tracker.....	163
A2.1. Pupil detection procedure.....	163

A2.2.	Projection of the coordinates	165
A2.3.	Possibilities of this device	167
A2.4.	Drawbacks.....	168
Annex III.....		169
High Speed VET©		169
References.....		171

Index of figures

Figure 1 Cones distribution in the central fovea. Adapted from a work by Mark Fairchild accessible at http://rit-mcsl.org/fairchild/WhyIsColor/images/ConeMosaics.jpg under a Creative Commons Attribution-Share Alike 3.0 Unported license.....	43
Figure 2 Examples of the behaviour of the ganglion cells when the opponent areas are stimulated. Adapted from a work by delldot accessible at https://commons.wikimedia.org/wiki/File:Receptive_field.svg Image under public domain	45
Figure 3 VA vs Contrast. From Artigas et al. 1995, elaborated from Legge et al. 1987	54
Figure 4 Logarithm of the decimal VA vs Pupil diameter for different luminance levels. From Artigas et al. 1995, elaborated from Leibowitz 1952	55
Figure 5 VA vs Accommodative demand, for the normal situation (left) and when the accommodative errors are compensated (right). From Artigas et al. 1995, elaborated from Johnson 1976.	56
Figure 6 CSF for sinusoidal gratings (open circles) and square wave gratings (open squares), the relation between both sensitivities is represented with the close circles. From Artigas et al. 1995, elaborated from Campbell and Robson 1968.	69

Figure 7 Sensitivity for different test sizes, 2 degrees (circles), 1 degree (squares), 30' (diamonds) and 15' (crosses). From Artigas et al. 1995, elaborated from Noorlander et al. 1980.....	71
Figure 8 CSF for different exposure times. 20 msec (open circles), 40 msec (squares), 500 msec (triangles), unlimited time (close circles). From Artigas et al. 1995, elaborated from Arend 1976.....	72
Figure 9 CSF for different pupil sizes. 2 mm (circles), 3.8 mm (squares) and 5.8 mm triangles. From Artigas et al. 1995, elaborated from Campbell and Green 1965..	75
Figure 10 Acromatic detection surface. From Artigas et al. 1995, elaborated from Kelly 1972.....	82
Figure 11 Effect on the CSF of brain damage for two patients and the posterior evolution over time. From Artigas et al. 1995, elaborated from Bodis-Wollner 1972.	85
Figure 12 The FD is the angular deviation ($\alpha_r + \alpha_l$) between the actual gaze position (represented with a grey triangle with the vertex to the bottom for right eye and with the vertex on top for the left eye) and the position of the real point. The angle is considered to be positive if it is towards the nose, in this example both angles are negative.....	90
Figure 13 Three examples. Left side, both angles are negative, the FD is negative, also called uncrossed disparity. Centre, both angles are positive, the FD is positive, also called crossed disparity. Right side, α_r is negative and α_l is positive, the FD could be zero, but how can we classify it in this case?.....	91

Figure 14 Scheme with the nomenclature used in the mathematical development	96
Figure 15 Boxplot of the FD per subject	99
Figure 16 Example of negative and divergent trend. Blue circles are the measurements, the blue line is the fitted linear regression model for all the measurements, red triangles are the local maxima, the red dashed line the fitted linear model for the maxima, green triangles are the local minima and the green dashed line the fitted linear model for the minima.....	102
Figure 17 Example of positive convergent trend.....	102
Figure 18 Boxplot of the FD per subject	103
Figure 19 Boxplot of the incremental threshold VS pedestal contrast for every frequency.	116
Figure 20 Boxplot of the incremental threshold VS pedestal contrast for every frequency.....	116
Figure 21 Boxplot of the exponents calculated for every subject.....	118
Figure 22 Adjusted model for the linear range of contrast, in grey for all the subjects and in black the mean exponent value.....	119
Figure 23 Effect of exposure time on the value of the exponent in equation 11. From Pons 1997.	120
Figure 24 Examples of the different designs.....	126
Figure 25 Mean contrast sensitivity. Solid markers for the foveal region, open markers for the perifoveal. Circles for the test without the fixation target, triangles for the test with the fixation target.	129

Figure 26 Mean difference in sensitivity between 'with fixation target' and 'without fixation target' for the two retinal locations.	130
Figure 27 Spectrum of the stimuli. Black for 'with the fixation target', grey for 'without the fixation target'. (a) foveal vision, 1 cpd, (b) perifoveal vision 1 cpd, (c) foveal vision 6 cpd, (d) perifoveal vision 6 cpd.	131
Figure 28 Boxplot of the standard deviations for a temporal window of 4 seconds. (a) for foveal vision, 1 cpd; (b) for perifoveal vision, 1 cpd; (c) for foveal vision, 6 cpd; (d) for perifoveal vision, 6 cpd.	132
Figure 29 Sensitivities for the three retinal areas. Black for the foveal, medium grey for the perifoveal and light grey for the near periphery.	134
Figure 30 i) Scheme of the device (a) is the IR camera and the IR illumination system, (b) is the hot mirror, (c) is the chinrest. ii) Representation of the far distance viewing setup, (d) is the target, (e) is a normal mirror.	142
Figure 31 Boxplot of the pupil size per subject for each viewing condition.	145
Figure 32 Boxplot of the differences per each variable.	147
Figure 33 Mean change in the pupil size.	147
Figure 34 Example of pupil size VS time.	151
Figure 35 Boxplot of the 2-second subsamples.	151
Figure 36 Pupil size VS time for different framerates: blue for 250 Hz, orange for 25 Hz and yellow for 5 Hz.	153
Figure 37 Boxplot of the measurement for different framerates.	154

Figure 38 Luminance generated by each digital values for every channel and the grey-scale. Red for the red subpixel, green for the green subpixel, blue for the blue subpixel and black for the three subpixels at the same time.....	159
Figure 39 a) original image, b) original histogram, c) optimised image, d) optimised histogram, e) binarized image, f) noise included in the binarized image, g) eroded image, h) dilated image, i) best fit circle on top of the binarized image, j) best fit circle on top of the original image.....	166
Figure 40 Scheme of the VET.....	169

Index of tables

Table 1 Examples of different tasks for each definition of VA.....	51
Table 2 Contrast definitions.....	65
Table 3 Summary of the measurements per subject.....	100
Table 4 Values for the model in equation 10 and the coefficient of determination. Please note that a negative coefficient of determination implies that a m value of 0 fits better than the actual value for m.....	101
Table 5 Number of subjects for each pattern.....	101
Table 6 Summary of the measurements per subject.....	104
Table 7 Values for the model in eq 5 and the coefficient of determination. Please note that a negative coefficient of determination implies that a m value of 0 fits better than the actual value for m.....	105
Table 8 Number of subjects for each pattern.....	105
Table 9 p-values of the Lilliefors test for every combination of frequency and pedestal contrast.....	115
Table 10 Median of the incremental contrast threshold.....	116
Table 11 Exponent values for the model in equation 11.....	118
Table 12 Radii in degrees for each retinal zone.....	125
Table 13 Average sensitivity for the different combinations.....	130
Table 14 Acronyms for the viewing conditions.....	140
Table 15 Summary of the results per subject.....	144

Table 16 Difference in pupil size generated by the illumination, all units are mm.....	146
Table 17 Difference in pupil size generated by the accommodation, all units are mm.....	146
Table 18 Difference in pupil size generated by the binocularity, all units are mm.....	146
Table 19 Pupil diameter in mm when using a monofocal contact lens fitted for near distance vision.....	148
Table 20 Comparison between the monofocal contact lens for far distance and the lens for near distance.....	149
Table 21 Number of significant matches per subject for each viewing condition.....	152
Table 21 p-values for the effect of the framerate value on the measurements.....	153
Table 23 Digital triplets corresponding to greyish colours which generates luminance levels between to grey steps in ascending order.....	162

Resumen

Objetivos

El principal objetivo de esta tesis es el desarrollo y testeo de nuevos test para la medida de parámetros optométricos bajo condiciones de visión natural. Estos test serán basados en paradigmas y procedimientos existentes que se utilizan en entornos clínicos y de investigación pero introduciendo nuevas aproximaciones en la metodología combinando procedimientos objetivos y subjetivos.

La visión natural se refiere a la situación estándar, visión binocular sin restricciones artificiales o asimetrías.

Como objetivo secundario nos hemos propuesto la moderación en el coste de los test desarrollados y del equipo necesario. Desarrollos de alta tecnología son comunes en el contexto de la investigación, pero esos prototipos, y dispositivos comerciales, no son siempre adecuados para entornos clínicos debido a su elevado coste.

Para alcanzar estos objetivos, cuatro experimentos con sus propias metodologías y resultados son descritos en los capítulos 2 a 5.

En el primer experimento analizamos la fijación bajo visión binocular, lo cual es un requisito para la visión natural.

En el segundo experimento nos centramos en implementar una técnica low-cost para aumentar la resolución en luminancia de los monitores de 8 bits para poder medir la discriminación de estímulos supraumbral.

El tercer experimento extiende el paradigma clásico de medida de sensibilidad al contraste para medir la sensibilidad en visión periférica bajo visión binocular.

El cuarto y último experimento se centra en las fluctuaciones de la pupila y como afectan al diámetro pupilar variaciones en la iluminación, vergencia del estímulo y binocularidad.

Experimento 1. Medida de la disparidad de fijación bajo condiciones de visión natural

Los movimientos fijacionales (microsacádicos, movimientos de deriva, trémores y torsiones) son un conjunto de movimientos que se producen aún

cuando intentamos fijar un estímulo y mantener el ojo quieto. En visión binocular, estos movimientos impedirán que los ejes visuales se crucen siempre en el mismo punto del espacio, haciendo que el ángulo de convergencia no sea constante.

La diferencia angular entre el punto del espacio que se intenta fijar y los ejes visuales mientras se mantiene la estereopsis, por la existencia de las áreas de Panum, se llama disparidad de fijación (FD). El test de FD se basa en la hiperagudeza Vernier en visión dicóptica. La tarea del observador es alinear los segmentos, entonces la FD será cero y el posible desalineamiento permitirá calcular el valor de la FD. La FD es positiva cuando los ejes se cruzan por delante del punto de fijación.

En función del método de medida se estará midiendo la FD objetiva (definición clásica de FD) o la subjetiva (cantidad de disparidad que no se puede compensar de forma sensorial por el sistema visual).

Metodología

Se determina la posición de los ejes visuales mediante el Web Cam Eye-Tracker que se ha desarrollado (hardware y software) para esta tesis (más información en el Anexo II). Mientras el sujeto fija un punto que se muestra en una pantalla posicionada 1 metro enfrente de la mentonera. Se utilizaron dos estímulos, punto negro sobre fondo blanco y punto blanco sobre fondo negro.

Quince sujetos participaron en el estudio, todos adultos jóvenes. Se midió la posición de los ojos durante 45 segundos, previamente cada sujeto se adaptó a la luminancia del laboratorio durante 15 minutos.

Resultados

Punto negro sobre fondo blanco

La distribución de las medidas no fue normal (según el test de Lilliefors con nivel de significación del 5%). La mediana promedio fue de -4.68 minutos de arco con un rango intercuartílico de 14.75 minutos de arco. Respecto a la evolución de la FD con el tiempo se encontraron diferentes patrones, tendencia positiva o negativa y tendencia convergente o divergente. La tendencia global de la medida se determinó mediante un modelo de regresión lineal, el valor de la pendiente determina la tendencia. Para analizar la convergencia/divergencia de los valores se ajusta una recta a los valores máximos de la medida y otra a los mínimos. Nueve sujetos presentaron tendencia negativa y 6 positiva mientras que 13 presentaron tendencia convergente y 2 divergente.

Punto blanco sobre fondo negro

Excepto para el sujeto 12, la distribución de las medidas no fue normal (según el test de Lilliefors con nivel de significación del 5%). La mediana promedio

fue de -7.22 minutos de arco con un rango intercuartílico de 15.13 minutos de arco. En este caso, 8 sujetos presentaron una tendencia negativa y 7 positiva, mientras que 9 presentaron tendencia convergente y 6 divergente.

Comparación entre ambos test

Debido a la no distribución normal de los resultados se usó el test de Kruskal Wallis para comparar ambos grupos de medidas. El p-valor fue de 0.6632, rechazando que existan diferencias estadísticamente significativas entre ambos diseños del test.

Conclusión

Pese a existir otros estudios de la FD basados en métodos objetivos no hemos encontrado ninguno que analice la variación de la FD con el tiempo. Tampoco hemos encontrado información sobre la influencia de la polaridad del estímulo sobre la FD, muy probablemente porque los métodos subjetivos, que son los más utilizados, se basan en visión dicóptica limitando bastante las posibles variaciones del estímulo. Así y todo, los descriptores estadísticos son compatibles con los resultados obtenidos con otros métodos objetivos y a la vez notablemente

Experimento 2. Medida de la sensibilidad supraumbral con pantallas de 8 bits

La función de sensibilidad al contraste (CSF) no es un descriptor ideal de la calidad visual. Su principal desventaja es que intenta describir el sistema por su capacidad en el límite de sensibilidad, pero en las imágenes naturales los contrastes son, en su gran mayoría, supraumbral. Esto significa que en general el sistema visual pasa más tiempo en entornos en los que debe detectar cambios en el contraste más que en detectar frecuencias espaciales con contrastes muy bajos.

Existe evidencia sobre que la función de discriminación del contraste (CDF) no sigue estrictamente la ley de Weber. Para frecuencias pedestal bajas (menores al 3%) la forma de la CDF es de bañera, para contrastes superiores al 3% se ajusta bien a una ecuación exponencial en el que el valor del exponente determina la pendiente de la recta cuando se representa en ejes logarítmicos. La ley de Weber requiere un valor de dicho exponente cercano a la unidad.

Metodología

Se desarrolló un test de dos alternativas de elección forzada (2AFC) para determinar el umbral de discriminación a los siguientes contrastes pedestal: 0.3, 0.5 y 0.7 (según la definición de contraste de Michelson) para las siguientes frecuencias espaciales: 2, 4, 8 y 16 ciclos por grado con una luminancia media de

60 cd/m². Las redes sinusoidales se presentaron dentro de ventanas cuadradas de 13.5 cm de lado (512 píxeles). El test consiste en dos ventanas en las que se muestran dos redes sinusoidales de la misma frecuencia espacial pero con diferentes contrastes, una con el contraste pedestal y la otra con mayor contraste. El orden en el que aparecían se aleatoriza. El orden de medida de las 4 frecuencias y los 3 pedestales también se aleatorizó. Se implementó un método de escalera modificado de forma que tras tres aciertos consecutivos se reducía el contraste un paso y tras un error se aumentaba. El test termina cuando se han producido cinco escalones y el valor de sensibilidad se determina a partir de la media de los cuatro últimos escalones. Se reclutó a 52 voluntarios, todos adultos jóvenes. Los criterios de exclusión fueron un error refractivo esférico mayor a 3 dioptrías, más de 0.75 dioptrías de astigmatismo y más de 1 dioptría de anisometropía. Las medidas se tomaron en visión natural. La pantalla de ordenador se situó a 1.12 metros delante del sujeto. Para incrementar la resolución en luminancia del monitor se implementó una técnica de *bit-stealing* para generar niveles intermedios de pseudogris. Se generaron 6 niveles intermedios entre cada pareja de gris puro, pasando a disponer de 1532 valores de luminancia posibles en lugar de los 256 valores normales de los sistemas de 8 bits. Esto es necesario puesto que la mínima diferencia de contraste que pueden generar los sistemas de 8 bits es bastante superior a la sensibilidad del sistema visual humano normal.

Resultados

Excepto para 2 y 8 ciclos por grado, pedestal de contraste 0.3 el resto de combinaciones no muestran una distribución normal según el test de Lilliefors. Los umbrales incrementales aumentan entre los contrastes pedestales 0.3 y 0.5 pero disminuyen entre 0.5 y 0.7. La mediana de los valores para las frecuencias espaciales en orden creciente fue: contraste pedestal 0.3 (2.55, 2.34, 2.59 y 5.68), contraste pedestal 0.5 (2.93, 3.91, 3.41 y 10.46) y contrastes pedestal 0.7 (1.51, 1.56, 3.46 y 6.87).

El incremento del umbral en función de la frecuencia espacial coincide con los datos que se encuentran en la literatura. En cambio, la disminución del umbral para el pedestal 0.7 es un dato nuevo puesto que a excepción de Kingdom el resto de investigadores midieron hasta un contraste pedestal de 0.5 asumiendo que para valores mayores el sistema visual humano seguiría el modelo exponencial. Kingdom midió los umbrales de contraste incremental para 0.9 y obtuvo caídas como las que se observan en nuestros datos. Si ajustamos el modelo exponencial de Legge a los resultados obtenidos para los pedestales 0.3 y 0.5 se obtienen los siguientes exponentes, ordenados para frecuencias espaciales en orden creciente: 0.488, 0.794, 0.818 y 1.846. Los exponentes para 2, 4 y 8 ciclos por grado coinciden con resultados previos de otros investigadores, en cambio, para 16 ciclos por grado no existe información con la que comparar. Hay que destacar que la desviación es elevada e implica algunos exponentes negativos, esto lo atribuimos

a que los sujetos no estaban acostumbrados a los experimentos psicofísicos y tal vez no mantuvieron criterios constantes o no prestaron la atención suficiente.

Conclusiones

Pese a la obtención de valores negativos para el exponente del modelo, que como se ha razonado lo atribuimos a errores en las respuestas por parte de los sujetos, los valores medios se ajustan a los valores que aparecen en la literatura. De esta forma se confirma que el test implementado proporciona valores fiables siempre que el sujeto responda correctamente. Esto también nos lleva a pensar en la modificación del algoritmo para detectar inconsistencias en las respuestas. Otra conclusión importante es que se puede confiar en el *bit-stealing* como método para incrementar la resolución en luminancia de equipamiento de 8 bits siempre que la combinación de pantalla y tarjeta gráfica esté bien caracterizada. Por último, nuestros resultados ponen en duda la validez del modelo exponencial de Legge más allá de contrastes pedestal de 0.5, efecto que ya se había apreciado por Kingdom para el contraste pedestal 0.9.

Experimento 3. Sensibilidad al contraste periférica bajo visión binocular en condiciones naturales

La CSF ha sido estudiada con detalle para la visión central, el número de estudios al respecto es muy elevado. En cambio, la visión central pese a ser

necesaria no es considerada suficiente por sujetos con problemas en la retina periférica para mostrarse completamente satisfechos con su visión o su nivel de funcionalidad. El elevado nivel de detalle de la visión central es adecuado para tareas como la lectura y el reconocimiento de caras, pero no es óptimo para otras tareas más básicas como caminar evitando posibles obstáculos. En cambio, el número de estudios sobre la sensibilidad al contraste en visión periférica es bastante reducido, y de los existentes las metodologías son diferentes dificultando comparaciones detalladas. Generalmente se usa como estímulo parches de Gabor (red sinusoidal envuelta por una Gaussiana) ya que permiten la exploración de diferentes sectores de la retina mediante el uso de puntos de fijación externos al estímulo. De esta forma se corrobora que los diferentes hemimeridianos de la retina presentan diferente sensibilidad, dato que coincide con las diferencias en la distribución de células ganglionares.

Esta estrategia no permite la medida en condiciones de visión binocular natural. En este estudio proponemos un diseño en forma de anillo con los bordes suavizados por una Gaussiana para medir dos regiones alrededor de la fovea. Para poder comparar también se mide la sensibilidad al contraste de la visión central mediante un estímulo de Gabor. Finalmente se compara la influencia del estímulo de fijación sobre la sensibilidad.

Metodología

Siguiendo la estructuración de las áreas de la retina propuesta por Polyak se definen tres conjuntos de radios con la condición de que la superficie, del círculo para la visión foveal y de las coronas circulares para las dos zonas periféricas, sea constante. El diámetro máximo, limitado por el tamaño subtendido por el monitor a la distancia de visionado (0.5 m) fue de 30 grados. Por tanto, definiendo una corona circular periférica de radio exterior 15 grados e interior de 14 grados el diámetro del estímulo de Gabor para la zona foveal es de 5.61 grados. Finalmente, la zona perifoveal se situó en un punto intermedio entre las otras dos de forma que su radio interior fue de 8.33 grados y el radio exterior de 10 grados.

Las frecuencias espaciales exploradas fueron: 0.5, 1, 2, 4, 6 y 8 ciclos por grado. La luminancia media de la red se fijó en 40 cd/m². Para este nivel de luminancia, con la técnica de *bit-stealing* implementada en el experimento anterior se generó un paso mínimo de contraste de 0.000495. El resto de la imagen se rellenó con un nivel de gris que proporcionase la luminancia media. El estímulo de fijación fue una cruz blanca de 36 píxeles (1.123 grados) de anchura y 3 píxeles de grosor (0.094 grados), posicionado en el centro del estímulo. Se compararon los espectros del test con y sin cruz no encontrándose diferencias significativas de forma cualitativa. Se generaron los siguientes sets de estímulos: región foveal, región foveal con cruz, región perifoveal, región perifoveal con cruz y región periférica con cruz. También se generaron dos imágenes referencia, ambas con el

nivel de gris con la luminancia media, una de ellas con el estímulo de fijación en la misma posición que en la imagen test.

El test consiste en primero la aparición de la imagen test durante 0.5 segundos, seguida de la imagen referencia durante otros 0.5 segundos de forma que no hubiese un parpadeo claro más allá de la aparición y desaparición de la red sinusoidal. La tarea del sujeto era mantener la mirada en el estímulo de fijación, o en el centro de la pantalla para los sets sin cruz de fijación e indicar mediante el teclado si detectaba la red o no. Se implementó un método de escalera modificado de tal forma que tras tres respuestas afirmativas se disminuía el contraste de la red en un paso y tras una respuesta negativa se incrementaba un paso. Tras 15 segundos sin respuesta se considera que el sujeto no detecta la red y por tanto la respuesta es negativa. El test termina tras cinco escalones y el valor de la sensibilidad se calcula promediando los últimos cuatro escalones. Las medidas se tomaron en total oscuridad, excepto la iluminación generada por el monitor. Antes de tomar las medidas cada sujeto se adaptó a las condiciones de iluminación durante 15 minutos. El orden de presentación de frecuencias y excentricidades se aleatorizó y se tomaron tres medidas para cada combinación. Esto alargó la toma de medidas a una semana para cada sujeto con el objetivo de obtener respuestas lo más fiables posible.

Para este estudio los criterios de inclusión fueron más estrictos que para el experimento anterior. Era imprescindible que los sujetos estuviesen

familiarizados en la realización de experimentos psicofísicos, una VA unidad o mejor y prácticamente emétopes jóvenes que pudiesen mantener el esfuerzo acomodativo que requería el test. Cuatro adultos jóvenes, tres hombres y una mujer participaron en el estudio.

Resultados

Efecto del estímulo de fijación

En visión foveal la sensibilidad es menor para frecuencias inferiores a 6 ciclos por grado cuando el estímulo de fijación está presente. En visión perifoveal se produce el mismo efecto para frecuencias espaciales inferiores a 4 ciclos por grado.

Para uno de los sujetos se repitió la medida de dos frecuencias especiales analizando los movimientos oculares mediante el High Speed VET (Annex III). Definiendo un tamaño de ventana temporal de 2 segundos se determinó la desviación de las posiciones del centro pupilar durante toda la medida y se representaron los resultados mediante gráficos de cajas y bigotes (*boxplots*). El resultado fue que para 1 ciclo por grado las desviaciones durante la medida presentan menos dispersión cuando la cruz de fijación está presente en el estímulo para ambas condiciones, en cambio para 6 ciclos por grado dichas desviaciones no varían tanto en función de la presencia del estímulo de fijación.

Sensibilidad periférica

Los datos obtenidos en el subexperimento previo sugieren comparar la sensibilidad de las tres zonas retinianas con el estímulo de fijación presente. El resultado promedio de los cuatro sujetos muestra una serie de características destacables. Primero la sensibilidad general se reduce al aumentar la excentricidad del estímulo. Segundo, esta reducción no es igual para todas las frecuencias y cambia la forma de la curva, pasando de una forma pasabanda a una forma pasabaja. Tercero el máximo de sensibilidad se desplaza hacia las frecuencias más bajas al aumentar la excentricidad.

Conclusiones

Estos resultados son consistentes con los que aparecen en la literatura. El efecto de la cruz de fijación en la sensibilidad es destacable y se debe tener en cuenta. Los datos de eye tracking sugieren que el estímulo de fijación restringe los movimientos oculares, y podría ser esta la causa de la disminución de la sensibilidad. El estímulo en forma de corona circular es apto para la medida de la sensibilidad al contraste en la periferia de la zona foveal.

Experimento 4. Medida objetiva de las variaciones del tamaño pupilar en el tiempo bajo diferentes condiciones de visión

La pupila regula la cantidad de luz que llega a la pupila. Los músculos que controlan la pupila nunca se mantienen quietos, esto produce una serie de contracciones y dilataciones que reciben diferentes nombres, siendo el más popular hippus pupilar. Existen diferentes mecanismos que pueden afectar al tamaño pupilar. En este experimento se pretende medir las variaciones de pupila al modificar tres parámetros: iluminación, proximidad del estímulo y binocularidad.

Metodología

Para testear la influencia de los tres parámetros citados se definieron ocho situaciones: Fotópica binocular de lejos, fotópica binocular de cerca, fotópica monocular de lejos, fotópica monocular de cerca, mesópica binocular de lejos, mesópica binocular de cerca, mesópica monocular de lejos y mesópica monocular de cerca.

El estímulo de fijación fue una cruz negra inscrita en un círculo. Para las dos distancias de presentación del estímulo (6 m y 0.5 m) el ángulo subtendido fue el mismo. Las dos iluminaciones fueron fotópica (100 lux) y mesópica (0.3 lux). Se

midió en binocular y monocular. El orden de estas condiciones fue aleatorizado. Se dejó un tiempo de adaptación de 15 minutos al cambiar las condiciones de iluminación y/o de binocularidad.

Mediante el High Speed VET se midió el diámetro de la pupila durante 45 segundos a una velocidad de captura de 250 fotogramas por segundo, por tanto se tomaron 11250 medidas para cada una de las ocho combinaciones.

Siete adultos jóvenes participaron en el estudio. Los criterios de inclusión fueron error refractivo esférico menor a 3 dioptrías y menos de 1 dioptría de astigmatismo y una VA unidad o mejor con la compensación habitual. Pupilas simétricas y circulares. Aquellos sujetos que necesitasen compensación llevaron sus lentes de contacto habituales.

Resultados

Se analizó la distribución de los resultados para cada medida con el test de Lilliefors, en todos los casos el p-valor fue inferior a 0.0001. Al comparar las diferentes condiciones para cada sujeto mediante el test de Kruskal Wallis se obtuvieron diferencias estadísticamente significativas para todas las condiciones de todos los sujetos excepto para el sujeto 5 en las que la variación del diámetro pupilar en condiciones fotópicas monoculares de lejos y cerca no fueron diferentes.

Comparando para cada sujeto entre diferentes condiciones y promediando se obtuvo que la diferencia media al cambiar de nivel de iluminación fue de 2.50 ± 0.20 mm, al cambiar la proximidad del estímulo la variación del diámetro pupilar fue de 0.34 ± 0.15 mm y al cambiar las condiciones de binocularidad la variación fue de 0.71 ± 0.28 mm.

Se repitió las medidas con el estímulo a 0.5 esta vez con una lente diaria desechable con un incremento de potencia de 2 dioptrías respecto a la refracción de lejos de cada ojo con el objetivo de relajar la acomodación. Estos datos se compararon con los obtenidos en visión de lejos y la variación promedio en el diámetro fue de -0.07 ± 0.12 mm.

La variación debida a la iluminación se ajusta a los resultados y modelos presentes en la literatura. La variación debida a la proximidad del estímulo también coincide con datos de otros investigadores. Respecto a la binocularidad existen pocos estudios en los que se hace hincapié en las diferencias que induce, nuestros resultados también son comparables a los efectos reportados por otros investigadores.

Usar un dispositivo que tenga una velocidad de captura de 250 fotogramas por segundo no es algo común en la práctica clínica debido a su alto costo. Otros dispositivos clínicos presentan una velocidad de captura muy inferior. Para comparar con otros estudios que miden la variación de la pupila en intervalos de

tiempo más cortos y a menor velocidad de captura se tomaron todas las medidas de forma aleatoria, se dividió en ventanas equivalentes a 2 segundos y se compararon los resultados. De 171 comparaciones posibles entre cada medida de cada sujeto, en el mejor de los casos el número de comparaciones consideradas equivalentes por el test de Kruskal Wallis fue de 61, siendo la mayoría de los casos en torno a 30 parejas. Para determinar el efecto de la velocidad de captura se redujo el muestreo de cada medida de 250 Hz se pasó a 25 y 5 Hz. Al comparar los tres vectores con el test de Kruskal Wallis no se encontró ninguna diferencia estadísticamente significativa.

Conclusiones

La primera conclusión de este estudio es que a pesar de mantener constantes las condiciones de iluminación, proximidad del estímulo y binocularidad es un error considerar que el tamaño pupilar se mantiene constante. La segunda conclusión es que la variación del diámetro pupilar no sigue una distribución normal. Pese a que diferentes dispositivos de uso normal en clínica como autorrefractómetros o queratómetros miden el diámetro pupilar, la utilidad de dicha medida es más que cuestionable debido a las enormes diferencias entre las condiciones de medida y las de visión natural. Otra conclusión importante es que mediante la definición de condiciones de medida próximas a la visión natural y a los entornos en los que se sitúan las necesidades visuales del paciente se obtendrán valores para el diámetro pupilar fidedignos

siempre y cuando la duración de la medida sea lo suficientemente larga (45 segundos) aunque la velocidad de captura del dispositivo no sea especialmente elevada (5 Hz).

Conclusiones finales

- La medida objetiva de la FD mediante la WCE es confiable
- Los resultados proporcionados por nuestra metodología no se pueden comparar directamente con otros estudios debido a la falta de información de la evolución temporal de la FD o de la influencia de la polaridad del estímulo
- El uso del *bit-stealing* para incrementar la resolución en luminancia de los monitores habituales proporcionan resultados confiables al medir la discriminación del contraste de estímulos supraumbral
- La ley exponencial para la discriminación del contraste formulada por Legge podría no ser adecuada para contrastes pedestal mayores de 0.5 y para las frecuencias espaciales elevadas
- Al situar un estímulo de fijación en un test de sensibilidad al contraste se disminuye la sensibilidad para las frecuencias espaciales bajas.
- El uso de un estímulo de Gabor para medir la sensibilidad de la visión central es adecuado para condiciones de visión natural, el equivalente en áreas periféricas son las coronas circulares.

- El tamaño pupilar no se puede considerar constante bajo condiciones constantes de iluminación, proximidad del estímulo y binocularidad
- Las variaciones en el diámetro pupilar no siguen una distribución normal
- El tamaño pupilar medido en condiciones de visión no naturales es diferente al que se obtiene en condiciones naturales
- La mejor estrategia para determinar las variaciones de pupila de un sujeto es medir la pupila en condiciones de visión naturales durante un periodo de tiempo razonable incluso a una velocidad de captura baja

Summary

Objectives

The main goal of this thesis is the development and testing of new tests for the measurement of optometric parameters. These tests will be based in existing paradigms and procedures but introducing new approaches in the methodology combining objective and subjective procedures.

Natural vision refers to binocular viewing without any artificial restriction or asymmetry.

As a second goal, we have decided to limit the cost of the developed tests and the necessary equipment to make it suitable for the clinical context.

To achieve these goals four experiments with their own methodologies and results are described in chapter 2 to 5.

In the first experiment the fixation stability under binocular viewing is analysed. The second experiment is centred in the implementation of a low-cost technique to increase the luminance resolution of common displays. The third

experiment extends the classical paradigm for measuring the contrast sensitivity to the peripheral vision under binocular viewing. The last experiment focuses on the pupil size fluctuations and how changes of illumination, the position of the stimulus and the binocularity affect the pupil.

Experiment 1. Measurement of the fixation disparity under natural viewing conditions

The fixational eye movements prevent the eye from remaining still, this implies that the visual axes do not cross on the point of interest. The stereopsis is allowed by the existence of the Panum's areas. The angular difference between the actual angle formed by the visual axes and the required angle to fixate the point of interest is known as fixation disparity (FD). The clinical tests for measuring the FD are based in subjective methods and do not measure the FD in its original definition.

Methods

Using the Web Cam Eye-Tracker (Annex II) the visual axes of both eyes were determined in each frame of a video sequence. Two stimuli were designed, a black dot over a white background and a white dot over a black background. The task for the subject was to stare the fixation point for 45 seconds. Fifteen subjects participated.

Results

For the black dot the median FD was -4.68 minutes of arc, for the white dot the median FD was -7.22 minutes of arc. Regarding the evolution of the FD over time different trends were found: positive, negative trends of all the measurement and convergent, divergent trends of the maxima and minima values. The differences in the results depending on the polarity of the stimulus were not statistical significant.

Experiment 2. Measurement of the suprathreshold sensitivity with common displays

The contrast sensitivity function measures the capabilities of the system at the threshold level, but in the real world we are dealing with suprathreshold contrasts most of the time. This task can be assessed by means of the contrast discrimination function.

Methods

A simple two alternative forced choice (2AFC) test was developed implementing a bit-stealing technique (Annex I) in order to increase the luminance resolution of the display. Three pedestal contrasts were tested: 0.3, 0.5

and 0.7 for the following spatial frequencies: 2, 4, 8 and 16 cycles per degree. A modified staircase method was implemented, the test finishes after five reversals and the sensitivity is calculated by averaging the four last reversals. 52 subjects were recruited.

Results

The incremental contrast discrimination thresholds increase between the pedestal contrasts 0.3 and 0.5 but decrease between 0.5 and 0.7. The threshold also increases for increasing spatial frequencies. When adjusting the results to the power law model defined by Legge the values obtained are in agreement with those reported in the literature when excluding the thresholds measured for the pedestal contrast of 0.7.

Experiment 3. Peripheral contrast sensitivity under binocular natural viewing conditions

The CSF has been deeply studied for the central vision. But central vision is not enough to achieve a high degree of satisfaction with the vision or to normal

tasks such as walking and avoiding obstacles. Those studies about the peripheral sensitivity were not done under binocular natural conditions.

Methods

To test three different areas of the retina (foveal, perifoveal and the near periphery) three different stimuli were designed, a Gabor patch for the fovea, and two rings for the other regions. The area of the three stimuli was exactly the same. Two versions of the stimuli were generated, with and without a fixation target. The task for the subject, 4 in total, was to press a key when the stimulus was detected.

Results

The sensitivity measured when the fixation cross was present was lower for the low frequencies in comparison with the stimuli without the cross. The sensitivity diminishes when increasing eccentricity, changing the shape of the curve from a band-pass shape in central vision to a low-pass shape.

Experiment 4. Objective measurement of the pupil size variation over time under different viewing conditions

The pupil regulates the amount of light reaching the retina. The muscles that modify its diameter are never still. Many different factors can affect the size of the pupil. In this experiment we want to test the influence of the illumination, the stimulus proximity and the binocular conditions.

Methods

Eight combinations of illumination, stimulus proximity and binocularity were defined. The pupil size of the right eye was measured during 45 seconds at a framerate of 250 Hz when staring at a fixation target. Seven young adults participated in this study.

Results

All the measurements did not follow a normal distribution. When comparing with the Kruskal Wallis all the conditions were statistical different except from the photopic monocular far and near conditions of subject 5. The mean effect of the change in illumination was 2.50 ± 0.20 mm, the proximity of the stimulus generated a mean change of 0.34 ± 0.15 mm and the variation in the

binocularity produces a change of 0.71 ± 0.28 mm. When adapting a disposable contact lens to match the vergence of the near stimulus the mean change due to the position of the stimulus was -0.07 ± 0.12 mm. When reducing the sampling rate from 250 to 25 and 5 Hz no statistical significant differences were found. When dividing the 45 second measurement into 2 second measurements the differences were statistically significant.

General conclusions

- The objective measurement of the FD by means of the Web Cam Eye-Tracker is reliable.
- The results provided by our methodology cannot be compared directly with other studies because we have not found any data about the temporal evolution of the FD or the influence of the polarity of the stimulus.
- The use of bit-stealing for increasing the luminance resolution of common displays provides reliable results when measuring suprathreshold contrast discrimination and for the contrast sensitivity measurement for different retinal areas.
- The power law for contrast discrimination formulated by Legge may be not accurate for pedestal contrasts higher than 0.5 and for high spatial frequencies.

- When placing a fixation target in a contrast test the sensitivity for low frequencies diminishes.
- The use of Gabor patches for measuring the sensitivity for central vision is reliable for natural viewing conditions, the equivalent for peripheral areas are the ring patches.
- Pupil size cannot be considered constant under constant conditions of illumination, stimulus proximity and binocularity
- The variations of the pupil size do not follow a normal distribution
- When the pupil size is measured under not natural conditions the values will differ from those obtained under natural vision
- The best strategy for determining the pupil size is to measure it under natural viewing conditions and taking measurements for a reasonable period of time even at a low capture speed

Chapter 1

Introduction and objective

1.1. Anatomy and physiology of the human eye

The human visual system is a really fascinating neural mechanism which deals with the visible light to generate a whole group of complex perceptions known as vision. It is able to extract physical information, such as the length of wave, from light emitted or reflected by the objects in the scene. It is also able to obtain information about the geometry of those objects and their position inside the scene through a series of optical properties, for example the blur generated by the vergence of the object. And, in a final step, produce a mental representation of the real world through the combination of all the information contained and derived from both monocular images in a fused three-dimensional perception taking into account the disparities generated by the different perspectives of the scene captured by each eye.

This sophisticated process has been crucial for the development of the human kind. Most of the information that we must deal with is acquired through sight. The human visual system provides information to other systems that regulate the reading, the memory, etc.

Light comes through the cornea and the pupil to the posterior chamber and generates an image on the inner surface of the eyeball. In this surface is where the phenomenon of vision begins.

1.1.1. Retina

The retina is the tissue inside the eye that contains the photoreceptors, rods and cones, which transforms the photons into electrical impulses that will travel to the visual cortex through the axons of different neurons inside the retina and those conforming the optic nerve.

The retina is not uniform through all its area. The most important part for the vision is the central retina, known as the macular region. This area has a diameter about 7 mm. The photoreceptor density is high for the cones and low for the rods. The density of the cones increases to the centre of the retina and reaches its maximum value in the foveal region, about 147300 cells/mm² (Osterberg 1935). The rod density is maximum in the periphery of the macular region, at 20 degrees (5.5 mm) from the centre with a mean value of 150000 cells/mm² (Osterberg 1935).

An important characteristic of the foveal region is that except from the photoreceptor layer the rest of the layers in the retina are displaced to their sides in order to not occlude the cones (Osterberg 1935) and to facilitate the perception of light with the highest spatial sampling in this tissue.

1.1.2. Photoreceptors

The photoreceptors are the cells in charge of capturing the photons and generating electrical impulses. There are two types of photoreceptors, cones and rods. The biggest difference between these two groups is that rods are responsible for the perception of light and their density is high outside the fovea while the cones are responsible for the colour perception and their density is higher in the central retina (Osterberg 1935).

The diameter of the photoreceptors depends on their eccentricity regarding to the central retina. Typical sizes of the peripheral rods are comprised between 2 to 5 microns while the cones size is found between 5 to 8 microns (Osterberg 1935). In the centre of the fovea, where rods are absent, the diameter of a cone is reduced to 1.5 microns. So, the image sampling by the photoreceptors is not constant and

homogeneous through the retina. A representation of the photoreceptor mosaic is shown in figure 1.

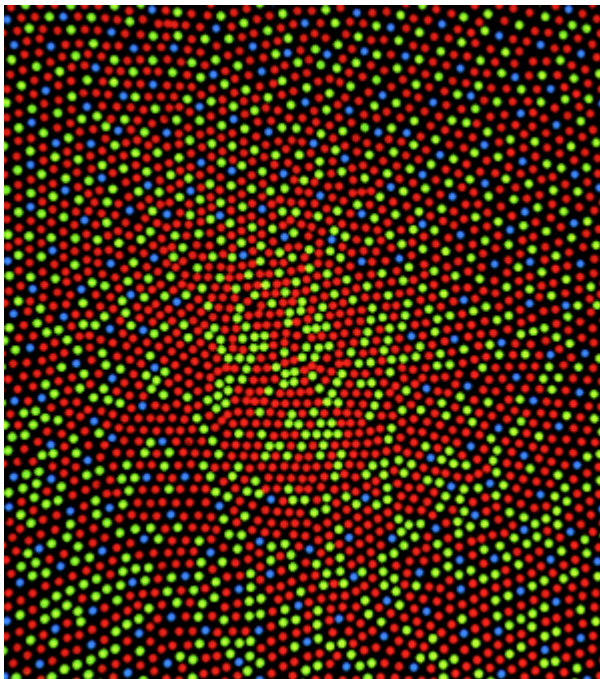


Figure 1 Cones distribution in the central fovea.
Adapted from a work by Mark Fairchild accessible at <http://rit-csl.org/fairchild/WhyIsColor/images/ConeMosaics.jpg> under a Creative Commons Attribution-Share Alike 3.0 Unported license

1.1.3. Ganglion cells

The electrical signals triggered by the photons are gathered by a group of specific neurons inside the retina, the ganglion cells. In the fovea, every ganglion cell is connected to a single cone, but when increasing the eccentricity more than one photoreceptor are connected to a single neuron, this is known as convergence (Thibos et al. 1987). The axons from the ganglion cells form the optic nerve. So, the spatial sampling of the retina is limited by the ganglion cells instead of the photoreceptors. For central retina the density of the ganglion cells is high, but it diminishes in the periphery (Drasdo 1989).

The receptive field of the ganglion cell is the portion of visual space that forms an image over the photoreceptors converging on that ganglion cell. For the central fovea, up to 3 degrees, this convergence has a ratio of 1:1 (Curcio & Allen 1990). Due to this convergence ratio in the centre of the fovea, there is no practical difference between cones and ganglion cells when talking about the spatial sampling of the image. For cones, the convergence with ganglion cells remains almost constant for the central 10 degrees (Curcio & Allen 1990). Starting at 10 degrees the convergence increases rapidly up to 30 degrees and from there it stabilises. For rods the convergence increases up to 30 degrees and from there it remains almost constant (Goodchild et al. 1996).

These receptive fields are organised following a centre and surround opposition scheme (Wiesel 1960), an example of the receptive fields properties is shown in figure 2. Because of this structure, ganglion cells will respond to different spatial structures present in the image. When using a patch of light to stimulate the receptive field both areas will be activated and because of their opposite effect on the response of the cell little effect will be generated. When using a grating of, for example, straight bars with a certain width that matches the response profile of the cell the total response will be maximum.

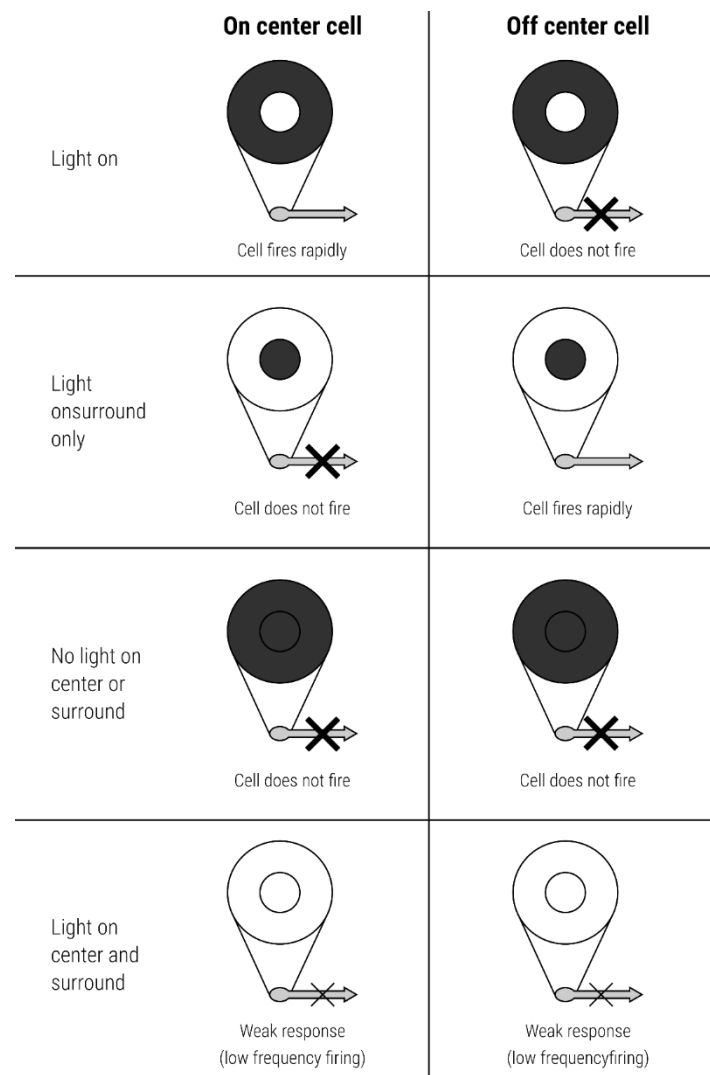


Figure 2 Examples of the behaviour of the ganglion cells when the opponent areas are stimulated. Adapted from a work by delldot accessible at https://commons.wikimedia.org/wiki/File:Receptive_field.svg Image under public domain

The density of ganglion cells is lower than for photoreceptors, but at the same time there are notorious asymmetries in the ganglion cell distribution between temporal and nasal retina (there are approximately three times more cells in the nasal retina than in the temporal retina) and superior and inferior retina (the density of ganglion cells is up to 60% higher in the superior retina in comparison to the inferior retina) (Curcio & Allen 1990).

Two classes of ganglion cells can be found, they received different names because there are important anatomical and physiological differences (Fukuda & Stone 1974). The first group, the Y cells, are bigger than the X cells, the other group. Y cells show a quick and brief response to changes in luminance while X cells are related to the colour vision and their responses are much longer in time.

1.1.4. Optic nerve

The axons of these neurons leave the retina forming the optic nerve. The optic nerves cross in the optic chiasm, where the information of the nasal retina crosses to the other hemisphere of the brain travelling together with the information of the temporal retina (Artigas et al. 1995).

1.1.5. Lateral geniculate nucleus

The axons of the optic nerve reach the lateral geniculate nucleus (LGN) where the visual information is projected into the visual cortex in the occipital region of the brain (Artigas et al. 1995).

The lateral geniculate nucleus is stratified in six layers. The visual information is projected into these layers following a retinotopic representation of the image. The first and second layer are formed by big neurons known as magnocells, the Y cells are connected to these cells. The other layers are formed by small cells called parvocells which are connected to the X cells (Fukuda & Stone 1974, Artigas et al. 1995). No convergence of the retinal information is produced in the visual pathway up to the lateral geniculate nucleus, so every single cell in it has the same receptive field of the ganglion cell that synapses to it.

Due to the limited resources in the human visual system, not every single photoreceptor signal arrives to the visual cortex through an isolated channel. There is a reduction in the number of neurons from the photoreceptors layer in the retina to the lateral geniculated nucleus (Artigas et al. 1995). This reduction implies that several photoreceptors responses converge to the same cell. From the LGN to the visual cortex the opposite phenomenon is produced: divergence (Barlow 1981). So, the visual pathway seems to be organised to process the signal

and extract the important features that will be analysed by the visual cortex (Tsotsos 1988).

1.1.6. Visual cortex

The visual cortex is stratified in six layers containing different kinds of neurons showing relevant differences in their receptive fields (Hubel & Wiesel 1962, Hubel & Wiesel 1972). These cells are organised in columns, perpendicular to the surface of the cortex, that respond to a particular orientation of a light bar (Hubel & Wiesel 1962).

The experiments of Hubel and Wiesel (Hubel & Wiesel 1962, Hubel & Wiesel 1972) showed that the neurons in the visual cortex have receptive fields different than the ganglion cells. Instead of being circular, the cortical receptive fields are more elongated generating this way different sensitivities for different orientations (Daugman 1980). This is the reason why it is commonly said that the cortical neurons are tuned to frequency and orientation. It is known that the proportion of cortical cells tuned for horizontal and vertical orientations is higher than those tuned for other orientations generating a higher sensitivity for vertical and horizontal gratings in comparison to oblique directions (Mansfield 1974).

1.2. Visual Acuity

1.2.1. Introduction

The Visual Acuity (VA) is the most popular metric to express the visual quality of an observer. It is the most common way of expressing the subject's ability to perform certain tasks related to the sharpness of his or her vision. The possible tasks related to the VA are detection, resolution, recognition and location:

- Detection refers to the smallest stimulus that can be detected, also known as minimum visible.
- Resolution is the ability to distinguish whether two objects are separated or not, it is known as minimum separable.
- Recognition refers to the capacity of identifying a shape or a detail inside the shape, it is the minimum recognizable.
- Location task refers to detect small displacements or misalignments inside the test.

For these tasks the mathematical definition of VA would be: the inverse of the minimum angle subtended by the smallest object that the subject can see (detection); the inverse of the minimum separation angle between two objects so that they are perceived as different objects (resolution); the inverse of the angle subtended by the smallest recognizable detail in the test (recognition) or the

inverse of the minimum angle subtended by the smallest deviation perceived by the observer. Table 1 contains examples of the visual tasks.

Due to the differences between the tasks related to the VA there is not a single and unique definition for this metric. A possible definition is: the VA is the capacity to detect, resolve, recognize or discriminate details in objects under conditions of high contrast and photopic illumination.

1.2.2. Factors affecting the VA

1.2.2.1. *Photoreceptor size*

The VA is maximum in the central fovea where the photoreceptors are tightly packed following a hexagonal distribution (Osterberg 1935, Curcio et al. 1993). Because of the circular shape of the iris the point spread function (PSF) of the eye is an Airy's disk (Artigas et al. 1995). The Rayleigh criterion for the resolution of the images of two points says that those images will be perceived as separated when the maximum of the Airy's disk of one point coincides with the first minimum of the other Airy's disk (Artigas et al. 1995). Doing some calculations and taking some assumptions about the optical system of the eye the smallest distance between two images in retina that can be detected as different points is around 4 microns (0.68 arc min).


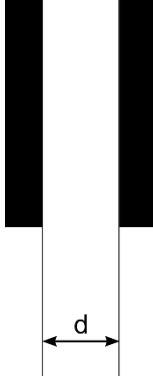
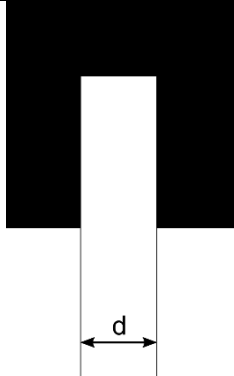

Task	Definition	Example
Detection		Smallest object that can be seen
Resolution		Smallest separation between two objects that can be seen
Recognition		Smallest detail that can be seen
Vernier		Smallest deviation between two lines that can be seen

Table 1 Examples of different tasks for each definition of VA.

Considering a diameter for the cones in the fovea of 1.5 microns and a separation of 0.5 microns this would mean that two images formed in two adjacent cones can be resolved (Artigas et al. 1995, Montés-Micó et al. 2011). This criterion refers only to the optical performance of a system so if two adjacent cones are excited the brain will not perceive two different spots of light, it is necessary, at least a third cone between the two images to resolve the spots.

1.2.2.2. *Photoreceptor mosaic*

The discrete nature of the retina should be considered so there is another limit imposed to the maximum resolution, the theorem of Nyquist-Shannon (Nyquist 1928, Shannon 1949) which imposes that the maximum frequency that can be detected by an array of receptors is slightly inferior than the half of the frequency of the receptors. When the stimulus is more complex than a pair of dots at least two pair of adjacent photoreceptors have to be stimulated by the detail inside the stimulus. In the central retina the cones are distributed following a quite regular hexagonal distribution (Hofer et al 2005). This distribution loses its regularity with increasing eccentricity and age (Curcio et al. 1993). This irregularity could help to avoid a possible subsampling of the retinal image (Williams & Collier 1983, Bossomaier et al. 1985).

1.2.2.3. Luminance

VA increases when the luminance is increased (Artigas et al. 1995). This increase is lineal with the logarithm of the luminance (Sheedy et al. 1984). The increment is slow for luminance levels lower than 0.05 cd/m^2 , that corresponds to the scotopic vision. At this level vision is sustained only by the rods which are not present in the central fovea (Osterberg 1935, Curcio et al. 1993). In the photopic range, more than 0.1 cd/m^2 , the angle of the slope is much higher than in the scotopic range. Above 100 cd/m^2 the angle diminishes reaching an asymptotic value.

Due to this relationship between VA and luminance it is recommended to measure it in the photopic range. Unfortunately, there is no consensus about the illumination range: while Artigas suggest more than 85 cd/m^2 (Artigas et al. 1995), the British standards are 120 to 150 cd/m^2 (Tunnacliffe 1993) but for the clinical practice the range of values are in the interval between 80 to 320 cd/m^2 .

1.2.2.4. Contrast

The VA is proportional to the inverse of the square-root of the contrast of the optotype (Legge et al. 1987) as can be seen in figure 3. The British standards (Tunnacliffe 1993) establish a lower limit of 0.9 for the contrast of the optotype while Sloan suggest a minimum contrast of 0.84 (Sloan 1951).

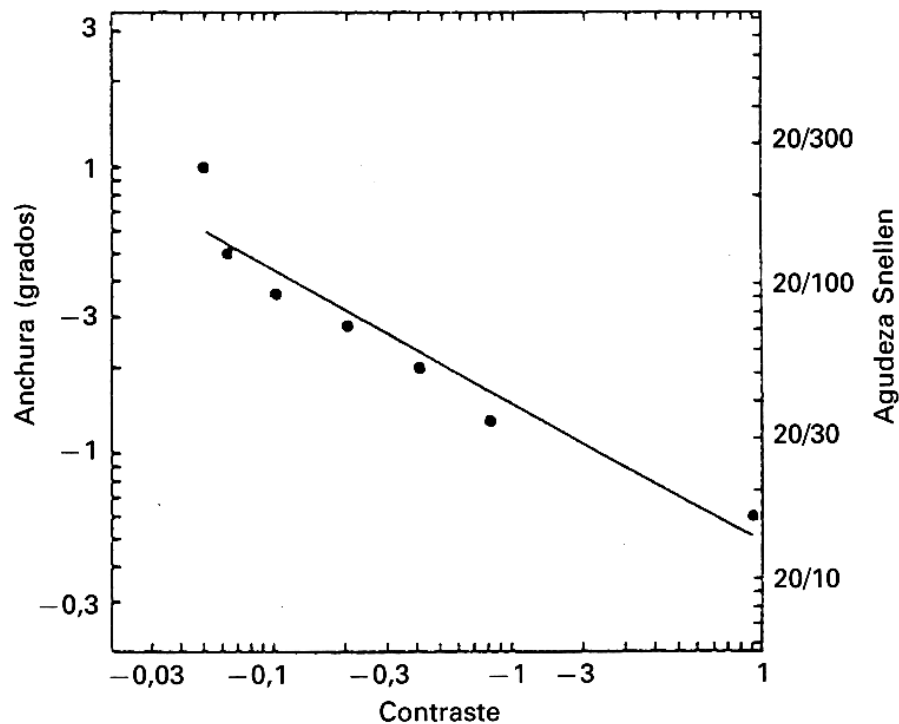


Figure 3 VA vs Contrast. From Artigas et al. 1995, elaborated from Legge et al. 1987

1.2.2.5. Exposure time

The exposure time is not a variable to consider in the clinical practice, but it plays a role on the VA. For luminance over 100 cd/m² and for exposure times longer than 0.1 seconds the effects are imperceptible, for shorter times the relationship is of inverse proportionality (Niven & Brown 1944, von Boehmer & Kolling 1998). For lower luminance levels VA show a noticeable and significant variation when the exposure time is in the range of 0.1 to 1 second (Graham & Cook 1937).

1.2.2.6. *Defocus*

The relationship between the VA and the spherical defocus is of inverse proportionality (Legge et al. 1987). This effect is the most relevant from the clinical point of view because the refraction process is based on it.

1.2.2.7. *Pupil*

Pupil diameter determines whether the aberrations or the diffraction limits the resolution of the eye. Leibowitz determined that the best VA is achieved with a pupil diameter between 2 and 4 mm (Leibowitz 1952, Campbell & Gubisch 1966). In figure 4 can be seen that the best VA is obtained for pupil sizes between 3 to 4 mm, in function of the luminance level.

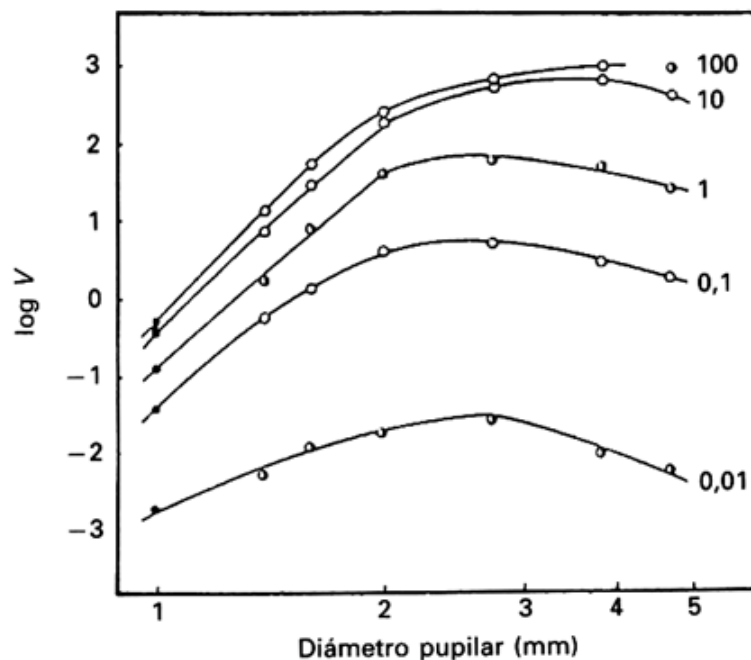


Figure 4 Logarithm of the decimal VA vs Pupil diameter for different luminance levels. From Artigas et al. 1995, elaborated from Leibowitz 1952

1.2.2.8. Accommodation

The accommodative response differs from the accommodative demand. Only for one accommodative demand the accommodative response shows the same value, that distance is known as the dark focus (Miller 1978). Because of this deviation the VA is modified lightly, but when correcting the accommodative error the VA remains constant for all the accommodative demands (Johnson 1976) as can be seen in figure 5.

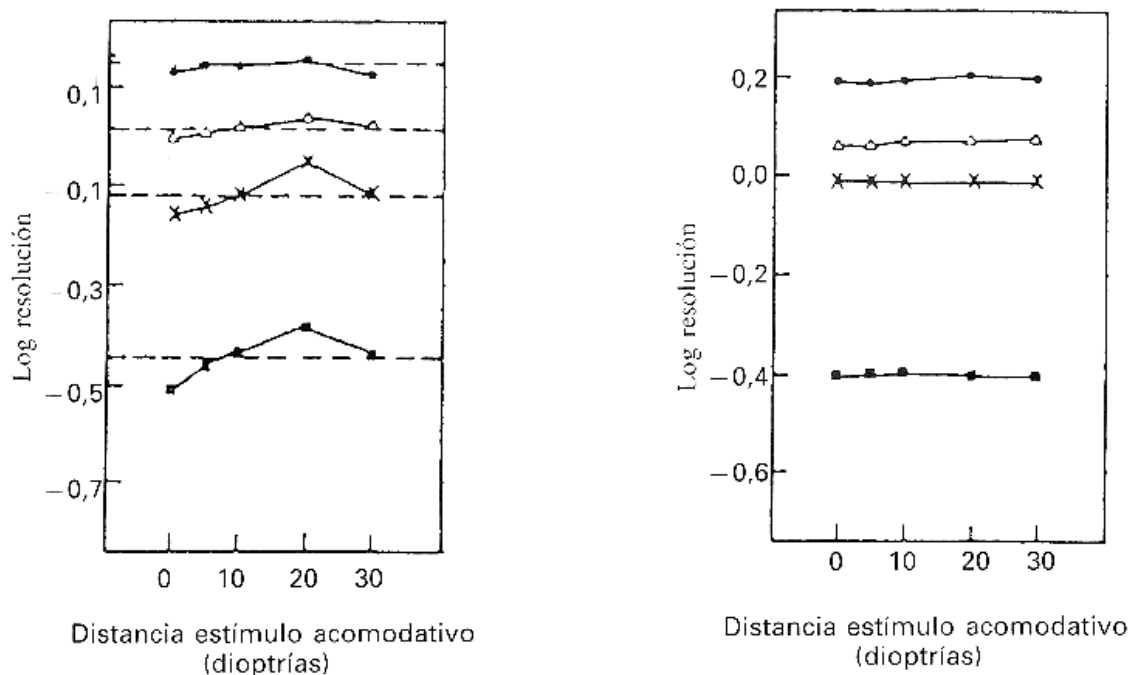


Figure 5 VA vs Accommodative demand, for the normal situation (left) and when the accommodative errors are compensated (right). From Artigas et al. 1995, elaborated from Johnson 1976.

1.2.2.9. *Adaptation state*

The VA value is influenced by the state of adaptation to the illumination of the visual system. The best values are obtained under photopic illumination when the luminance level for the test and the adaptation field are similar. Under mesopic and scotopic conditions the VA is better when the luminance of the test is higher than the luminance of the adaptation field (Craik 1939).

1.2.2.10. *Eccentricity*

For foveal vision the VA is maximum and it diminishes with increasing the eccentricity of the stimulus under photopic conditions as has been shown by different authors (van Doorn et al. 1972, Berkley et al. 1975, Johnson et al. 1978, Jacobs 1979).

1.2.2.11. *Other*

Other factors such as the experience of the observer with the test (Fahle & Edelman 1993), fatigue, attention (La Fleur & Salthouse 2014) and age (Adams et al. 1988) play a role on the value of the VA.

1.2.3. Methods of measurement of the VA

1.2.3.1. *Notations*

Once exposed the different tasks, and subsequently the ambiguity, that can be used for defining and measuring the VA concept it is necessary to find a metric to report that value. There are different ways to express it based in the recognition task.

1.2.3.1.1. Snellen

The Snellen notation is a fraction between the distance of observation and the distance in which the detail subtends 1 arc minute (Snellen 1862, Bennett 1965). Because it is based in distances there are two options to express the Snellen notation. The first is using meters, so the denominator will be 6 meters in general (this depends on the design of the optotype) and the second one is using feet and in this case the denominator will be 20 feet.

With this notation the normal VA is 6/6 or 20/20. Acuties below this value have a numerator minor than the denominator, acuties higher than the normal value have a numerator major than the denominator. It is quite simple to change the viewing distance and calculate the right value for VA, being this its main advantage.

1.2.3.1.2. Decimal

This notation is related to the Minimum Angle of Resolution (MAR). Defined as the quotient between 1 arc minute and the MAR in arc minutes (Bennett 1965). Because of the quotient this notation has no dimension.

The normal VA in decimal notation is 1. Acuties lower than the normal have a value smaller than one and values higher than one represent smaller sizes for the MAR. Some clinicians communicate the VA to their patients as a percentage in an attempt to help patients to understand their visual situation. To calculate this percentage it is necessary to multiply the decimal value by one hundred.

To convert from the Snellen notation to the decimal notation is as simple as to calculate the Snellen quotient. To convert from decimal to Snellen it is only necessary to multiply the decimal value by the standard denominator of the Snellen notation (6 if using meters, 20 if using feet).

1.2.3.1.2. logMar

Because of the limitations of the Snellen chart such as problems with the progression of sizes, number of letters per row, difficulty for recognizing some letters, etc. (Sloan 1951, Sloan 1959, Ferris et al. 1982, Wick & Schor 1984, Friendly & Weiss 1985, Elliott & Sheridan 1988) Bailey and Lovie proposed another design for an optotype chart and a new notation for the VA (Bailey and Lovie 1976, Bailey

and Lovie 1980). This notation uses the MAR again, but instead of calculating a quotient respect to the standard value for the MAR the logarithm is calculated.

1.2.3.1.3. Other

There are other metrics to express the VA value, some of them designed for specific sets of patients such as those who have low vision.

1.2.4. Standard values

While a logMar value of 0.0 is considered the standard and desirable VA this value is not realistic. The idea comes from initial studies at the end of the nineteenth century (Snellen 1862). The optical quality of the eye allows higher resolutions and the neural sampling is also capable of resolving smaller details than those subtending 1 arc min (Campbell & Green 1965, Green 1970). Many people show a VA better than the 0.0 so this value should be considered a lower limit for the normal VA. The value considered normal or standard is of crucial importance because refractive surgery, refraction algorithms, contact lens fit, etc. pretend to achieve it.

For example, during a refraction, in order to relax the accommodation, a considerable amount of positive defocus is induced. This defocus is reduced in steps of 0.25 dioptries until the VA reaches the 0.0 logMar. This is done to prevent the hypercorrection of the eye due to the effects of an increase of the total

refractive power of the eye due to the accommodation (Montés-Micó et al. 2011). This procedure is known as maximum positive maximum visual acuity. When following this algorithm there is the risk of hipocompensating the patient when the target VA value is lower than the VA of the patient. The result of that is an excess of positive value for the prescription of the eye, blurring the vision and reducing the VA value.

Since the invention of the nonius scale by the French mathematician born in the sixteenth century Pierre Vernier there is evidence that for certain tasks the capabilities of the human visual system go beyond the limits imposed by the anatomy and the diffraction. Westheimer reported (Westheimer 1975) an increasing number of examples for these hyperacuity tasks, known as Vernier acuity, during the nineteenth century. Using a Vernier task for measuring the VA a much higher value is expected, around 1 second of arc, equivalent to 60 in decimal notation (Artigas et al. 1995). This implies that there is a process to increase the capabilities of the visual system for some specific tasks.

Even though, the VA when measured with letters is an easy way to make the patient to understand its visual capabilities and at the same time is a good tool for performing a refraction there are some problems. First, there is not a single and unique definition making it difficult in order to establish a global standard for measuring and reporting its value. Second, the many possible factors that affect it make the standardization even more difficult. Third, the human visual system

show, under some circumstances, capabilities far beyond its optical and anatomical limits. And finally, the most important thing, in the real world what matters is not always small and black over white.

1.3. Contrast Sensitivity Function

1.3.1. Introduction

Despite the VA is the most used metric to assess human vision there are some situations in which having a good VA is not synonym of having a good quality of vision. Cataracts at early stages may not diminish the VA but can alter the quality of vision. In fact, in McCarty (McCarty et al. 1999), 462 subjects out of 2300 people with a VA of 0.0 logMar or better reported dissatisfaction with their vision, few of them related to the presence of cataract. VA is related to satisfaction but not equivalent (Sletteberg et al. 1995), for example, for cataracts it has been shown that the VA value is not a good predictor of satisfaction, quality of life and performance after surgery (Schein et al. 1995) due to the ambiguous definition of outcome (Lundström et al. 1999).

The contrast sensitivity is the ability of the visual system to detect changes of luminance (Artigas et al. 1995, Barten 1992, Barten 1999). This ability is used when we try to distinguish between an object and the background.

Optotypes can be used to test the contrast sensitivity (Pelli & Robson 1988, Pelli & Bex 2003), but the most used and more appropriate object to measure the contrast sensitivity are the sine-wave gratings. Firstly introduced by Schade in the fifties (Schade 1956) after his studies on the application of Fourier analysis on television systems. Some years later, Hubel and Wiesel provided the first physiological evidence that different cells from the visual cortex responded to different orientations of a luminous bar (Hubel & Wiesel 1959). Different researchers have demonstrated that the visual system is sensitive to these kind of stimuli (Campbell & Robson 1968, Campbell et al. 1969, Guth & Mcnelis 1969, Maffei & Fiorentini 1973, De Valois et al. 1982, Watson & Barlow 1983, Ginsburg & Cannon 1984) or more specifically to Gabor functions (a sinusoidal grating enveloped by a Gaussian function as seen in equation 1) (Marçelja 1980, Pollen & Ronner 1981, Kulikowski et al. 1982).

$$g(x, y, \lambda, \theta, \psi, \sigma, \gamma) = \exp\left(-\frac{x'^2 + y'^2 \gamma^2}{2\sigma^2}\right) \cos\left(\frac{2\pi x'}{\lambda} + \psi\right)$$

Where

$$x' = x \cos \theta + y \sin \theta$$

$$y' = -x \sin \theta + y \cos \theta$$

Equation 1

λ is the wavelength of the sinusoid grating

θ is the orientation of the normal of the stripes

ψ is the phase of the grating

σ is the deviation of the Gaussian

γ is the ellipticity

Sinusoidal gratings are characterised with three parameters: frequency, contrast and phase (equation 2). The frequency is the number of times that a period is repeated per unit of length. Common units for the frequency are cycles per image, cycles per segment and, the most used, cycles per degree of viewing angle (cpd). The contrast is the difference in luminance between two points of the grating, in particular, is the relationship between the maximum and the minimum luminance and is defined by three different expressions: Michelson, Weber and Root Mean Square (RMS) (Peli 1990, Pelli & Bex 2013). Michelson contrast is the ratio between the maximum luminance minus the minimum luminance and the maximum luminance plus the minimum luminance, this definition is suitable for periodic stimulus such as the sinusoidal gratings or checkerboards (Peli 1990). Weber contrast is the ratio between the maximum luminance minus the minimum luminance and the background luminance, this definition is frequently used for optotypes (Peli 1990). The RMS contrast is the standard deviation of

luminance and is the appropriate definition for complex and non-periodic images (Peli 1990, Pelli & Bex 2013). The different contrast definitions are summarized in table 2. Please note that while Michelson and Weber contrast have no units, RMS contrast is measured in cd/m^2 so making direct comparison between them is difficult or impossible. Phase refers to the position of the bars in respect to a reference. An interesting property of sine-wave gratings is that the defocus only diminishes their amplitude (or contrast) and not their frequency and phase.

$$y(x) = A \sin\left(\frac{2\pi}{T}x + \varphi\right)$$

Where

Equation 2

A, half of the contrast

T, the period

φ , initial phase

Michelson	$\text{Contrast} = \frac{\text{luminance}_{\text{maximum}} - \text{luminance}_{\text{minimum}}}{\text{luminance}_{\text{maximum}} + \text{luminance}_{\text{minimum}}}$
Weber	$\text{Contrast} = \frac{\text{luminance}_{\text{maximum}} - \text{luminance}_{\text{minimum}}}{\text{luminance}_{\text{background}}}$
RMS	$\text{Contrast} = \sqrt{\frac{1}{MN} \sum_{i=0}^{N-1} \sum_{j=0}^{M-1} (I_{ij} - \bar{I})^2}$ <p>I_{ij} are the i-th j-th normalized pixel value of a digital image of size M by N. \bar{I} is the mean pixel intensity of the image</p>

Table 2 Contrast definitions.

The minimum contrast at which a grating is distinguishable from a uniform field with the same luminance than the mean luminance value of the grating is known as the threshold contrast. Its inverse is known as sensitivity as seen in equation 3. The Contrast Sensitivity Function (CSF) are the values of contrast sensitivity (CS) for each spatial frequency. The normal CSF under high photopic conditions is a continuous band-pass curve when plotted in logarithmic axes showing a peak value around 5 to 7 cycles per degree (cpd), the cut-off frequency is around 60 cpd.

Equation 3

$$Sensitivity = \frac{1}{Contrast_{threshold}}$$

The CSF is not only due to the sensorial part of the visual system. All the optical systems can be characterised through their Optical Transfer Function (OTF) which indicates the loss in contrast of an image formed by an optical system. This is a complex function with two components, the Modulation Transfer Function (MTF) and the Phase Transfer Function (PTF). The OTF is a complex function while the MTF is the absolute value of the OTF. The MTF measures how the system is filtering and attenuating the different spatial frequencies of the object, in fact, it can be used to characterise the effect of a system on the signal by analysing the differences between its input and its output. In the case of the eye, the MTF characterises how the optics (tear film, cornea, crystalline lens, aqueous and vitreous humours) attenuate the contrast of the spatial frequencies. The MTF and the CSF are related but are not the same. The MTF refers only to the filtering

generated by the optical system, in this case the optics of the eye, and the CSF refers to the sensitivity of the system (brain) for an image modified by the optics of the eye (Campbell & Green 1965, Bour 1980, Barten 1992, Barten 1999).

1.3.2. Relationship between the VA and the CSF

The cut-off frequency is the biggest frequency (and the smallest cycle) that can be seen at maximum contrast (Campbell and Green 1965, Barten 1992, Barten 1999). Depending on the definition and the task, this frequency is related with the smallest detail that can be resolved, being, this way the relationship between the CSF and the VA. The VA is the one-dimensional and the CSF the two-dimensional limits of the vision. CSF determines the value of the contrast below which nothing can be detected regardless of its size while the VA determines the physical size below which nothing can be resolved regardless of its contrast (National Research Council 1985).

1.3.3. Factors influencing the CSF

1.3.3.1. *Those related to the stimulus*

1.3.3.1.1. Mean luminance

As stated before, for high luminance levels the maximum of the CSF is around 5-7 cpd, and the cut-off frequency is up to 60 cpd. As the mean luminance decreases, the height of the maximum sensitivity decreases as well and the frequencies for the maximum and the cut-off are displaced towards lower values. The CSF shape goes from a band-pass curve to a low-pass curve. (Campbell & Robson 1968, van Nes 1968, Sheedy et al. 1984). Another factor related to the luminance has to be taken into account, the luminance changes exponentially when changing the viewing distance.

1.3.3.1.2. Grating profile

Sensitivity is different for sine-wave gratings (band-pass) than for square-wave gratings (low-pass) (Campbell & Robson 1968). The differences in sensitivity for the low spatial frequencies can be seen in figure 6.

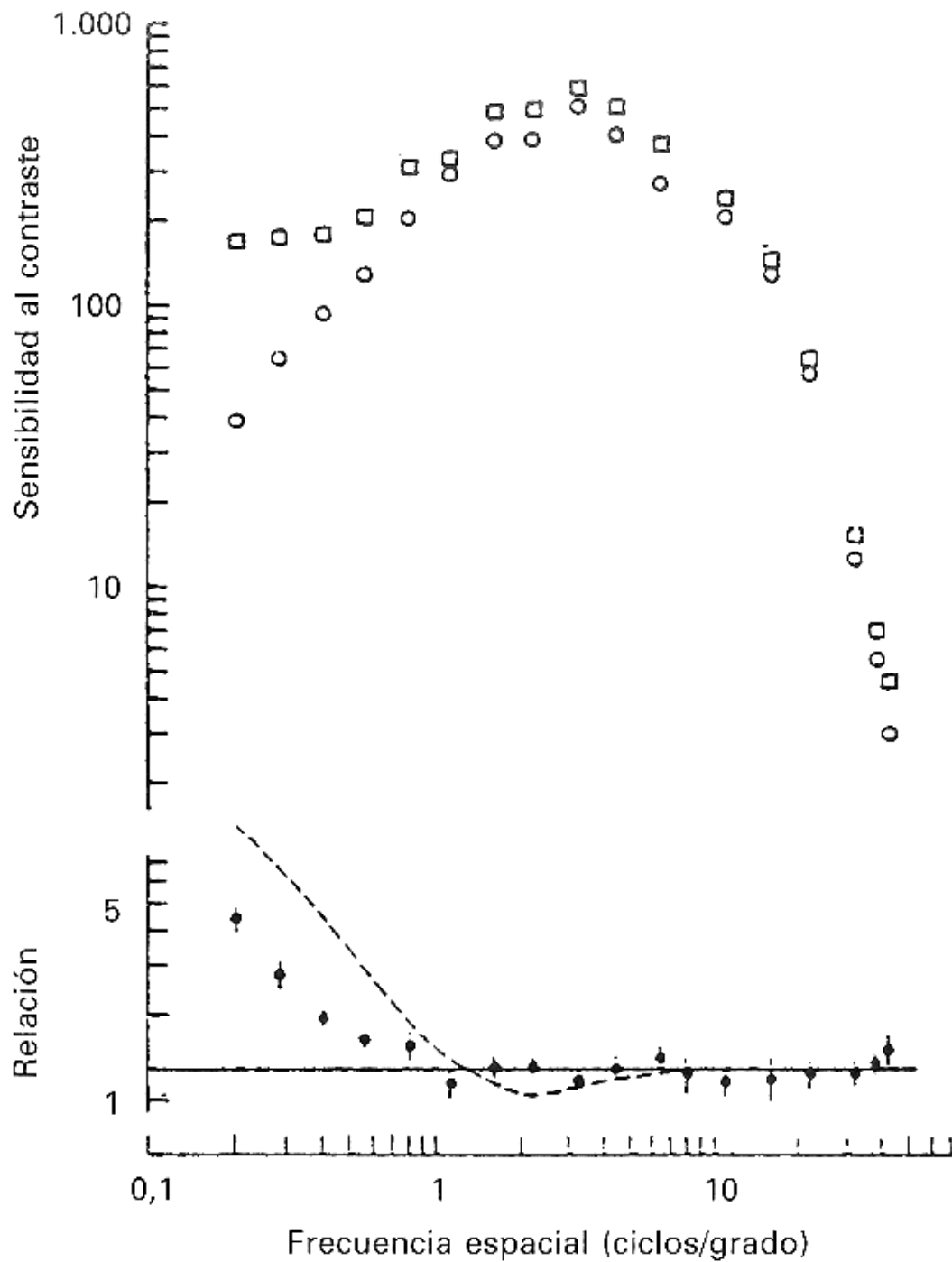


Figure 6 CSF for sinusoidal gratings (open circles) and square wave gratings (open squares), the relation between both sensitivities is represented with the close circles. From Artigas et al. 1995, elaborated from Campbell and Robson 1968.

1.3.3.1.3. Field size and number of cycles presented

The number of cycles present in the stimulus affect the sensitivity. The contrast threshold diminishes as the number of cycles increase up to ten (McCann et al. 1978). Sjostrand (Sjostrand 1979) studied the influence of the field size and concluded that low frequencies are detected outside the fovea. Researchers have determined that 6 degrees of visual angle is the critical value, a grating subtending less than that quantity generate false depressions in the sensitivity (Heul 1977, Arden 1978, Sjostrand 1979, Kruk et al. 1981, Kruk & Regan 1983, Trick et al. 1988). This parameter is related to the number of cycles that are presented.

1.3.3.1.4. Eccentricity

Sensitivity diminishes as the eccentricity of the stimulus increases (Virsu & Rovamo 1979, Robson & Graham 1981, Kelly 1984, Johnston 1987, Pointer & Hess 1989, Thibos et al. 1996). Across the retina the sensitivity varies different depending on the direction (Robson & Graham 1981, Pointer & Hess 1989).

1.3.3.1.5 Test size

This effect is only noticeable for a stimulus size of 2 degrees or less. For smaller sizes the sensitivity is lower for the low and mid frequencies than for the high frequencies, this is related to the number of frequencies present in the stimulus patch (Noorlander et al. 1980). The results for different sizes are shown in figure 7.

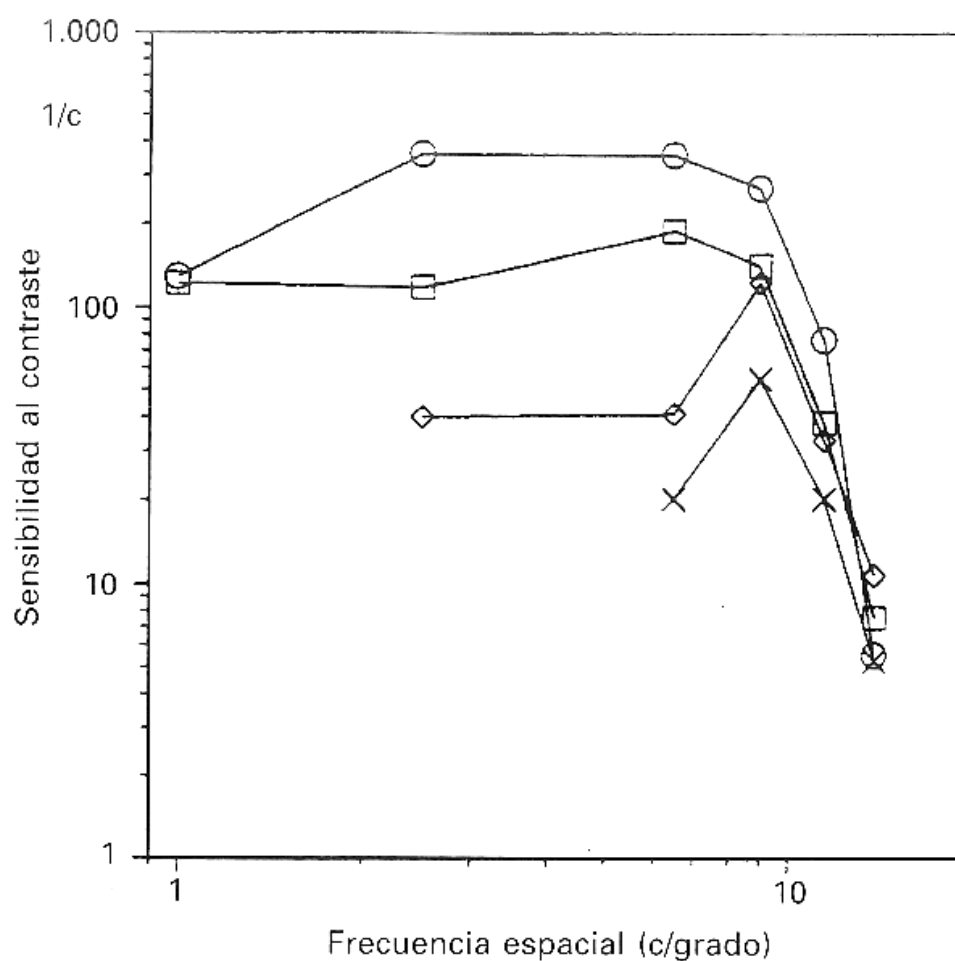


Figure 7 Sensitivity for different test sizes, 2 degrees (circles), 1 degree (squares), 30' (diamonds) and 15' (crosses). From Artigas et al. 1995, elaborated from Noorlander et al. 1980.

1.3.3.1.6. Time

The overall shape of the CSF depends on the interval of time while the stimulus is presented and the on-set time (Arend 1976). For small exposure times the CSF shows a low-pass shape, the sensitivity increases with the exposure time changing the CSF into a band-pass shape (figure 8).

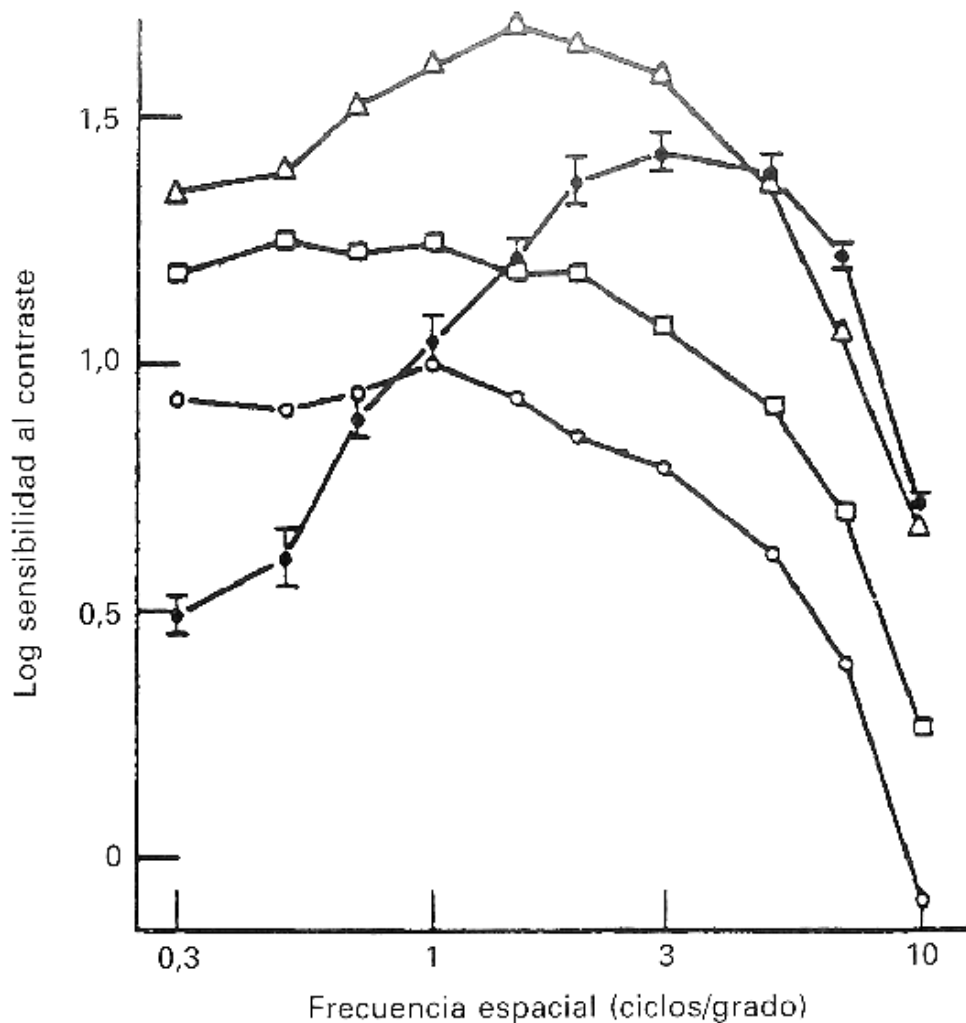


Figure 8 CSF for different exposure times. 20 msec (open circles), 40 msec (squares), 500 msec (triangles), unlimited time (close circles). From Artigas et al. 1995, elaborated from Arend 1976.

1.3.3.1.7 Orientation

As has been explained in section 1.6, sensitivity is higher for vertical and horizontal gratings than for oblique orientations (Campbell & Kulikowski 1966) due to the higher amount of cortical cells tuned for vertical and horizontal directions (Mansfield 1974).

1.3.3.1.8 Edge interactions

The function than envelopes the sine-wave grating introduce new spatial frequencies so it should be considered when measuring low frequencies. If possible, the best option is to use a wide Gaussian envelope to prevent the appearing of sharp edges which are composed by high frequencies and to not generate an abrupt gradient of contrast. The circular envelope generates another effect on the grating, the central lines are longer than the peripheral, and that generates a different summation (National Research Council 1985).

1.3.3.2. *Those related to the subject*

1.3.3.2.1. Adaptation state

The optimum response is obtained once the visual system is adapted to the mean luminance level (Sheedy et al 1984).

1.3.3.2.2. Defocus

Campbell and Green reported a loss of sensitivity for mid and high frequencies when increasing the power of ophthalmic lenses but not for low frequencies (Campbell & Green 1965), this agrees with the impact of the defocus on the visual acuity (Arden 1988). Due to the nature of the gratings, a cylindrical defocus has different impact on sensitivity depending on the relationship between the orientation of the cylinder and the grating. So, it is crucial to compensate all the refractive errors before measuring the contrast sensitivity to prevent optical generated alterations, notches, in the CSF curve (Apkarian et al. 1987).

1.3.3.2.3. Pupil

Pupil diameter is crucial for the quality of the image over the retina. For big diameters the optical aberrations affect the quality while for small diameters the diffraction limits the quality. Campbell reported lower sensitivities for bigger pupil diameters (Campbell & Green 1965, Campbell et al. 1966), the sensitivity for different pupil sizes are plotted in figure 9. The impact of the pupil size on the retinal illumination is proportional to the area of the pupil, so the variation is

exponential (Charman 1991) this in combination with the natural oscillation of the pupil diameter (Stark et al. 1958) hinders the stabilization of the retinal illumination. Also, the pupil diameter is affected by adaptation to the luminance level of the test (Sheedy 1984).

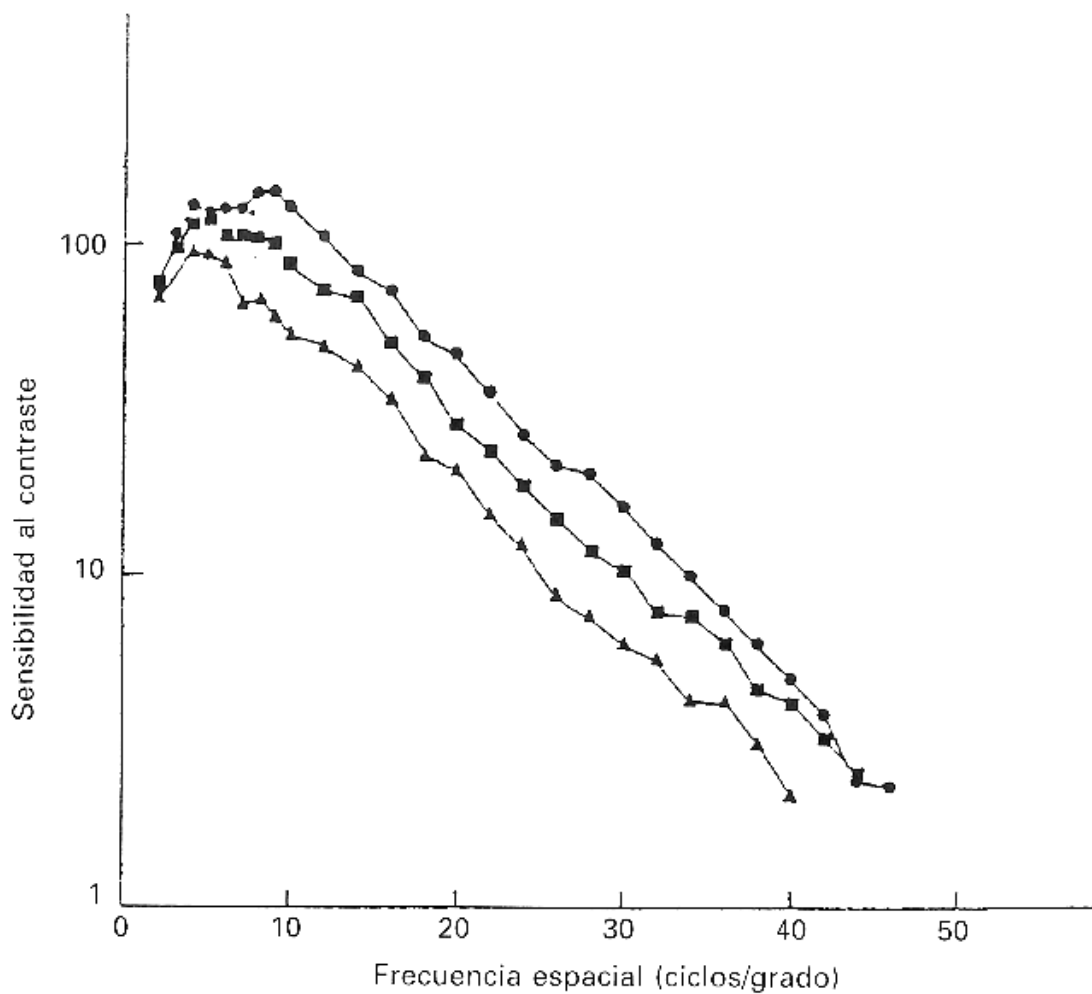


Figure 9 CSF for different pupil sizes. 2 mm (circles), 3.8 mm (squares) and 5.8 mm triangles. From Artigas et al. 1995, elaborated from Campbell and Green 1965.

1.3.3.2.4. Binocularity

Campbell & Green (Campbell & Green 1965) and Legge (Legge 1984a, Legge 1984b) reported better sensitivity when the test was made under binocular vision. This is known as binocular summation and implies that two eyes are better than one at the threshold level. In fact, Legge did not find significant differences under monocular and binocular viewing when the test was done at suprathreshold contrast levels (Legge 1984a).

Meese tested the influence of different viewing conditions and found that the results were different depending on them. The binocular summation process is more complicated than the expected and the equivalence of the results obtained under monocular, binocular or dichoptic vision should be questioned (Meese et al. 2006).

1.3.2.3.5. Psychological factors

There is a list of factors such as tiredness, the focus level on the task (La Fleur & Salthouse 2014), reflexes, etc. that can modify the results of the measurement for all the psychophysical measurements.

1.3.2.3.6. Age

The overall sensitivity reduces with age (Owsley et al. 1983, Higgins et al. 1988, Sloane et al. 1988). Probably, optical changes seem to have no effect on this loss as Morrison and Owsley showed (Morrison & McGrath 1985, Owsley et al. 1985). A possible explanation is that the photoreceptor distribution increases its disorder with age (Werner et al. 1990).

1.3.4. Measuring methods

Contrast threshold is not a single value for a determined combination of frequency, mean luminance, spatial position, and other factors affect the CSF. Due to neural noise, sometimes the observer will perceive the stimulus at some contrast, other times will not perceive it. The proportions between perceived and not perceived can be used to define the threshold. A common criterion is the value of contrast at which the probability of detection is the 50%.

1.3.4.1. *Limits*

In this method the stimulus is always present and two different approaches can be used. In the first, that is called ‘ascending’ the stimulus is below the threshold of the observer the contrast (or the magnitude under study) is increased until the observer can perceive the stimulus. In the ‘descending’ method, a suprathreshold stimulus is presented and the contrast is diminished until the observer cannot detect the image (Artigas et al. 1995).

The results of both submethodologies are averaged to obtain a definitive value for the threshold, but for some situations both submethodologies provide quite different results so the limits method is used to estimate the range of values that should be used for each observer in other psychophysical methodologies.

1.3.4.2. *Adjustment*

In this method the subject controls the variation of the magnitude and its task is to reach the threshold modifying the test controls. In fact, the adjustment method is a small but important variation to the limits method with a greater degree of involvement by the subject. This method usually is faster than others and psychologically less boring for the subject.

1.3.4.3. *Simple stimuli*

This method consists in determining the psychometric function by presenting a reduced sample of stimuli with different levels of contrast. The bigger contrast has to be a value that is always seen and the smaller contrast has to be a value that is never seen. The stimuli are presented in random order many times to determine the probability of detection for each value of contrast (Artigas et al. 1995).

1.3.4.4. Constant stimuli

This is a variation of the previous method, in this case next to the test stimulus a reference stimulus is presented and the task for the subject is to compare both stimulus.

1.3.4.4.1. Psychometric function

The psychometric function describes the detection probability as a function of the signal intensity (Nachmias 1981, Wichmann & Hill 2001) and it is a cumulative normal probability function also known as Galton's ogive. In the equation 4 p is the probability of detection, c is the contrast, c_0 is the contrast value with a 50% of detection probability, x is an integration variable and σ is the standard deviation of the distribution.

Equation 4

$$p(c) = \frac{1}{\sigma\sqrt{2\pi}} \int_{-\infty}^c e^{-\frac{(x-c_0)^2}{2\sigma^2}} dx$$

There are external and internal sources of noise that affects detection, this noise follows a Gaussian distribution (Thurstone 1927). The internal noise is the one related to the visual system, composed by the optics of the eye and neurons (Chichilnisky 2001), while the external is the one related to the image.

1.3.4.5. *Forced Choice*

One of the principal disadvantages of the previous described methods is that all of them rely on the stability of the subject criterion while doing the test. This is not always possible, especially between non-trained observers and for time consuming or boring tests. To prevent the effects of the guessing by the subject the forced choice methods appeared (Blackwell 1946).

The experimenter is accepting and forcing that near the threshold level the subject will answer randomly. The stimuli are presented in different spatial locations or time intervals and the subject has to choose one of the options even if the stimulus is not perceptible. These methods have shown a greater degree of stability in the threshold estimation in comparison to previous methods (Artigas et al. 1995).

1.3.4.6. *Staircase methods*

Dixon developed another method to estimate the threshold in psychophysical experiments (Dixon 1965). Starting, usually, at a perceptible contrast level, while the subject perceives the stimulus for the next iteration of the test the stimulus contrast is lowered by a certain amount and when the answer is negative the contrast is increased. By repeating the test at some point the answers

will be an alternation of YES and NO which indicates that the threshold is located between those contrast values.

This method admits different modifications such as the step size that can be modified depending on the answer of the observer to prevent memorization or to require a number of sequential positive answers before reducing the contrast.

1.3.5. Temporal CSF

The equivalent to the CSF in the temporal domain is known as flickering sensitivity curve (FSC) (de Lange 1958a, de Lange 1958b). The maximum in the FSC is around 10 Hz for an uniform stimulus (spatial frequency zero) (de Lange 1958a, de Lange 1958b). As for the CSF, the FSC is affected by different factors that can change its shape. Robson (Robson 1966) reported a change in the band-pass shape of the CSF to a low-pass shape when the temporal frequency is increased, a similar change happens on the FSC when increasing the spatial frequency.

Kulikowski reported an interesting discovering (Kulikowski & Tolhurst 1973). The thresholds for the flicker detection and the grating detection are different. In particular, the FSC showed a band-pass shape while the CSF had a low-pass shape under that experimental conditions. This means that two different channels were involved. One sensitive to low spatial frequencies and high temporal frequencies (the magnocellular) and the other sensitive to high spatial

frequencies and low temporal frequencies (the parvocellular). Some characteristics of the neurons of each mechanism are explained in section 1.5.

When representing the sensitivity versus the spatial and the temporal frequencies at the same time a surface arise. Known as the acromatic detection surface, it represents the response of the visual system to a spatial-temporal stimulus (Kelly 1972), this surface can be seen in figure 10.

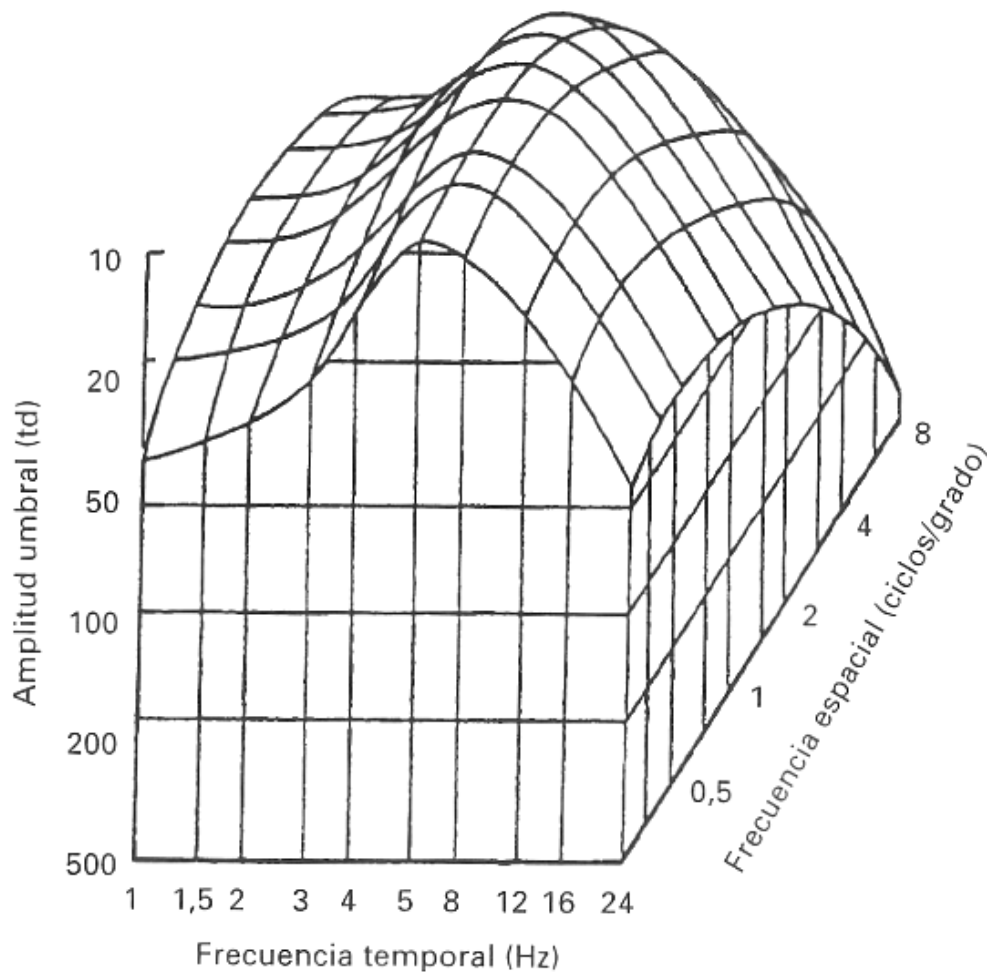


Figure 10 Acromatic detection surface. From Artigas et al. 1995, elaborated from Kelly 1972.

1.3.6. Spatial channels

The organisation of the cells in the visual system permits to speak about orientation mechanisms or channels (Kline et al. 1983). The shape of the curve describing the sensitivity of this channels when plotted using logarithmic axes is like a parabola. The peaks of this channels are separated by octaves of frequencies.

The psychophysical experiments done show a series of characteristics of the visual system that support the idea of the spatial channels. These experiments show some phenomena related to the visual system: adaptation, discrimination at threshold, subthreshold summation and masking. When a channel is continuously stimulated its sensitivity for the range of frequencies to which the channel is tuned decreases for a period of time, this is known as adaptation (Blakemore & Campbell 1969). Another way to analyse the channels is to test whether the visual system can discriminate between two frequencies at threshold or not. The idea is if both frequencies stimulate the same channel the response will be similar and it will not be possible to detect the differences, but if each frequency is detected by different channels there will not be any problem to distinguish between them (Watson & Robson 1981, Nachmias 1975, Thomas 1982). Using a similar reasoning when presenting two subthreshold gratings of similar frequency, if the channel is tuned for both frequencies there will be a summation and the visual system will detect a stimulus. If each frequency stimulates a different channel there will not be any

detection because the summation process will not occur (Graham & Nachmias 1971, Olzak 1981). The masking phenomenon consists on a raise in the sensitivity threshold for a grating when a second grating with a neighbouring frequency is presented only if the second frequency stimulates the same channel (Wilson et al. 1983).

Using these properties of the frequency channels the previous studies estimated a different number of channels, between 6 to 8 frequency channels. This estimation varies in function of the stimulus properties. Orientation is also a factor to consider, Olzak estimated that each channel is tuned for a set of orientations between 5 to 20 degrees (Olzak 1986). So, the CSF has to be understood as the result of the responses of all the channels.

1.3.7. Clinical application

1.3.7.1. *Diagnosis and screening*

Some pathologies like glaucoma, macular degeneration, optic neuritis and problems like cataracts in early stages have no impact on the VA but produce a significant decrease in the sensitivity for mid and low frequencies (Hess & Woo 1978, Loshin & White 1984, Ross et al. 1984, Fleishman et al. 1987). In figure 11 is represented the follow up of two patients with different brain damaged (Bodis-

Wollner 1972), it is remarkable how the recovery is not uniform for all the frequencies.

Despite the solid evidence that different conditions affect the CSF in specific ways it is not clear that those changes are enough for a diagnostic. The visual channels can be affected by certain conditions, producing a diminishing in the sensitivity of the frequencies transmitted by that channel. Identifying the alterations on the CSF can provide a cue on the origin of the problem. Notches in the CSF can be produced by refractive errors (Apkarian et al. 1987). A weird relationship between the values of the VA and the CSF of a subject indicates that the problem has an optic origin.

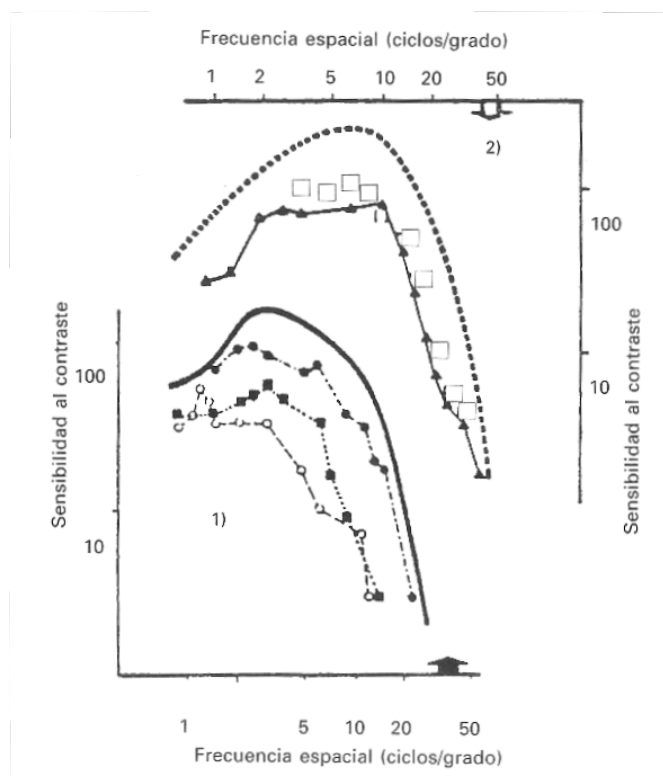


Figure 11 Effect on the CSF of brain damage for two patients and the posterior evolution over time. From Artigas et al. 1995, elaborated from Bodis-Wollner 1972.

1.3.7.2. *Follow up and documentation*

The CSF is a more detailed assessment of the visual function so it is a better way to document the visual impairment and its progression. But because of the number of different factors, including the effect of the psychophysical procedures, that affect the sensitivity mentioned in previous sections there are significant problems in order to correlate the results obtained in the laboratories among them and with the clinical practice (Ginsburg & Cannon 1983, Corwin & Richman 1986, Long & Pen 1987, Long & Tuck 1988, Pelli & Robson 1988, Rubin 1988). An example of follow up is shown in figure 11.

The lack of a common standard when measuring the contrast sensitivity function, similar to the lack of an international standard for measuring the visual acuity, limits the interchangeability of the results when using different testing procedures.

1.3.8. Limitations

The existence of the frequency channels indicates that the exclusive use of the VA for assessing the spatial vision is not a good decision. Different conditions can affect low frequencies, or even mid frequencies and have no impact on the VA. But also, the influence of the temporal frequency on the contrast sensitivity function implies that the vision is a multidimensional phenomenon. What is more,

in the real world, the images are not always grey, they have colour and are not pushing the visual system to its limit of detection.

1.4. Objectives

The goal of this thesis is to develop new tests for measuring optometric parameters based in existing paradigms for assessing the visual quality, performance and other parameters under natural viewing conditions with new approaches combining subjective and objective procedures.

Natural vision refers to the normal viewing situation. Binocular viewing without any restriction or asymmetries.

A secondary goal will be the moderation in the cost of the tests developed and needed equipment. High-tech developments are common in a research context, but those prototypes, and commercial devices, are not always suitable for clinical setups due to its high-cost.

In the first experiment we will talk about the fixation under binocular viewing, which is a requirement for natural vision.

In the second experiment we will focus on a low-cost technique to increase the luminance resolution of common displays to measure the discrimination of suprathreshold stimuli.

The third experiment will extend the normal contrast measurement paradigms to test the peripheral sensitivity under binocular viewing.

The fourth and last experiment focuses on the fluctuations of the pupil and how is affected the pupil diameter by variations in the illumination, the vergence of the stimulus and the binocularity.

Chapter 2

Objective measurement of the fixation disparity under natural viewing conditions

2.1. Justification

Natural viewing conditions means, binocular vision. Under monocular vision the fixational eye movements (Ditchburn & Ginsburg 1953, Martínez-Conde et al. 2004, Otero-Millan et al. 2014) prevent the eye from remaining perfectly still. In fact, when measuring the fixation position using an eye-tracker device the result is a cloud of points around the target. Under binocular viewing the existence of the fixational movements implies that both visual axes will be moving constantly, so the angle of convergence cannot be considered constant.

The angular difference between the point in space that is intended to be stared and the visual axis of each eye in binocular condition while maintaining the depth perception is known as Fixation Disparity (FD) (Ogle et al. 1967), a basic scheme is shown in figure 12. When the deviation is towards the nose the angle is considered to be positive. Fusion, and stereopsis are possible because of the existence of the fusional areas of Panum (Mitchell 1966).

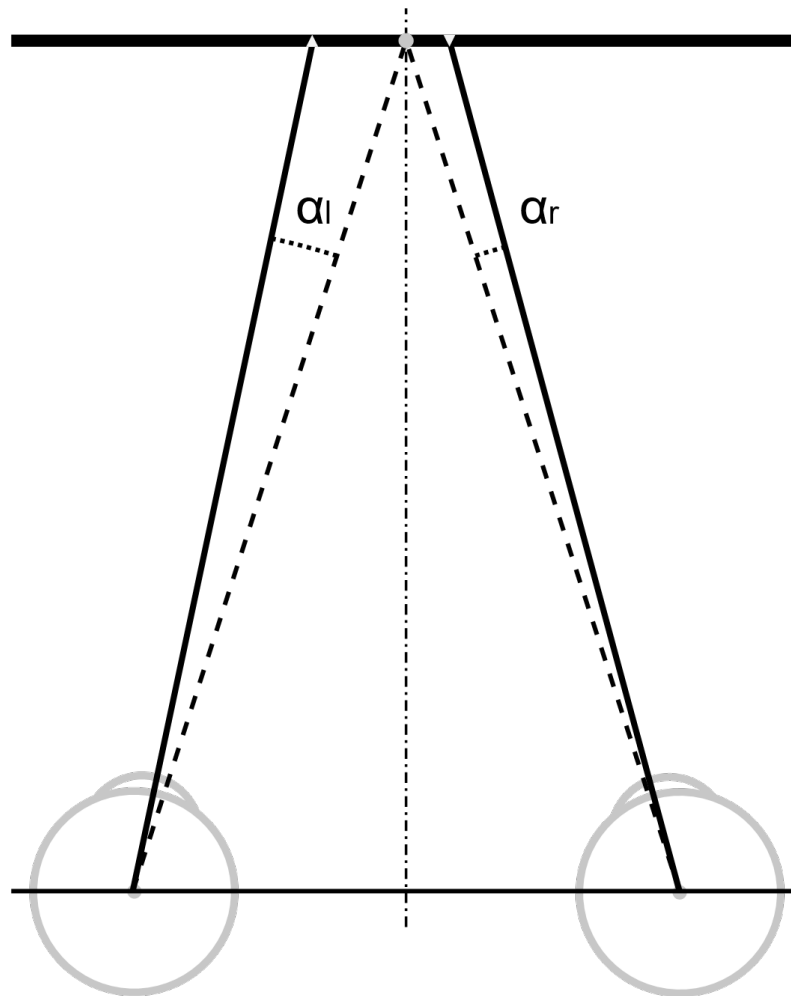


Figure 12 The FD is the angular deviation ($\alpha_r + \alpha_l$) between the actual gaze position (represented with a grey triangle with the vertex to the bottom for right eye and with the vertex on top for the left eye) and the position of the real point. The angle is considered to be positive if it is towards the nose, in this example both angles are negative.

Because of this misalignment, a binocular disparity is generated between the eyes and the stimulus, so many authors prefer to classify the FD as crossed or uncrossed in function of the depth. This classification is not adequate. Some examples of different possibilities of misalignment of the visual axes are provided in figure 13.

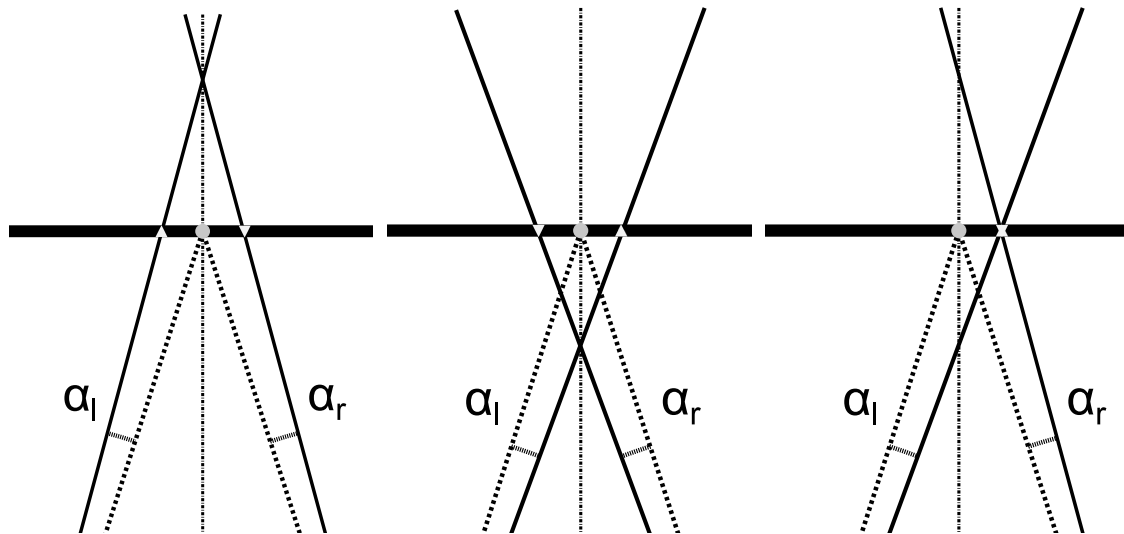


Figure 13 Three examples. Left side, both angles are negative, the FD is negative, also called uncrossed disparity. Centre, both angles are positive, the FD is positive, also called crossed disparity. Right side, α_r is negative and α_l is positive, the FD could be zero, but how can we classify it in this case?.

Ogle (Ogle et al. 1967) introduced the idea of FD, measuring it using a simple test based on the Vernier hyperacuity, see Chapter 1 for more details. Both eyes see a fusional stimulus binocularly and two segments in dichoptic vision. The task for the patient is to align the segments, assuming that when both segments were perceived as aligned the visual axes were aligned over the stimulus, and hence the FD being zero. From the amount of displacement of the movable segment the angle was calculated. During the sixties, Hebbard (Hebbard 1962) using a complex and invasive system obtained the first objective results. His results showed a little difference in comparison to the results reported by Ogle.

The development of eye-tracker systems has allowed to obtain information about the position of the visual axes in a non-invasive way. With these devices, different studies found significant differences in the value of the FD compared with the results of the subjective methods (Remole 1985, Kertesz & Lee 1987, Fogt & Jones 1998).

Accordingly to these differences, depending on the method used to measure the FD some authors differentiate two concepts: the Objective Fixation Disparity (OFD) and the Subjective Fixation Disparity (SFD) (Remole 1985, Fogt & Jones 1998, Schroth et al. 2015). The OFD is the traditional concept of FD (misalignment between the visual axes and the stimulus) measured by means of an objective method and the SFD is the FD measured by means of a subjective method and represents the amount of disparity that cannot be compensated sensorially by the visual system. These definitions imply that there is a mechanism, maybe related with the fusion itself, able to modify the retinal correspondence in order to compensate the misalignment of the visual axes and avoid the diplopia preserving the depth perception. Jaschinski calls the effect of this mechanism Shift in Retinal Correspondence (SRC) and defines it using the expression in equation 5. This means that once the eyes are misaligned the brain tries to compensate it modifying the retinal correspondence to some extent and the amount of FD not compensated can be measured with the subjective methods (Jaschinski et al. 2010).

Equation 5

$$SRC = -(OFD - SFD)$$

Objective measurements are more interesting than the subjective measurements if we consider the fixational movements. Due to these involuntary movements, the visual axes cannot keep their position over time. Fixational movements can be classified in the following types (Ditchburn & Ginsborg 1953, Martínez-Conde et al. 2004, Otero-Millan et al. 2014):

- Microsaccades: with frequency between 1 to 3 Hz and mean amplitude of 0.5 degrees. Usually microsaccades are conjugated and some authors think that can compensate vergencial errors (Collewijn & Kowler 2008). The target itself can influence the ratio of microsaccades, as target size increases the number of microsaccades diminishes (Steinman 1965).
- Drifts: this type of movements shows a small amplitude, from 3 to 15 minutes of arc (Martínez-Conde et al. 2004, Otero-Millan et al. 2014). Drifts happen between microsaccades while the eye is trying to fixate on the target. These slow movements are the results of different mechanisms (optokinetic, pursuit, vergencial, vestibule-ocular reflex and neural noise) (Otero-Millan et al. 2014).
- Tremors: these movements are characterized by high temporal frequency, up to 90 Hz, and low amplitude, less than 1 min of arc (Martínez-Conde

2004, Otero-Millan 2014). Little is known of these movements; spectral analysis reveals a degree of synchronization between eyes (Spauschus et al. 1999).

-Torsions: these movements rotate the eye up to 3 degrees, can be conjugated and non-conjugated. Binocular summation plays an important role improving the fixation stability in comparison to monocular viewing (González et al. 2012).

The influence of these movements over the FD cannot be measured using the subjective tests, but using objective methods we can collect information about some of these types of movements. Previous studies using infrared eye-trackers did not provide information about the dynamic measurements (Kirkby et al. 2013, De Luca et al. 2009).

2.2. Experimental development

2.2.1. Mathematical development

The FD is the addition of the two angles α_r and α_l (equation 6). Following the nomenclature in figure 14, each α can be calculated as the angle β minus the angle γ equations 7 and 8. The angle beta is formed by connecting the gaze position with the rotation centre and with the projection of the rotation centre over the fixation plane. The angle gamma is formed by the triangle connecting the fixation point,

the rotation centre of the eye and the projection of the rotation centre. Because these two triangles are rectangular triangles the calculation of the desired angles is simple. Equation 9 is the final expression for calculating the FD using only the values that can be measured. Two assumptions have been made. First, the line of sight (line connecting the centre of the pupil and the fixation point) and the visual axis (line connecting the nodal point of the eye with the fixation point) are the same (Chang 2011). Second, the baseline (line connecting the rotation centres of the eyeballs) and the interpupillary distance for far distance vision are the same, in fact, for the viewing conditions the difference is less than the absolute error of the measurement (1 mm).

Equation 6	$FD = \alpha_r + \alpha_l$
Equation 7	$\alpha_r = \beta_r - \gamma_r$
Equation 8	$\alpha_l = \beta_l - \gamma_l$ $\beta_r - \gamma_r = \arctan\left(\frac{d_r - c_r}{D}\right) - \arctan\left(\frac{d_r}{D}\right)$ $\beta_l - \gamma_l = \arctan\left(\frac{d_l - c_l}{D}\right) - \arctan\left(\frac{d_l}{D}\right)$
Equation 9	$FD = \left[\arctan\left(\frac{d_r - c_r}{D}\right) - \arctan\left(\frac{d_r}{D}\right) \right] + \left[\arctan\left(\frac{d_l - c_l}{D}\right) - \arctan\left(\frac{d_l}{D}\right) \right]$

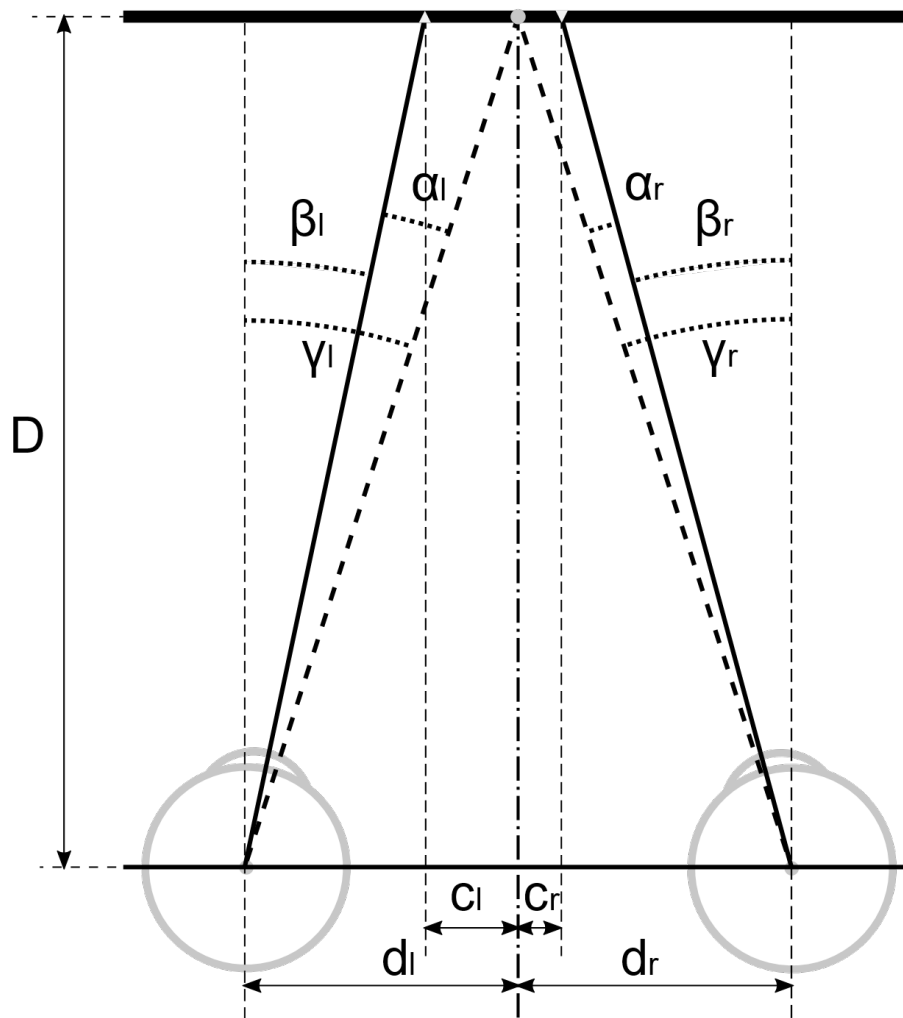


Figure 14 Scheme with the nomenclature used in the mathematical development

2.2.2. Participants

Fifteen subjects participated in this study. Their ages were between 21 to 33 years old. The inclusion criteria were to achieve a monocular visual acuity (VA) logMar of 0.0 or better without glasses or with their contact lenses, their phorias (assessed using the cover test and the prism bar) for far and near distance had to

be in the norm range. The exclusion criteria were to show a manifest deviation of the visual axes (tropia), more than one dioptre of anisometropia, amblyopia or alterations in the transparency of the optical structures. All participants underwent an optometric screening and slit lamp examination.

2.2.3. Stimuli

The stimulus consisted on a central fixation point surrounded by four calibration points. Following this design two different stimuli were generated, one with white background and black symbols, the other with black background and white symbols.

2.2.4. Apparatus

The Web Cam Eye-tracker (annex II) was used to record video sequences of both eyes simultaneously while the subject was fixating on the target over a period of 45 seconds, in these experimental conditions the video sequence was captured at a framerate of 7.33 ± 1.88 fps. The stimuli were displayed on a 16-inch CRT computer display (Phillips®, 109E5), with a resolution of 1280 per 1024 pixels and a luminance of 80 cd/m^2 . The display was placed in front of the subject, at 1 m. The video was recorded using the video capture tools integrated with Matlab®.

2.2.5. Procedure

Volunteers were informed about the nature of the experiment. During the optometric screening the interpupillary distance was taken. If the patient met the inclusion criteria the procedure of the test was explained using a sample of the stimulus printed on paper. The subject sat on a chair with adjustable height and rest on the chinrest. In front of the chinrest and slightly below the line of sight the webcam was centred respect to the nose.

The measurement consisted of three steps. First the calibration step, second the fixation step and finally another calibration step. Both calibration steps were exactly the same, the subject had to stare to every calibration point for three seconds. Starting with the upper left point and finishing at the lower left point. The fixation step consists in to fixate the central point for 45 seconds. After the video recording the sequence was analysed using an own Matlab© code to determine the gaze positions for every frame and using the equation 5 to calculate the FD.

The order of the stimulus was randomised. Both measurements were recorded in one session, before the first measurement a fifteen-minute adaptation time was completed in order to adapt to the illumination inside the laboratory.

2.3. Results

2.3.1. Black symbols on white background

The distribution of the FD was analysed using the Lilliefors test implemented in Matlab®, for all the subjects the null hypothesis was rejected at the 5% significance level. The p-values were all inferior to 0.001, except for subject 9 which showed a p-value of 0.0014. The statistical summary of the measurements is shown in table 3 and a boxplot per subject is represented in figure 15.

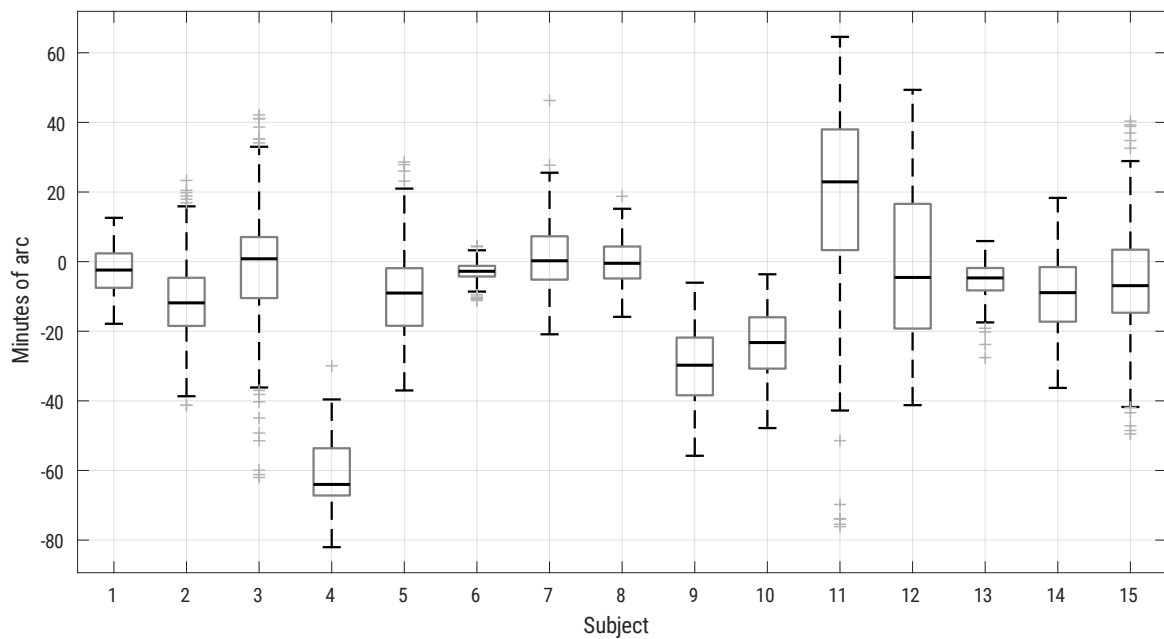


Figure 15 Boxplot of the FD per subject

Subject	Median	IQR
1	-2.42	9.89
2	-11.85	13.83
3	0.82	17.53
4	-64.01	13.57
5	-9.03	16.56
6	-2.77	3.05
7	0.24	12.45
8	-0.48	9.18
9	-29.75	16.58
10	-23.25	14.75
11	22.92	34.68
12	-4.55	35.82
13	-4.68	6.44
14	-8.92	15.69
15	-6.91	18.12

Table 3 Summary of the measurements per subject.

The average median was -4.68 minutes of arc with an interquartile range of 14.75 minutes of arc. When looking to the evolution of the FD value over time different patterns are recognised. Positive, negative trends, and convergent, divergent trends. To set the overall trend, a linear regression model was fitted to all the data (equation 10), the value of m determines the trend. To analyse the convergent or divergent trend of the data, the maximum and the minimum values were detected and two straight lines were fitted to each subgroup. The results for all the fits appear in table 4. The meaning of positive trend is that the FD tends to reduce its negative value, which is, the visual axes are crossing behind the stimulus and tend to increase their convergence over time. The negative trend

means that the visual axes reduce its convergence over time. The convergent trend of the maxima and minima means that the oscillations of the FD values diminish over time while the divergent trend is the opposite. The number of subjects per trend appears in table 5. Examples of the patterns are shown in figures 16 and 17.

Equation 10

$$FD = m * t + n$$

	All data			Maxima			Minima		
Subject	m	n	R ²	m	n	R ²	m	n	R ²
1	0.26	-8.50	0.14	0.14	2.44	-0.04	0.39	-18.88	0.30
2	0.10	-13.08	-0.08	-0.27	11.13	0.04	0.49	-40.30	0.17
3	-0.30	11.63	0.45	-0.79	34.48	0.42	0.33	-18.36	-0.03
4	-0.13	-58.40	-0.07	-0.08	-51.63	-0.16	-0.12	-67.36	0.18
5	0.29	-16.33	-0.08	0.17	4.80	0.04	0.28	-35.49	0.03
6	-0.01	-1.77	0.48	-0.04	4.01	0.02	0.14	-15.21	-0.13
7	-0.28	7.98	0.19	-0.62	32.93	0.15	0.03	-19.62	-0.21
8	-0.25	4.90	0.10	-0.34	15.67	0.22	-0.15	-5.96	0.02
9	-0.48	-18.76	0.01	-0.42	0.04	0.46	-0.34	-44.95	0.26
10	-0.34	-15.52	-0.06	-0.25	0.82	0.57	-0.23	-41.17	0.17
11	0.13	29.64	-0.06	0.00	57.05	0.57	-0.07	-36.44	0.45
12	-1.06	19.17	0.20	-1.04	40.02	0.20	-0.87	-0.70	0.18
13	0.05	-5.28	0.15	-0.04	5.51	-0.14	0.29	-23.59	0.00
14	0.25	-14.76	-0.08	0.20	7.62	-0.10	0.26	-38.01	0.04
15	-0.68	12.05	0.30	-0.79	30.58	0.35	-0.66	-5.22	0.14

Table 4 Values for the model in equation 10 and the coefficient of determination. Please note that a negative coefficient of determination implies that a m value of 0 fits better than the actual value for m.

Trend	Positive	Negative	Convergent	Divergent
Number of subjects	6	9	13	2

Table 5 Number of subjects for each pattern.

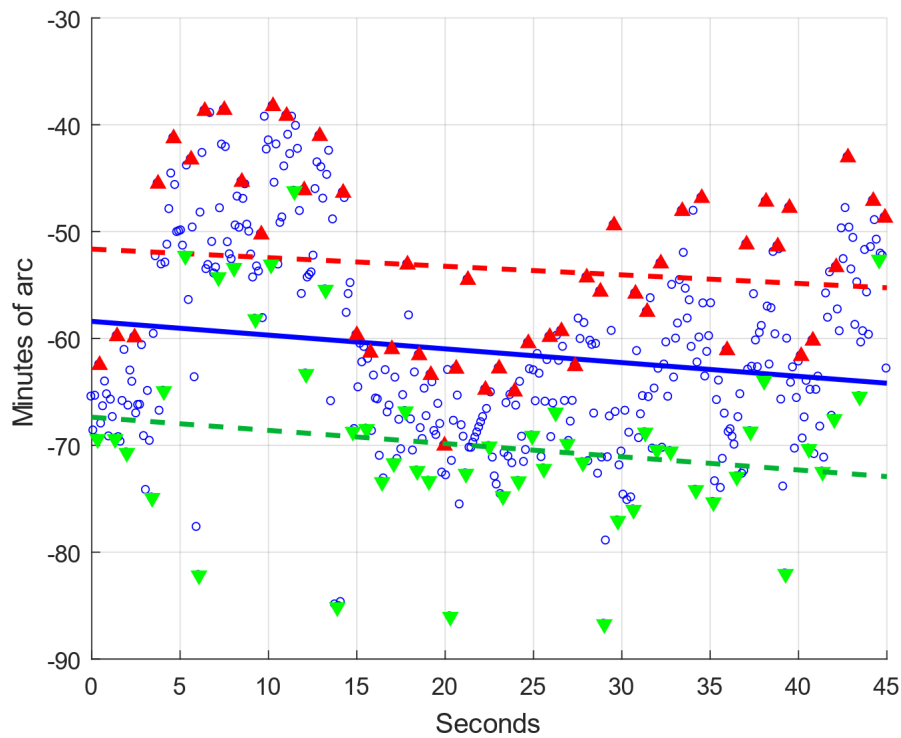


Figure 16 Example of negative and divergent trend. Blue circles are the measurements, the blue line is the fitted linear regression model for all the measurements, red triangles are the local maxima, the red dashed line the fitted linear model for the maxima, green triangles are the local minima and the green dashed line the fitted linear model for the minima.

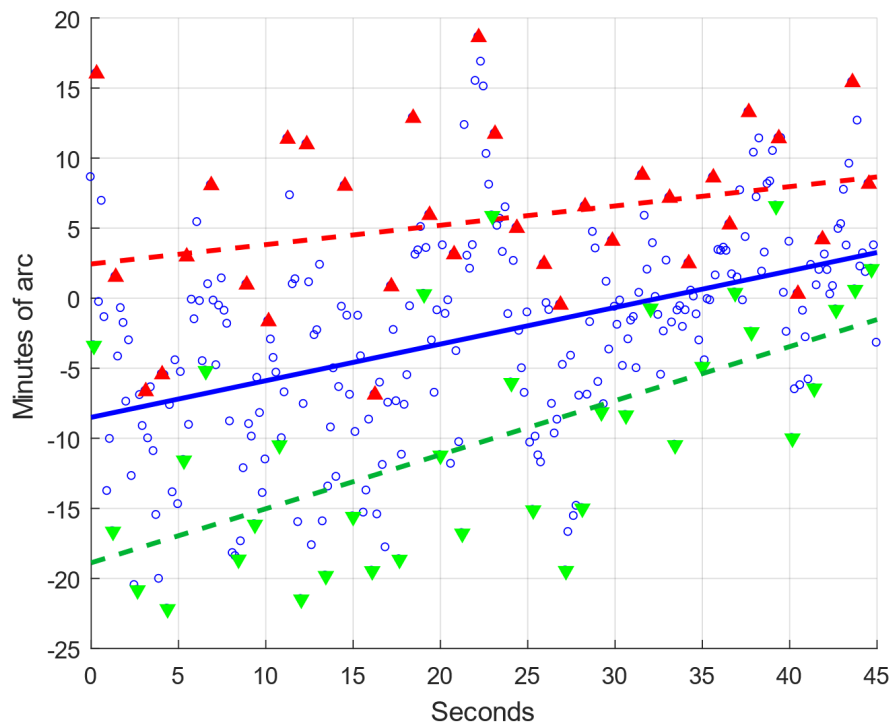


Figure 17 Example of positive convergent trend

2.3.2. White symbols on black background

The distribution of the FD was analysed using the Lilliefors test implemented in Matlab®, for all the subjects, except for subject 12, the null hypothesis was rejected at the 5% significance level. The p-values were all inferior to 0.001, except for subjects 12 and 14 which showed a p-value of 0.1102 and 0.0172 respectively. The statistical summary of the measurements is shown in table 6 and a boxplot per subject is represented in figure 18.

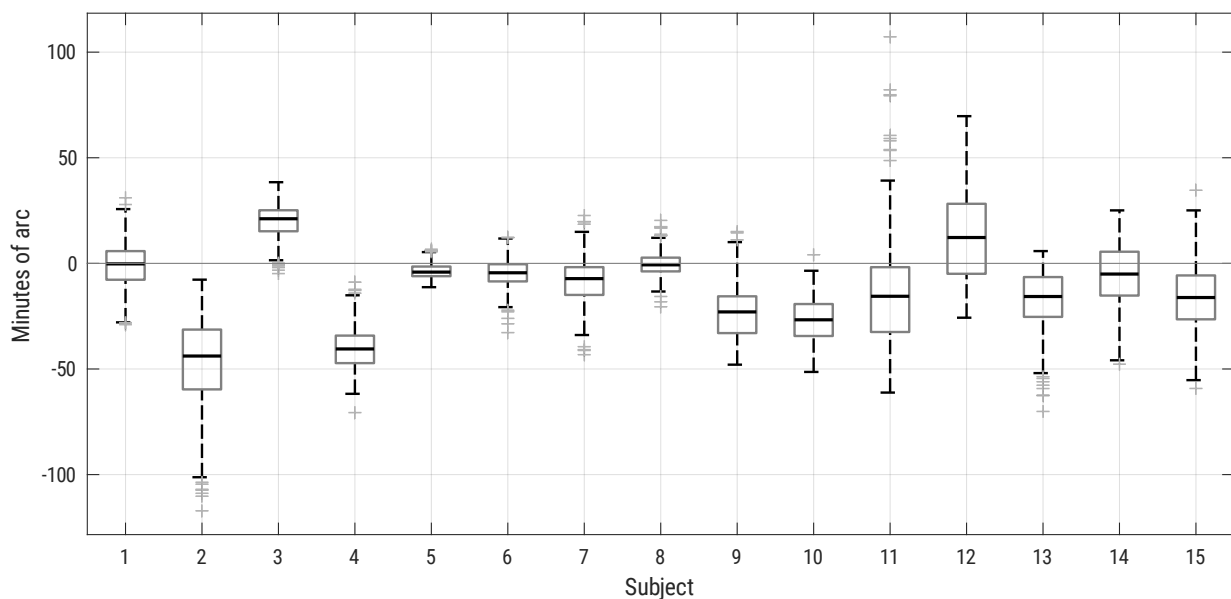


Figure 18 Boxplot of the FD per subject

Subject	Median	IQR
1	-0.24	13.56
2	-43.86	28.32
3	21.13	9.94
4	-40.51	13.03
5	-4.13	4.56
6	-4.45	8.13
7	-7.22	13.15
8	-0.69	6.51
9	-22.98	17.41
10	-26.71	15.13
11	-15.57	30.68
12	12.25	33.14
13	-15.69	18.85
14	-5.05	20.76
15	-16.17	20.77

Table 6 Summary of the measurements per subject.

The average median was -7.22 minutes of arc with an interquartile range of 15.13 minutes of arc. The dynamic analysis shows a different distribution of the previously explained patterns.

Subject	All data			Maxima			Minima		
	m	n	R ²	m	n	R ²	m	n	R ²
1	0.16	-4.95	-0.10	0.45	9.48	0.09	-0.18	-18.27	-0.10
2	-0.05	-31.78	0.06	-0.37	3.58	0.36	-0.72	-75.64	0.08
3	0.09	18.87	0.08	0.04	27.57	0.18	0.11	-9.37	-0.12
4	-0.10	-37.88	-0.01	0.01	-19.30	-0.15	0.01	-53.25	-0.02
5	-0.13	-1.30	0.05	-0.22	6.90	0.20	-0.03	-9.36	-0.01
6	-0.13	0.38	-0.04	-0.27	13.43	0.41	-0.05	-13.35	0.07
7	0.04	-8.89	-0.03	-0.33	18.31	-0.09	0.71	-44.61	0.34
8	-0.17	3.70	0.10	-0.24	13.58	0.37	-0.09	-8.48	-0.09
9	-0.43	-14.67	-0.07	-0.26	7.40	0.44	-0.27	-39.92	0.03
10	-0.10	-25.93	-0.14	-0.13	-2.29	0.05	-0.15	-44.97	0.29
11	0.20	-35.90	0.24	0.04	-14.44	0.56	0.47	-62.04	-0.02
12	0.33	4.36	-0.09	-0.27	46.73	-0.12	0.69	-26.15	0.26
13	0.03	-13.92	-0.12	0.02	8.33	0.14	-0.07	-39.51	0.04
14	0.28	-12.39	-0.10	0.02	19.37	0.06	0.32	-36.94	0.09
15	-0.07	-12.04	-0.04	-0.40	17.34	0.06	-0.09	-38.09	-0.20

Table 7 Values for the model in eq 5 and the coefficient of determination. Please note that a negative coefficient of determination implies that a m value of 0 fits better than the actual value for m.

Trend	Positive	Negative	Convergent	Divergent
Number of subjects	7	8	9	6

Table 8 Number of subjects for each pattern.

2.3.3. Differences between both designs

The distribution of data reported in tables 4 and 6 was determined with the Lilliefors test. The results were a p-value of 0.01 for the medians of the measurements under the B design and a p-value of 0.5 under the W design. Because of this difference in distribution, in order to analyse both groups, a Kruskal Wallis test was performed. The p-value was 0.6632, rejecting the differences between both conditions that can be seen in figure 19.

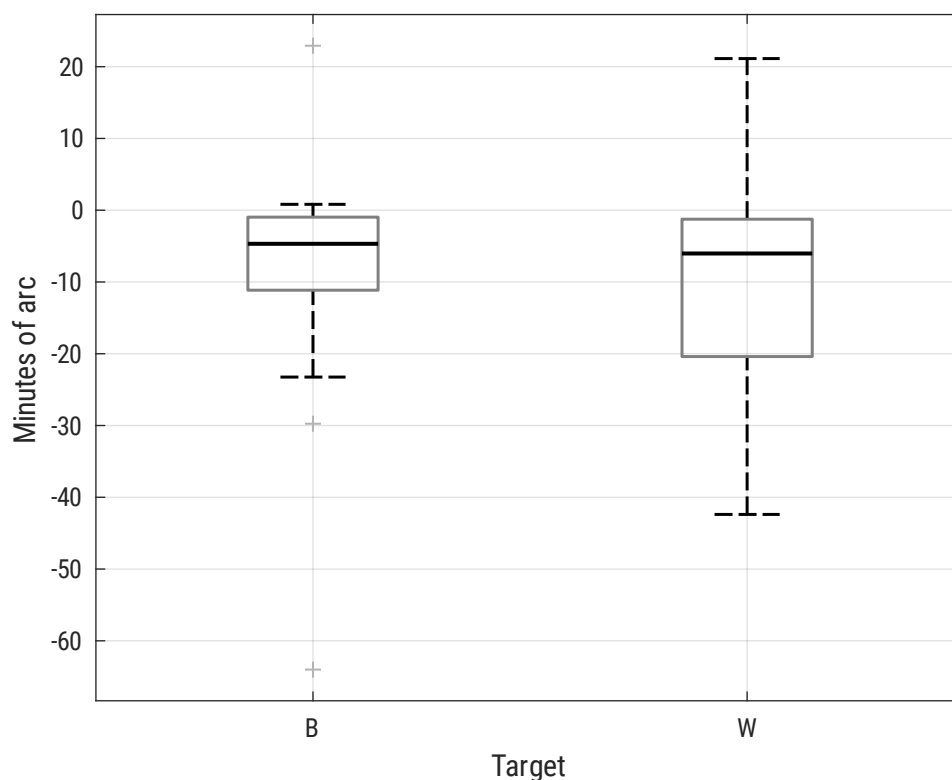


Figure 19 Boxplot of the median of the measurements for each design

2.4. Comparison with other systems

When comparing with other studies it is necessary to differentiate the type of FD that is being measured, the SFD or the OFD. Hebbard (Hebbard 1962) using a scleral lens with a mirror obtained the first OFD measurements. He reported measurements closer to zero with really small dispersion in comparison to the ones reported in this thesis and those reported by other researchers. For a measurement of 37.5 seconds, the mean value for the FD was 8.7 minutes of arc with a range of values between 8.3 to 9.1 minutes of arc.

Remole (Remole 1985) using an objective psychophysical procedure based on the border enhancement effect derived of the change in the neurophysiological structure of the retina with the eccentricity also reports values compatible with ours.

Fogt (Fogt & Jones 1998) used scleral coils to determine the variations in the horizontal position of both eyes at the same time, but they combined an anaglyph test to determine the SFD. Their results of the SFD and OFD are quite similar to the ones reported previously for the OFD.

De Luca (De Luca et al. 2009) developed a different approach using infrared eye-trackers. Nevertheless, he took measurements with one subject but he do not provide any information about the results except from the mean value and the

range. Using the mean value implies that the distribution of the measurement is normal but no information concerning this aspect is provided. For a viewing distance of 60 cm, 8 out of 12 measurements were in average -7.2 ± 5.4 minutes of arc and 4 out of 12 measurements were in average 11.4 ± 7.2 minutes of arc. Unfortunately De Luca did not report any information about the temporal evolution of the FD. A big difference is found in the methodology. De Luca is not measuring strictly the OFD, in fact, the task for the observer is to align two nonius lines in dichoptic vision, using polarizers and when the subject sees both lines aligned then the eye-tracker determines the actual visual axes position. So, De Luca is measuring the SRC as Jaschinski defined in equation 5. Our method measures the OFD under natural viewing conditions, that is an important difference due to the fact that vision, at least the contrast sensitivity and discrimination, depends on the viewing conditions (Meese et al. 2006).

Concerning the experiment conducted by Jaschinski et al. (Jaschinski et al. 2010) our results are in agreement. Despite the fact they did not provide with information about the distribution of the data or the mean values for every measurement, the average result for all the measurements is -6.6 ± 13.9 minutes of arc which is really similar to the average for the B design (-4.68 ± 14.75 minutes of arc) and the W design (-7.22 ± 15.13 minutes of arc). Interestingly, their data show a bigger dispersion for the “long” measurements (15 seconds) than for the short measurements (1.5 seconds), this also agrees with our data. Jaschinski

reports average positive values of disparity and lower dispersion for the SFD than for the OFD, that is in agreement with the results published by De Luca.

Unfortunately, we have not found in the literature studies about the influence of the polarity of the stimulus, being the default for all of them black symbols over white background.

2.5. Conclusions and future work

The developed material and software is a reliable methodology for objective and non-invasive measurement of the FD is reliable, providing a new approach for the study of this optometric parameter under natural vision. As far as we know data on the temporal variation of the OFD has not been published before, and we have described different patterns on the evolution of this parameter over time. Our data reflects the influence of the fixational eye movements on the fixation stability that should not be omitted in the evaluation of the visual function.

As options for future work a wide range of approaches emerge, from the clinical validation of the measurements described in this chapter to the research on the influence of other parameters such as the polarity of the test, the effect of a background with different spatial frequencies, a moving target, effects of blur, FD on the threshold of contrast, etc.

The potential applications of this objective test are: determining the binocular performance of different multifocal contact lenses, studying the asthenopia after near vision work, assessment of multifocal ophthalmic lenses, etc.

Chapter 3

Measurement of the suprathreshold contrast sensitivity with common displays

3.1. Justification

Similar to what has been reasoned about the insufficiency of the VA as a global metric for the vision, the CSF is also not an ideal descriptor. The major drawback of CSF is that it attempts to describe the visual function by measuring thresholds. An example of a real-world task related to the contrast threshold is to differentiate the object from its background. But in general, real images are not pushing the visual system to its limits of performance and most of the contrasts are at a suprathreshold level. A more natural task is to determine the suprathreshold contrast sensitivity, which means to determine the minimum increment of contrast that can be perceived for a pedestal contrast. First data on this kind of measurements was taken by Campbell and Kulikowski (Campbell and Kulikowski 1966).

The suprathreshold discrimination was expected to follow the Weber's law, in a similar way to the discrimination of luminance works (Artigas et al. 1995).

Different studies agree in the shape of the Contrast Discrimination Function (CDF). For low pedestal contrast it shows a dip shape. When increasing the contrast, around the 3%, the relation between the pedestal contrast and the threshold of the incremental contrast in a log representation shows a linear relation. This relation follows the equation 11. As said before, the discrimination of luminance follows Weber's law, in this case the equation for the luminance is equivalent to equation 11 and the value of N is 1. But for the contrast discrimination Legge reported N values lower than 1 (Legge & Foley 1980), other researchers reported similar values around 0.6. The value of N seems to be related to the methodology of the experiment, the adjustment methods (Kulikowski 1976, Kulikowski & Gorea 1978) produce higher values than the 2AFC (Pantle 1974, Pelli 1979). Other factors, such as the adaptation to a previous grating (Kulikowski 1976, Kulikowski & Gorea 1978) also increases the value of N .

Equation 11

$$\Delta C = kC^N$$

To obtain feasible results using psychophysical methodologies implies, in general, to take a large number of repeated measurements. This is the main drawback when trying to implement this kind of tests into a clinical context, the amount of time. For the clinical practice a test has to be simple, short and reliable. Another desirable characteristic would be the cost, as cheap as possible. For these

reasons in this experiment we will develop and test a quick contrast discrimination test using common equipment (an 8-bit computer display).

3.2. Experimental development

A suprathreshold contrast sensitivity test was developed using sine-wave gratings.

3.2.1 Display

A 19 inch Philips 109E5 computer display was used to show the gratings. This is an 8-bit display, with a maximum luminance of 113 cd/m^2 . The characterisation of the display was performed with a CL-200 Chroma Meter (Konica Minolta, Tokyo, Japan) photometer after a 30 minutes period of warm-up time for the display. In order to increase the luminance resolution of the display, a bit-stealing technique was implemented, more information about this can be found in the Annex I. The computer screen was placed at 112 cm in front of the subject.

3.2.2. Stimuli

The stimuli for this test were sine-wave gratings of 2, 4, 8 and 16 cpd inside a square window of 13.5 cm (512 pixels) which subtended 6.87 degrees at the

viewing distance. The pedestal contrasts, following the Michelson definition for contrast, were 0.3, 0.5 and 0.7.

3.2.3. Test

The procedure of the test is a 2AFC design with a modified staircase method. Both squared windows appear at the same time on the display. One is the reference image showing the reference sine-wave grating with the pedestal contrast and the other shows a grating with the same spatial frequency but with a higher contrast, in which of the two windows is shown the reference grating is randomly determined each time. The task for the observer was to determine which grating had a bigger contrast, in case both gratings had the same aspect, it was obligatory to pick one randomly.

After three correct answers the contrast of the test grating was diminished one step. After one incorrect answer the contrast of the test grating was increased one step. The test stopped after five reversals and the incremental contrast threshold was calculated averaging the last four reversals.

The test was done under binocular viewing conditions. The order of frequencies and pedestal contrasts were randomised. The measurement of the four frequencies and the three contrast pedestals for each frequency took for a single observer approximately 20 minutes.

3.2.4. Participants

Fifty-two volunteers participated in this study. With a mean age of 27.15 ± 4.12 years, 25 were women and 27 men. The inclusion criteria were healthy young adults with a VA of 0.0 logMar or better with their habitual correction, with no clinical history of refractive surgery. The exclusion criteria were, a refractive error higher than 3 dioptries of myopia or hyperopia, more than 0.75 dioptries of astigmatism, more than 1 dioptre of anisometropia and being under any medical treatment. Those patients who need prescription wore their habitual glasses or contact lenses.

3.3. Results

The data distribution for each combination of frequency and pedestal contrast was tested with the Lilliefors test, the p-values are showed in the table 9.

		Frequency (cpd)			
		2	4	8	16
Pedestal contrast	0.3	0.012	0.001	0.006	0.001
	0.5	0.001	0.001	0.001	0.001
	0.7	0.001	0.001	0.001	0.001

Table 9 p-values of the Lilliefors test for every combination of frequency and pedestal contrast.

A boxplot of the incremental contrast threshold is represented in figure 20. As can be noticed, the incremental threshold increases between the pedestal

contrast 0.3 to 0.5 and diminishes between the pedestal contrast 0.5 to 0.7. The average values of the incremental contrast threshold appear in table 10.

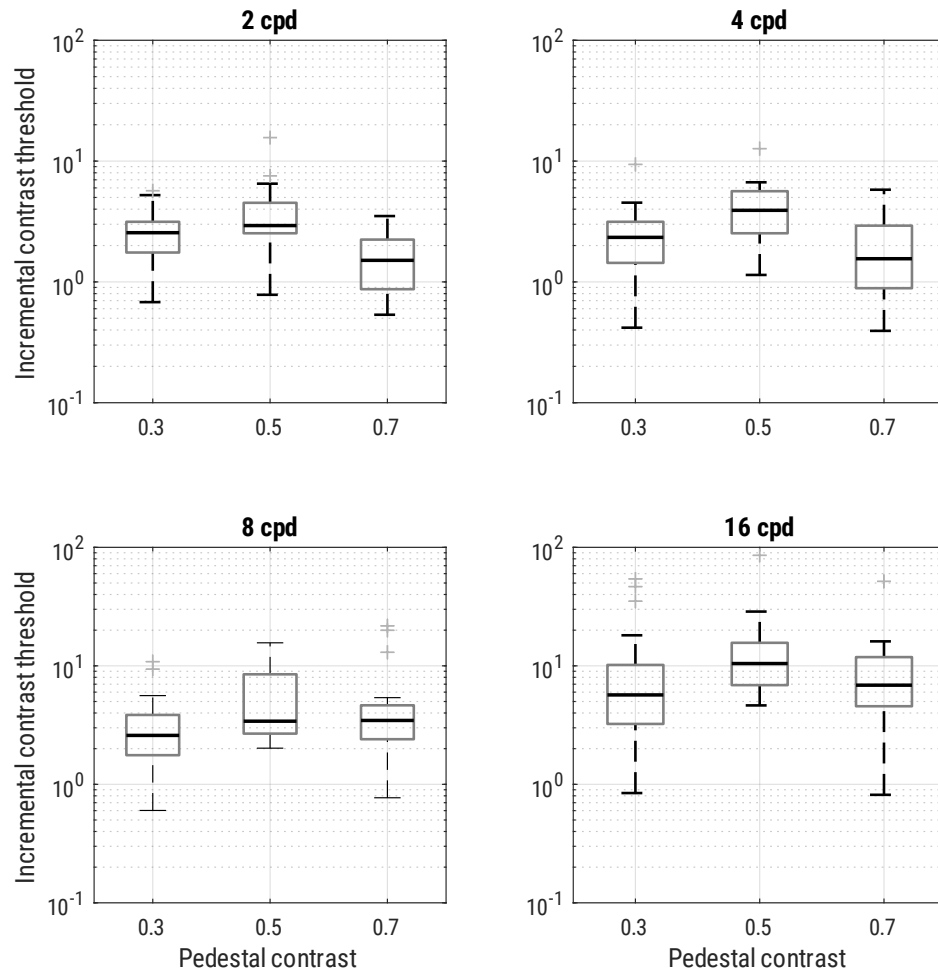


Figure 20 Boxplot of the incremental threshold VS pedestal contrast for every frequency.

		Frequency (cpd)			
		2	4	8	16
Pedestal contrast	0.3	2.55	2.34	2.59	5.68
	0.5	2.93	3.91	3.41	10.46
	0.7	1.51	1.56	3.46	6.87

Table 10 Median of the incremental contrast threshold.

3.4. Comparison with other studies

When comparing to previous studies the incremental thresholds up to 0.5 of contrast pedestal are in agreement with previous reported results. Results for the pedestal contrast of 0.7 are in disagreement with the proposed model in equation 11. This can be related to differences in the methodologies but also is due to the fact that the majority of the researchers have not measured the contrast discrimination far beyond a pedestal contrast of 0.5 (Campbell & Kulikowski 1966, Legge 1981, Legge & Foley 1980, Pantle 1974, Pelli 1979, Kulikowski 1976, Kulikowski & Gorea 1978, Barlow et al. 1976) and have assumed that the model is correct for higher contrasts. But Kingdom and Whittle (Kingdom & Whittle 1996) measured it for 0.1, 0.5 and 0.9 pedestal contrasts and reported the same effect with values in the same range. When trying to adjust the model to all the data, as it is evident, the values of the exponent are considerably low. But when doing the same adjustment with the values up to 0.5 of pedestal contrast the calculated exponents were in agreement with the literature (values between 0.3 and 0.9) except for 16 cpd, but we have not found previous values for this frequency.

The mean exponent values and deviations are in table 11 and a graphical representation appears in figure 20. The high variability between observers is attributed to the fact that the observers were not familiar with contrast sensitivity tests and the psychophysical methodology so they did not follow a constant criterion in their answers.

	Frequency (cpd)			
	2	4	8	16
Mean	0.488	0.794	0.818	1.846
Deviation	1.193	1.267	1.338	1.661

Table 11 Exponent values for the model in equation 11.

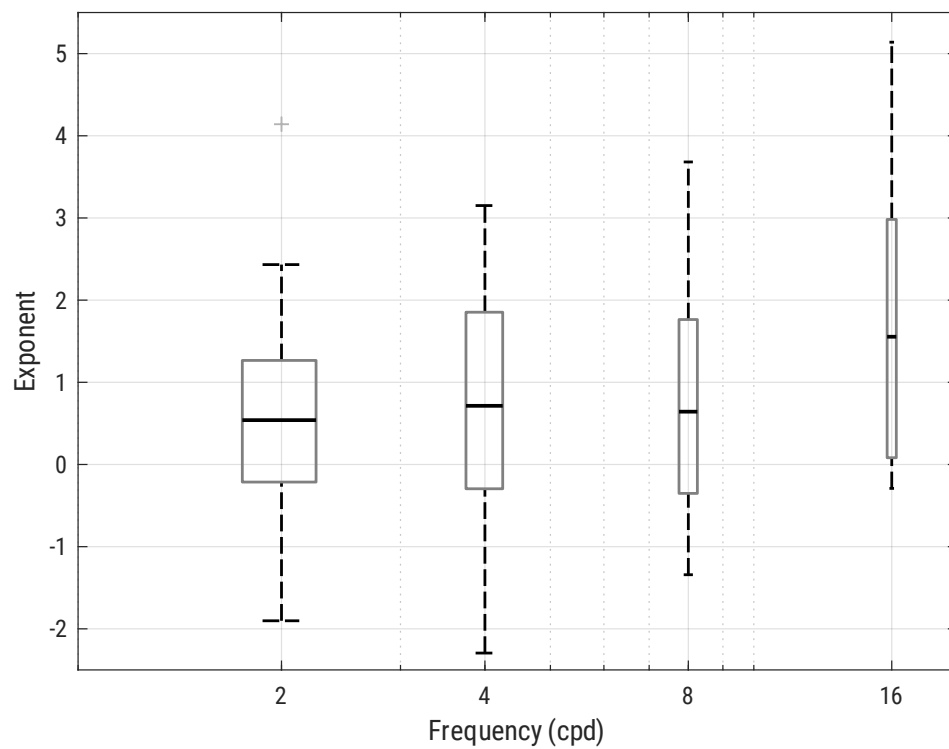


Figure 21 Boxplot of the exponents calculated for every subject

Figure 22 shows a representation of the linear part of the model in equation 11, for all the subjects and the median value.

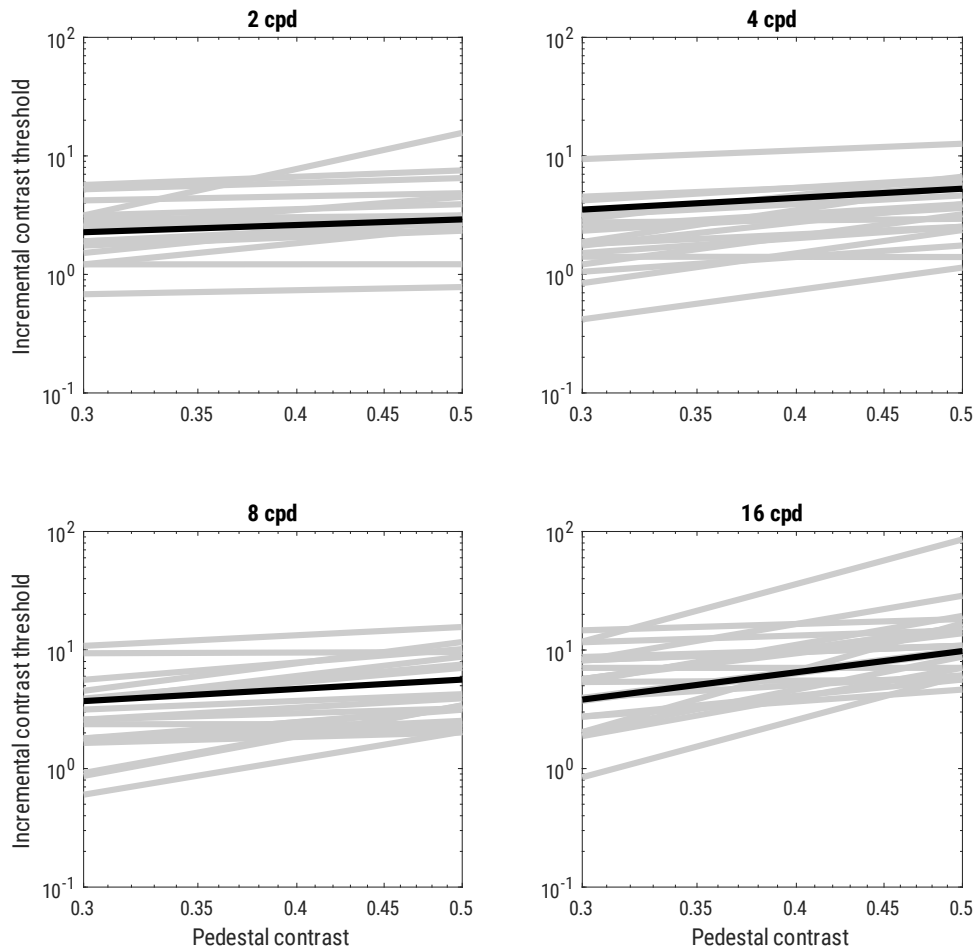


Figure 22 Adjusted model for the linear range of contrast, in grey for all the subjects and in black the mean exponent value.

The exposure time has to be considered as well, in fact, as Pons reported (Pons 1997), the value of N is modified by this parameter, increasing as the exposure time increases, this can be seen in figure 23 for frequencies higher than 0.5 cpd.

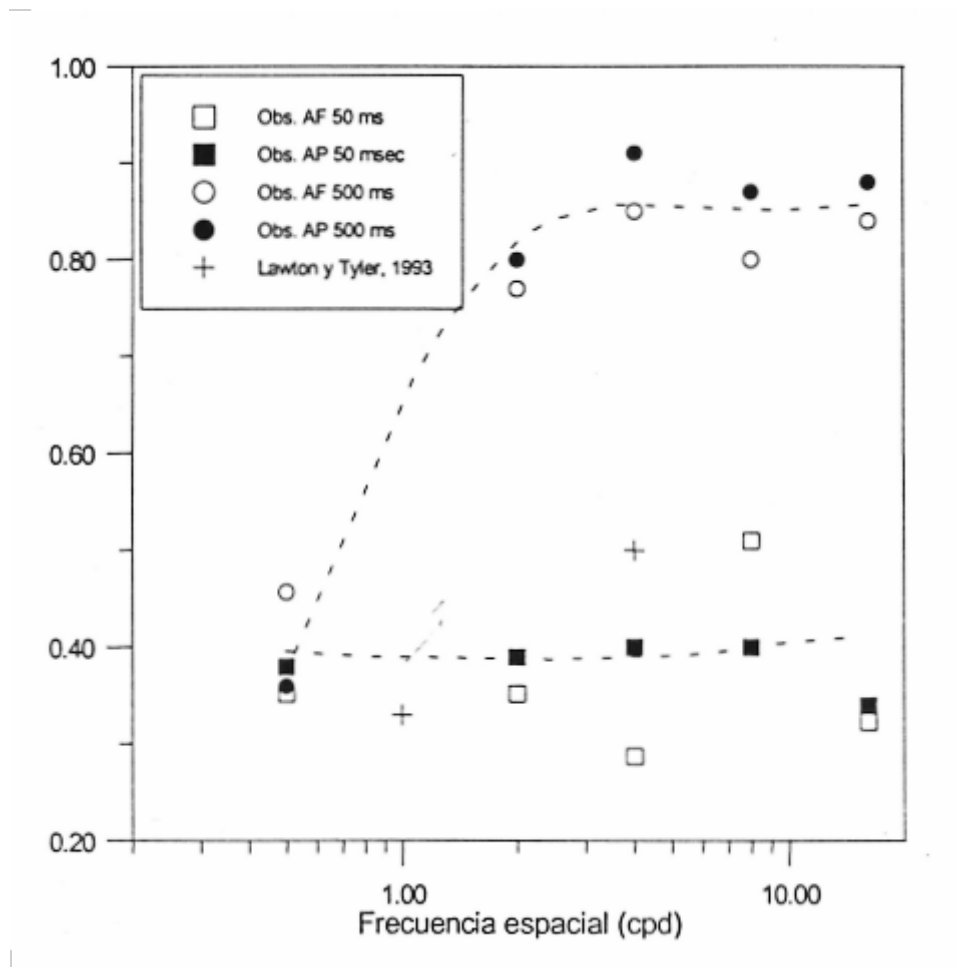


Figure 23 Effect of exposure time on the value of the exponent in equation 11. From Pons 1997.

3.5. Conclusions and future work

The conclusions of this work are that common 8-bit equipment can be used for sensitivity measurements when implementing a bit-stealing technique to increase the luminance resolution of the graphics card and the display. This is a

key point for implementing existing tests and new designs with low-cost equipment in comparison to the 10-bit and 12-bit hardware. Another conclusion from our data is that the power law for the suprathreshold discrimination may be not correct for pedestal contrasts higher than 0.5 as other researchers have shown.

In the near future we expect to adapt the present test to a portable device such as a tablet, that will help in the clinical evaluation of the described methodology in this chapter.

Chapter 4

Peripheral contrast sensitivity under natural binocular viewing

4.1. Justification

The CSF has been studied in depth for central vision (Campbell & Green 1965, Barten 1999, Virsu & Rovamo 1979, Thibos et al. 1987). But the central vision, being necessary, is not sufficient for a normal level of functionality or good satisfaction (Ramrattan et al. 2001). In fact, the central and near periphery vision because their high VA are crucial for high level tasks such as reading (Rayner & Bertera 1979, Osaka 1987) but not for other routine and semiautomatic tasks as walking (Turano et al. 1999, Turano 2004). The near periphery has an active role in reading. While reading the eye is not foveating every single letter, it stops in key points and determines which point is the next to foveate. The next saccade will place that point of interest in the fovea, the reading is controlled, then, by means of a mechanism that uses the visual information around the fovea (Ikeda & Saida 1978, Legge et al. 1989, Rayner 1998).

As has been showed in the introduction, sine-wave gratings are good stimuli for measuring the contrast sensitivity. Generally, the grating is showed

inside a circular patch whose edges are smoothed by a Gaussian, this is known as a Gabor patch. For the peripheral regions the classical experiments (Virsu and Rovamo 1979, Johnston 1987, Thibos et al. 1987) chose to use the Gabor stimulus and an external fixation point. The position of the fixation point in relation to the stimulus determines the peripheral angle that is being tested. This configuration is useful to test the asymmetries in sensitivity along a retinal direction due to the asymmetrical distribution of ganglion cells (Goodchild et al. 1996, Curcio & Allen 1990), but is not representative of the natural viewing conditions. Under binocular viewing, this design will stimulate corresponding areas, but those areas show a different contrast sensitivity. It would be more interesting to stimulate symmetrical areas at the same time. Another question arises, what is the effect of the fixation point in the sensitivity? Summers (Summers & Meese 2009) studied the influence of different configurations of a fixation target on the contrast sensitivity for central vision and demonstrated that the fixation target generates a masking effect that reduces sensitivity when the number of cycles per image is small.

For these reasons, we decided to measure the contrast sensitivity for the foveal, the perifoveal and the near periphery using concentrically rings and checking the possible effects of the presence of the fixation target on the contrast sensitivity for the foveal and perifoveal areas.

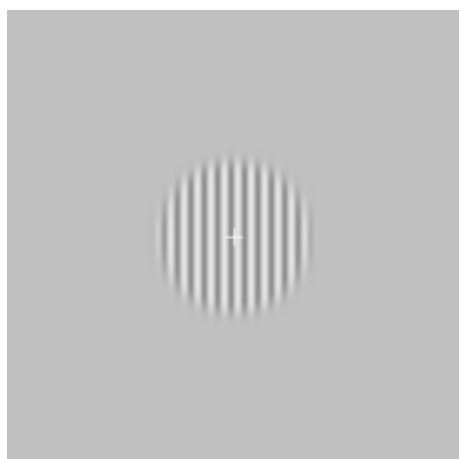
Polyak (Polyak 1941) divided the retina in regions, assigning to the fovea a diameter of 5.2 degrees, to the perifovea a diameter of 8.6 degrees and to the perifovea a diameter of 19 degrees. For Polyak the peripheral retina starts at 14.5 degrees from the foveola.

4.2. Experimental development

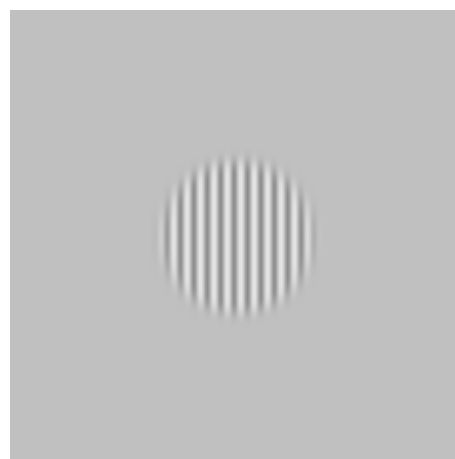
A 24 inch 8-bit per channel backlit led computer display was placed 50 cm in front of a chinrest, at this distance the display subtended 30.5 degrees. The maximum retinal region that could be tested was up to 15 degrees. Trying to match what Polyak considers peripheral retina the radii for the biggest ring was set to 14 and 15 degrees. The radii for the other stimuli were chosen to match the same area than the peripheral ring. This implies a radius of 5.61 degrees for the foveal patch, this radius comprises Polyak's foveal and perifoveal regions. An intermediate ring was generated with radii of 8.33 and 10 degrees, this can be considered as perifoveal region. Radii are summarized in table 12.

Region	Foveal circle	Perifoveal ring	Near periphery ring
Degrees	5.61	8.33 to 10	14 to 15

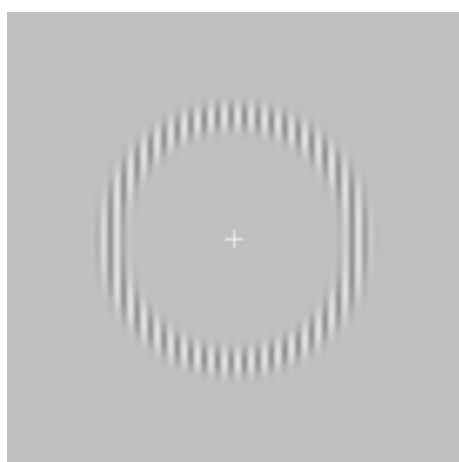
Table 12 Radii in degrees for each retinal zone.



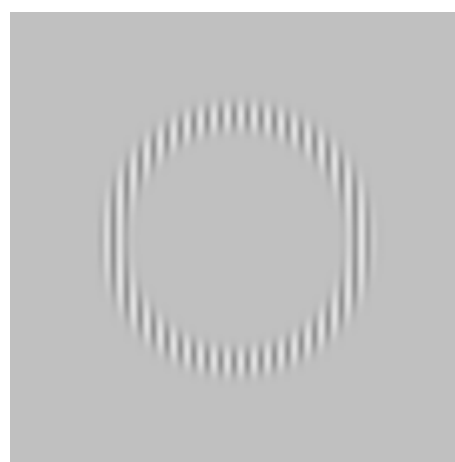
Foveal stimulus with fixation target



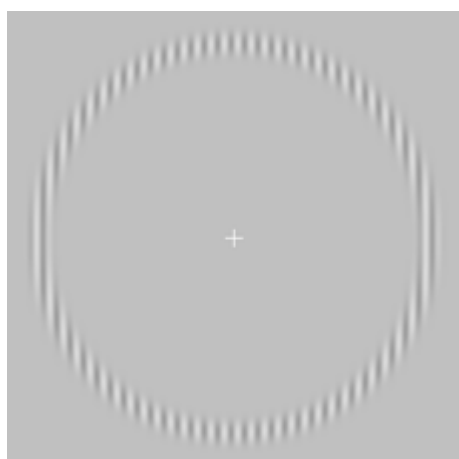
Foveal stimulus without fixation target



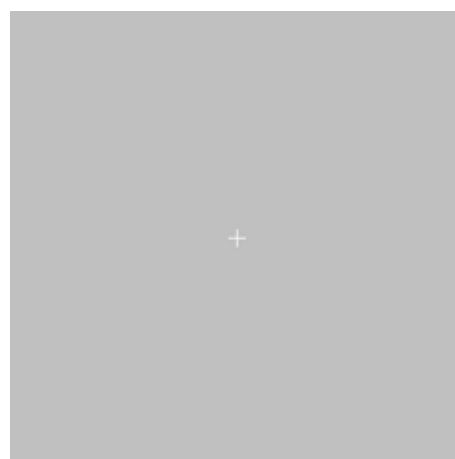
Perifoveal stimulus with fixation target



Perifoveal stimulus without fixation target



Near periphery stimulus with fixation target



Reference image with fixation target

Figure 24 Examples of the different designs

Vertical sine-wave gratings of 0.5, 1, 2, 4, 6 and 8 cycles per degree were used. The mean luminance for all the gratings was 40 cd/m^2 . The area outside the grating was filled with a grey of the mean luminance. In order to increase the luminance resolution of the display a bit-stealing technique was implemented, more information about this can be found in the Annex I. The contrast step, using the Michelson definition, was 0.000495.

The fixation target was a white cross placed in the centre of the screen. The cross was 36 pixels wide and 3 pixels of thickness, which is equivalent to 1.123 and 0.094 degrees of visual angle. To check the effect of the cross on the sensitivity the foveal and perifoveal stimuli were generated with the target and without the target, the near periphery ring was generated only with the fixation target due to the difficulty to maintain the stability of the gaze in the centre of the ring without any visual aid. Examples are shown in figure 24.

The test consisted in showing first the test image for 500 ms followed by the reference image (with the mean grating luminance) for another 500 ms. For the stimuli with the fixation target the cross was placed in the centre of the stimulus, which is the centre of the display, for both the reference and the test image. The task for the observer was to keep the eyes fixating in the centre of the stimulus and press the spacebar in case they perceived a difference between the test and the reference image, any other key to indicate a negative answer. After 15 seconds without any key pressed the algorithm considered it as a negative answer. A modified staircase method was used (Leek 2001). After three consecutive

detections the contrast of the grating was reduced one step, after one negative answer the contrast was increased one step. The test finishes after five reversals and the threshold value is averaged from the last four reversals. The experiment was conducted in a laboratory under total darkness, except for the light emitted by the computer display.

Four young adults, three men and one woman, participated in this pilot study. The mean age was 30 years old, with a range from 26 to 32. The inclusion criteria were healthy young adults with experience in psychophysical tests with a monocular visual acuity of 0.0 logMAR or better and a refractive error close to emmetropia (range between 0.5 dioptries of myopia to 0.5 of hyperopia and up to 0.5 dioptries of astigmatism) and an accommodation capacity of more than 2 dioptries. Exclusion criteria were a history of eye surgery, any kind of illnesses, to be under a drug treatment up to two weeks before the measurements and any problem with respect to the tear film, cornea and/or pupil size. Subjects were informed by the experimenter about the nature and possible consequences of the experiment. The tenets of the Declaration of Helsinki were followed in this research. Before the experiment subjects had to adapt to the low light conditions of the laboratory for 15 minutes.

4.3. Results

4.3.1 Effect of fixation target

The averaged sensitivities for the four combinations of areas and presence of target are shown in figure 25, table 13 contains the plotted values.

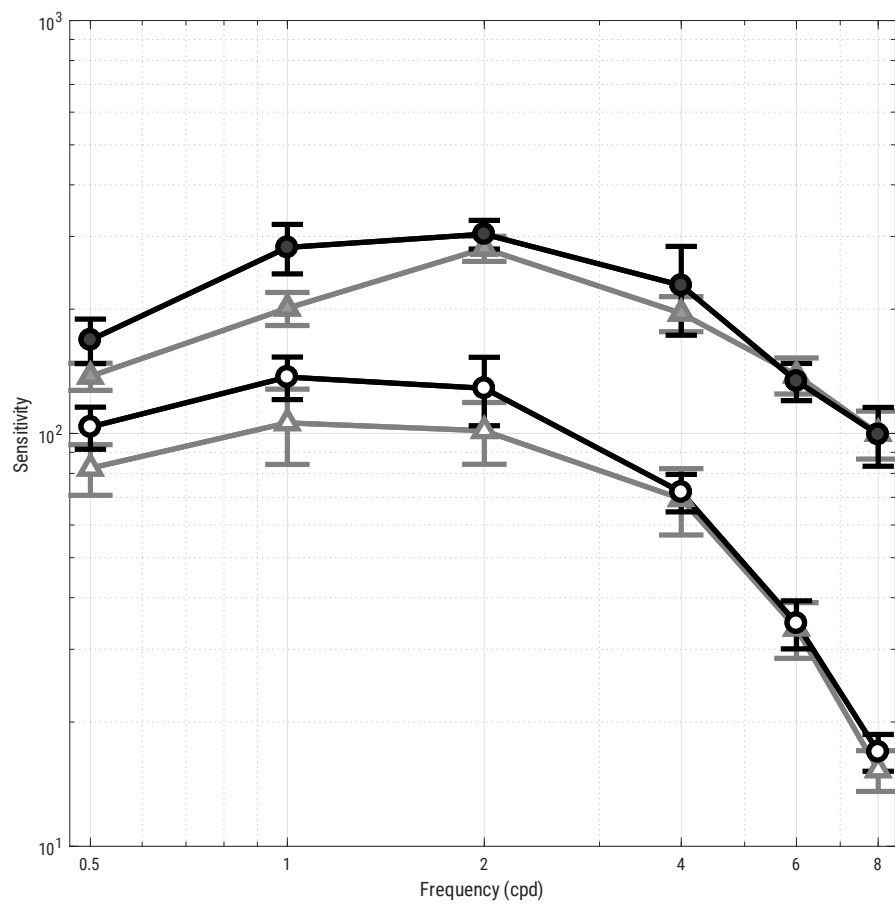


Figure 25 Mean contrast sensitivity. Solid markers for the foveal region, open markers for the perifoveal. Circles for the test without the fixation target, triangles for the test with the fixation target.

	With the fixation target				Without the fixation target			
	Foveal		Perifoveal		Foveal		Perifoveal	
Frequency (cpd)	Mean	Standard error	Mean	Standard error	Mean	Standard error	Mean	Standard error
0.5	138	10.39	82	11.55	168	20.79	104	12.12
1	201	18.48	106	21.94	282	38.68	137	16.17
2	281	19.63	102	17.32	304	24.25	129	24.25
4	195	19.05	69	12.70	228	55.43	72	7.51
6	138	13.86	34	5.20	134	13.86	35	4.62
8	100	13.28	15	1.73	99	16.17	17	1.73

Table 13 Average sensitivity for the different combinations.

Results show a reduction in the sensitivity when testing the same retinal area depending only on the presence of a fixation target, being higher for the “without the fixation target” condition. This effect is more noticeable in low spatial frequencies as can be seen on figure 26. The loss in sensitivity is noticed both in the foveal area and in the perifoveal area.

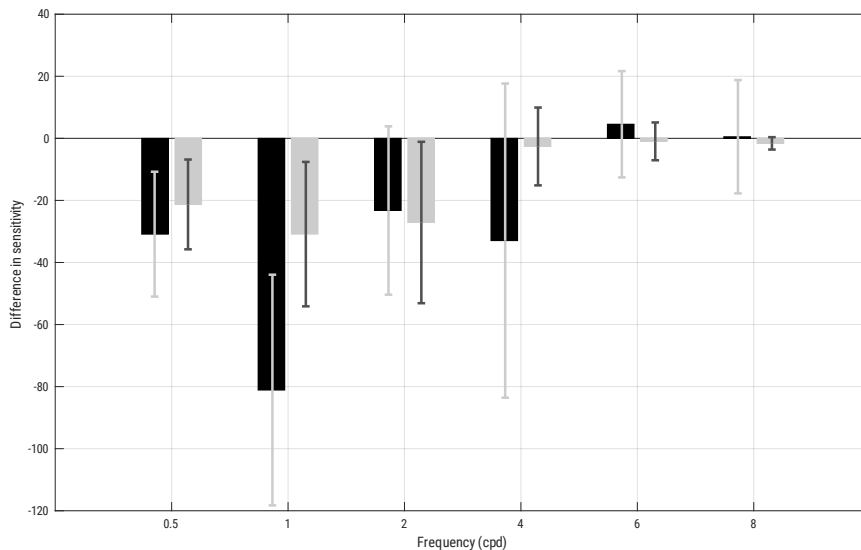


Figure 26 Mean difference in sensitivity between 'with fixation target' and 'without fixation target' for the two retinal locations. Black for central vision, grey for perifoveal.

We found differences in the sensitivity between “with the fixation target” and “without the fixation target” stimuli for both areas. The differences are more noticeable for the lower frequencies, especially for 1 cycles per degree (cpd) in foveal vision. The effect of the fixation target over the stimulus spectrum is small. Taking two different stimuli, 1 and 6 cpd, and analysing their spectra, little differences can be seen (figure 27); this would not justify any significant change in the contrast sensitivity.

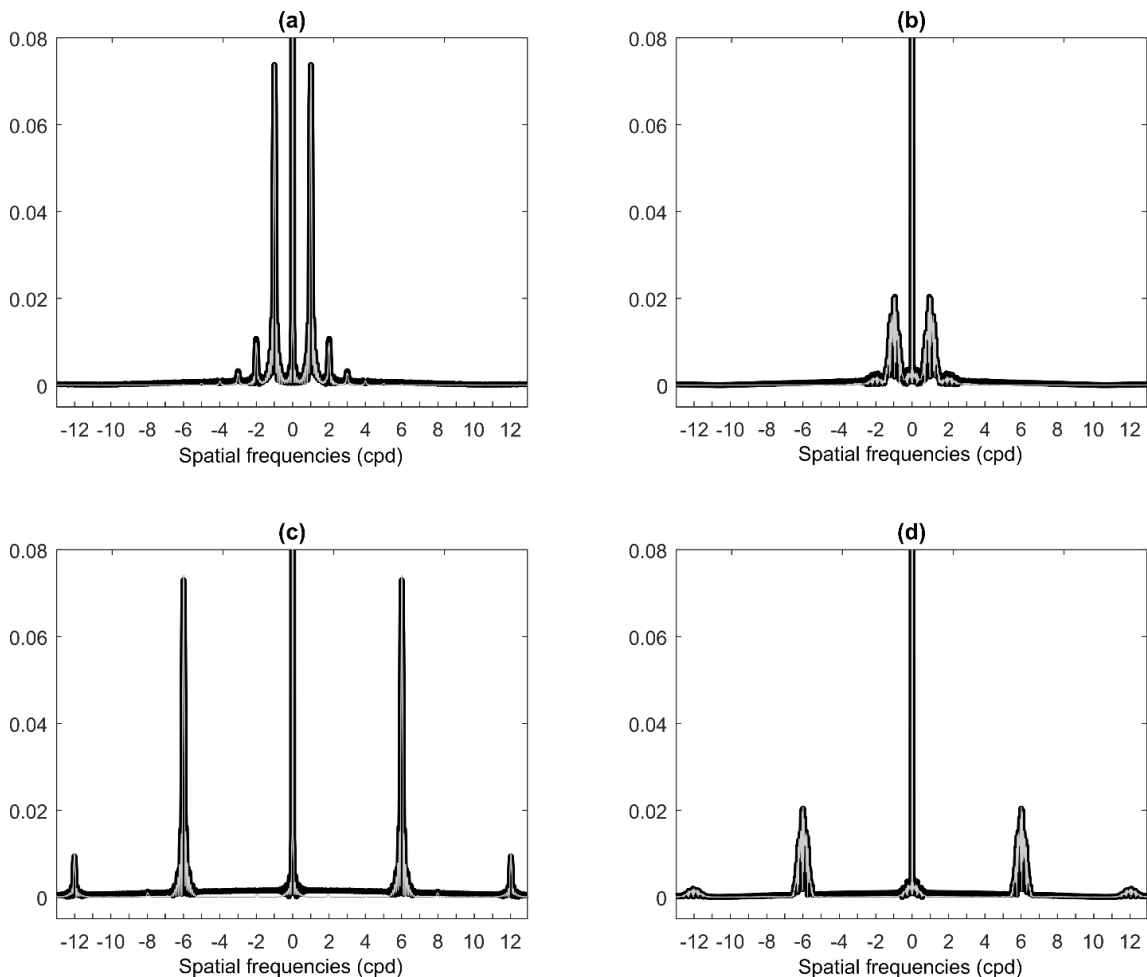


Figure 27 Spectrum of the stimuli. Black for 'with the fixation target', grey for 'without the fixation target'. (a) foveal vision, 1 cpd, (b) perifoveal vision 1 cpd, (c) foveal vision 6 cpd, (d) perifoveal vision 6 cpd.

The other factor that should be considered is the gaze stability due to the presence of the fixation target. The fixation target acts as a stimulus for the gaze stability and for the accommodation and convergence as well (Legge & Campbell 1981). Using an infrared eye-tracker (High-Speed Video Eye-Tracker Toolbox, Cambridge Research Systems Ltd, Rochester, Kent, United Kingdom), for more details please check the Annex III, we determined the gaze position of the right eye of one of the volunteers while doing the test for two different frequencies. The chosen frequencies were 1 and 6 cpd, because they are representative of the two different behaviours described. The eye-tracker captures the information about the pupil centre and the pupil size with a temporal frequency of 250Hz. To analyse all this information we chose a temporal window of 4 seconds (1000 values). This window was placed in the beginning of the sequence and moved towards the end moving step by step. The standard deviation was calculated for all the positions of the window and the results are represented in the figure 28.

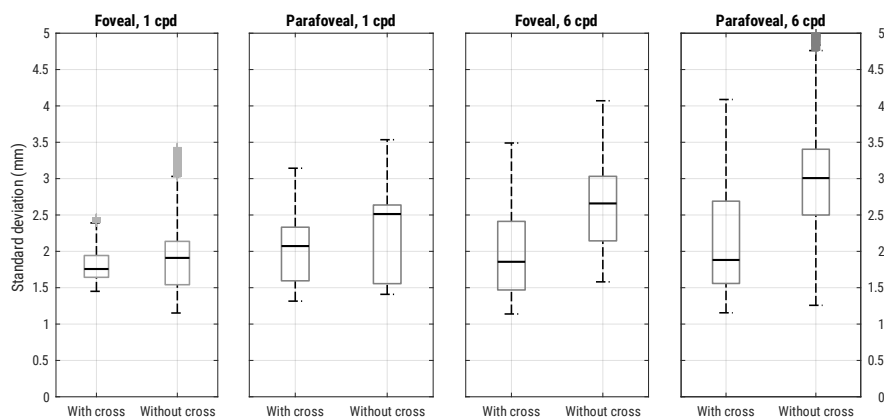


Figure 28 Boxplot of the standard deviations for a temporal window of 4 seconds. (a) for foveal vision, 1 cpd; (b) for parafoveal vision, 1 cpd; (c) for foveal vision, 6 cpd; (d) for parafoveal vision, 6 cpd.

For 1 cpd and foveal vision, in the horizontal direction the dispersion of the deviations is lower for the stimulus with the cross in comparison to the stimulus without the cross. A small height in the boxplots of figure 28 means a small variation of the deviations over time, and this can be interpreted as a more stable fixation over time.

In conclusion, the use of a fixation target has effects over the sensitivity values for a wide range of low to mid frequencies over different concentric areas of the retina. This reduction can be related to the fixation stability. As Pons (Pons et al. 2000) demonstrated, fixational eye movements act as a low-pass filter degrading the quality of the retinal image. In this pilot study we found different patterns of eye movements for different frequencies of the test that can be related to relevant loss in sensitivity. The use of a ring mask to measure the peripheral sensitivity provides results compatible with those reported by other studies. We consider necessary to further test the effects on contrast sensitivity of other designs for the fixation stimulus and to improve the integration of the eye-tracking techniques as fixational eye movements play a role in vision but in general are not considered in vision research.

4.3.2. Peripheral sensitivity

The previous results suggest to compare the sensitivity for the three areas using the fixation target. The average result for all the observers are plotted in the figure 29.

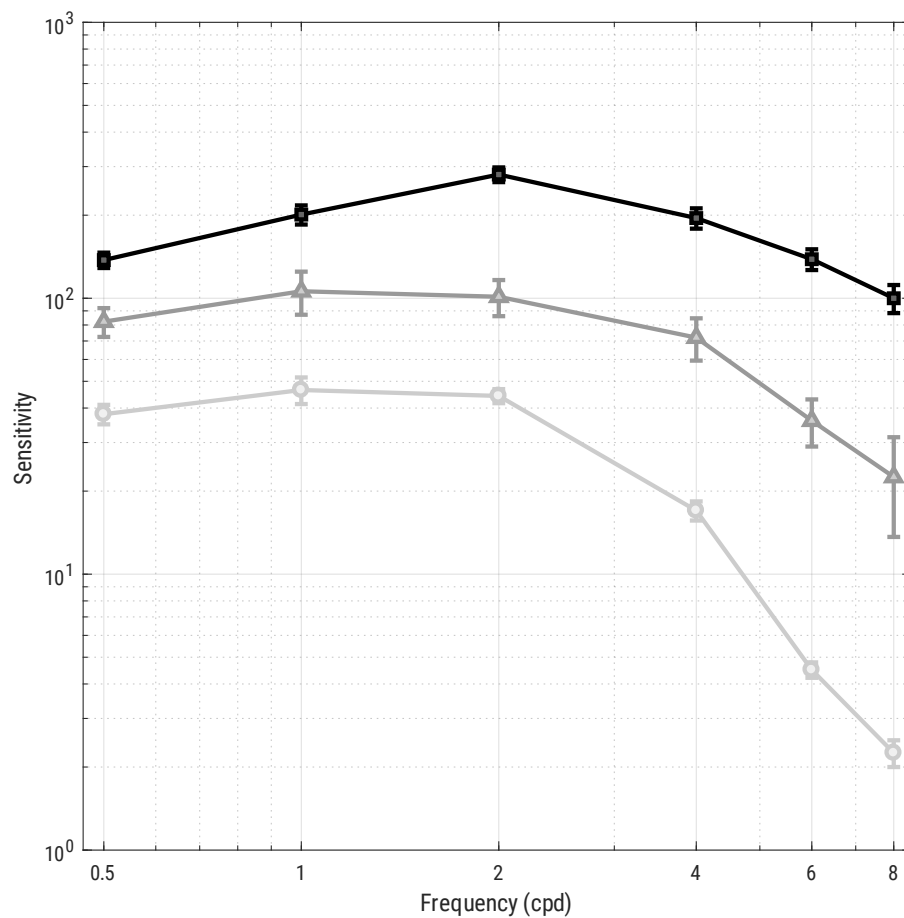


Figure 29 Sensitivities for the three retinal areas. Black for the foveal, medium grey for the perifoveal and light grey for the near periphery.

The overall sensitivity diminishes with increasing eccentricity, and at the same time, the maximum of the sensitivity is displaced towards lower frequencies changing from a band-pass shape for the foveal vision to a low-pass shape for the near periphery area.

4.4. Comparison with other systems

The first results, influence of the fixation point on the sensitivity, are in agreement with the experiment done by Gilbert that compare the change in the threshold sensitivity between stabilized and non-stabilized gratings (Gilbert & Fender 1969). They found a significant reduction in sensitivity when the test grating was stabilized. This reduction had more effect in frequencies lower than 0.5 cycles per degree. In our study we are restricting the eye movements (except from the fixational eye movements) using the fixation cross. The goal of Gilbert was to measure the effects of stabilization of the retinal image, while ours is to stabilize the fixation.

The influence of the fixation point on the sensitivity have been studied by Summer (Summers et al. 2009). Their results disagree with the ones that we report in the present study. Summers reports an increase in the contrast threshold (reduction in the sensitivity) in 4 and 8 cpd; and a little or almost no effect in 1 and 2 cpd, in our study, the effects are the contrary. We attribute the difference in the results to the differences between the stimuli in the two studies. Summers used a black square and we use a white hair cross of 3 pixels of thickness, they reported a small reduction in the masking effect when changing the colour of the fixation point to white. They found a relation between the size of the square, the size of the patch (or the number of visible cycles) and the masking effect. In fact, in their experiment 4, they compared the effects of the fixation point for 4 cpd between a

patch of 0.75 degrees and another of 3 degrees. The results showed an increase in the threshold for the small patch but no effect for the big patch. In comparison, we are using a patch with a surface almost five times bigger.

Despite the influence of the fixation target, the overall behaviour under the same conditions agree with those reported by other researchers (Virsu & Rovamo 1979, Kelly 1984, Johnston 1987, Thibos et al. 1996) validating the results of this experiment. The sensitivity diminishes when the eccentricity of the stimulus is increased and the maximum of the CSF is displaced towards lower frequencies (Thibos et al. 1996). Thibos reports a change in the shape of the CSF from a band-pass to a low-pass and a lower sensitivity for the peripheral stimulus (30 degrees from the fovea). In our study the changes are compatible taking into account the different intermediate areas that we are testing in comparison to Thibos.

The test results ensure that the annular design is suitable for testing the contrast sensitivity in the periphery of the fovea. This test has application both in the laboratory and in clinical setups.

4.5. Conclusions and future work

The conclusion of the work described in this chapter is that it is possible to measure the contrast sensitivity under natural vision for the centre and the periphery of the fovea using 8-bit colour depth equipment and stimulus with a

ring shape, the results are reliable and in agreement with the literature. An original result from this work is the difference in the sensitivity generated by the presence or absence of a fixation target on the stimulus to make sure that the test image is stimulating the desired area of the retina. An eye-tracking measurement for one of the subjects suggests that the pattern of the eye movements while fixating on the stimulus differs in function of the presence or absence of the stimulus. To compare the differences between monocular and binocular viewing would be of interest as well.

As future work it is necessary to take more measurements to validate the described test. A possible application in the clinical practice of this test is to assess the vision performance of multifocal contact lens wearers. This kind of lenses have a not uniform power profile (Plainis et al. 2013) to generate focused images for far, near and intermediate objects at the same time, also known as simultaneous vision. It is also of interest for measuring the quality of vision on the periphery, thinking in the efforts of studying the peripheral refraction and its impact on the myopia onset, a peripheral CSF tool should be of great interest. Other possible work would be to measure the suprathreshold contrast discrimination.

Chapter 5

Objective measurement of the pupil size variation over time under different viewing conditions

5.1. Justification

Pupil size determines the quantity of light reaching the retina, in fact, the retinal illuminance unit, the Troland is calculated considering the pupil area, equation 12. So, even in controlled conditions, the pupil can change the amount of light entering towards the retina.

The muscles that regulates the pupil diameter never remain still, there is a continuous oscillation. There are different names for this phenomenon: pupil unrest (Beatty & Lucero-Wagoner 2000), pupil activity (Sosnowska et al. 2015) and pupilar hippus (Yoss et al. 1970, Beatty & Lucero-Wagoner 2000, Ukai et al. 1997). Pupillary hippus refers to irregular but rhythmic oscillations of the pupil size, around 0.2 Hz (Ukai et al. 1997), other authors report a much lower frequency, 0.04 Hz or even lower frequency (Beatty & Lucero-Wagoner 2000). These oscillations are mediated by different mechanisms in the central nervous system

(sympathetic and parasympathetic) (Beatty & Lucero-Wagoner 2000). Its study allows to assess the state of those mechanisms, the effect of drugs, diseases such as Parkinson (Jain et al. 2011) or narcolepsy (Prasad et al. 2011).

$$T = L \cdot \pi \cdot r^2$$

Equation 12

Where

L the luminance in cd/m^2

r the pupil radius in mm

5.2. Experimental development

The eye-tracker VET (Annex III) was used to record high-speed video sequences of the right eye at 250 fps. The considered viewing conditions were: far distance (6 m), near distance (0.5 m), photopic (100 lux), mesopic (3 lux), binocular viewing, monocular viewing. These conditions are representative of different situations in the real life. All the conditions considered appear in table 14

Photopic Binocular Far	PBF
Photopic Binocular Near	PBN
Photopic Monocular Far	PMF
Photopic Monocular Near	PMN
Mesopic Binocular Far	MBF
Mesopic Binocular Near	MBN
Mesopic Monocular Far	MMF
Mesopic Monocular Near	MMN

Table 14 Acronyms for the viewing conditions.

The stimulus for far distance was a black cross inscribed in a circle of 72 mm in diameter (approximately 41 arcmin). For the near distance target the stimulus was the equivalent. Both targets were printed on white paper. The illumination level was 100 lux, measured using a photometer model CL-200 Chroma Meter (Konica Minolta, Tokyo, Japan), the probe was placed on the corneal plane. The measurements lasted for 45 seconds, this means, a total number of $45 * 250 = 11250$ measurements were taken per each condition per each subject. For the monocular viewing condition a patch was placed on the left eye. A scheme of the experimental setup appears in figure 30, for the near distance the stimulus was placed 0.5 m in front of the subject, for the far distance the stimulus was placed 1 meter behind the chinrest and was viewed through a flat mirror placed 2 m in front of the chinrest, so the viewing distance was equivalent to 6 m.

Seven young adults, 2 women and 5 men, participated. Mean age was 28.29 ± 2.98 years old. The inclusion criteria were healthy young adults with a monocular visual acuity with the best correction 0.0 logMAR or better, with a refractive error between 3 dioptries of hyperopia and 3 dioptries of myopia and up to 1 dioptre of astigmatism and round and symmetrical pupils (up to 0.5 mm of difference in diameter) (Lam et al. 1987, Ettinger et al. 1991). Those subjects who need compensation were fitted with daily disposable contact lenses. Exclusion criteria were a history of eye surgery, any kind of illnesses, to be under a drug treatment up to two weeks before the measurements and any problem on the tear film, cornea and pupil size. All measurements were taken between 9 am to 12 am

and subjects were asked to not drink any caffeinated beverage from the afternoon before the day of the measurement (Wilhelm et al. 2014).

A fifteen-minute light adaptation period for each condition was carried out in order to let the pupil fluctuations stabilize. The volunteer task was to rest on the chin rest, and fixate the target while trying to move as few as possible during the 45 seconds the measurement lasted. Pupil size was calibrated before measuring each subject using the provided scale.

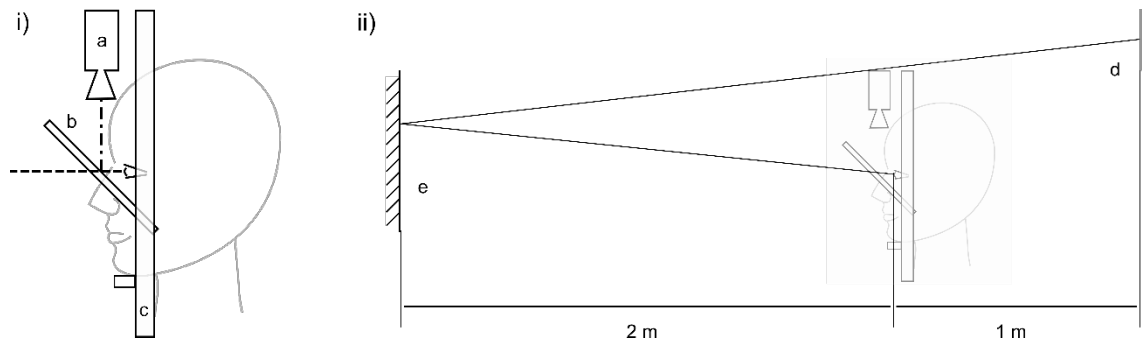


Figure 30 i) Scheme of the device (a) is the IR camera and the IR illumination system, (b) is the hot mirror, (c) is the chinrest. ii) Representation of the far distance viewing setup, (d) is the target, (e) is a normal mirror.

5.3. Results

The distribution of all measurements was checked using the Lilliefors test implemented in Matlab©. For all the measurements, the p-value was inferior to 0.0001 so, it can be accepted that none of the measurements follow a normal distribution. For this reason, in table 15 appears the summary as median, interquartile range (iqr), maximum and minimum values. Analysing the variations in pupil diameter for the different viewing conditions for each subject the results were statistically significant for all the cases except for PMF and PMN for subject 5. Boxplots of the measurements are shown in figure 31.

		Subject							Average	Standard Deviation
		1	2	3	4	5	6	7		
MBF	median	6.66	7.31	6.93	4.64	5.25	6.24	7.34	6.34	1.04
	Iqr	0.10	0.19	0.14	0.32	0.55	0.16	0.38	0.26	0.16
	Max	6.85	7.61	7.06	4.97	6.01	6.52	7.77	6.68	0.97
	Min	6.47	7.01	6.67	4.23	4.73	5.95	6.81	5.98	1.09
MBN	median	6.35	5.90	7.09	4.03	4.99	5.82	7.38	5.94	1.17
	Iqr	0.20	0.36	0.14	0.42	0.85	0.33	0.31	0.37	0.23
	Max	6.62	6.43	7.31	4.43	5.98	6.32	7.80	6.41	1.07
	Min	5.98	5.11	6.78	3.41	4.22	5.27	6.95	5.39	1.30
MMF	median	6.91	7.68	6.81	NaN	6.17	6.41	8.37	7.06	0.82
	Iqr	0.07	0.18	0.06	NaN	0.33	0.16	0.16	0.16	0.10
	Max	7.02	7.95	6.93	NaN	6.89	6.70	8.73	7.37	0.80
	Min	6.80	7.43	6.70	NaN	5.38	6.12	7.97	6.73	0.92

MMN	median	6.63	7.41	7.13	5.12	5.60	5.97	7.98	6.55	1.03
	Iqr	0.09	0.27	0.07	0.17	1.07	0.24	0.29	0.32	0.34
	Max	6.78	7.82	7.24	5.39	6.68	6.37	8.29	6.94	0.96
	Min	6.47	6.95	7.03	4.81	4.61	5.57	7.62	6.15	1.17
PBF	median	3.81	3.74	3.40	2.91	3.18	3.81	4.39	3.61	0.49
	Iqr	0.23	0.33	0.24	0.11	0.35	0.32	0.23	0.26	0.08
	Max	4.20	4.24	3.75	3.08	3.66	4.25	4.75	3.99	0.54
	Min	3.43	3.25	3.06	2.75	2.84	3.37	4.02	3.25	0.43
PBN	median	3.68	3.64	3.09	2.85	3.00	3.55	3.56	3.34	0.35
	Iqr	0.23	0.29	0.44	0.21	0.25	0.19	0.27	0.27	0.08
	Max	4.01	4.09	3.66	3.12	3.32	3.87	3.98	3.72	0.37
	Min	3.34	3.20	2.52	2.58	2.69	3.24	3.16	2.96	0.35
PMF	median	4.85	5.28	5.12	3.79	3.61	4.40	5.37	4.63	0.71
	Iqr	0.42	0.90	0.33	0.22	0.37	0.25	0.51	0.43	0.23
	Max	5.46	6.19	5.52	4.07	4.13	4.81	6.14	5.19	0.88
	Min	4.24	4.26	4.69	3.49	3.10	3.93	4.56	4.04	0.58
PMN	median	4.32	4.69	4.30	3.68	3.53	4.20	4.49	4.17	0.42
	Iqr	0.26	0.54	0.63	0.32	0.27	0.34	0.49	0.41	0.15
	Max	4.66	5.59	5.04	4.13	4.03	4.66	5.15	4.75	0.56
	Min	4.00	3.70	3.69	3.23	3.03	3.73	3.93	3.62	0.36

Table 15 Summary of the results per subject.

Using the Kruskal Wallis test for non-parametric data, the p-values calculated for all the subjects were zero. This is due to the amount of measurements per subject. Repeating the test with a reduced sample of the first 50 values the p-values ranged between $2.29 \cdot 10^{-31}$ to $1.05 \cdot 10^{-80}$.

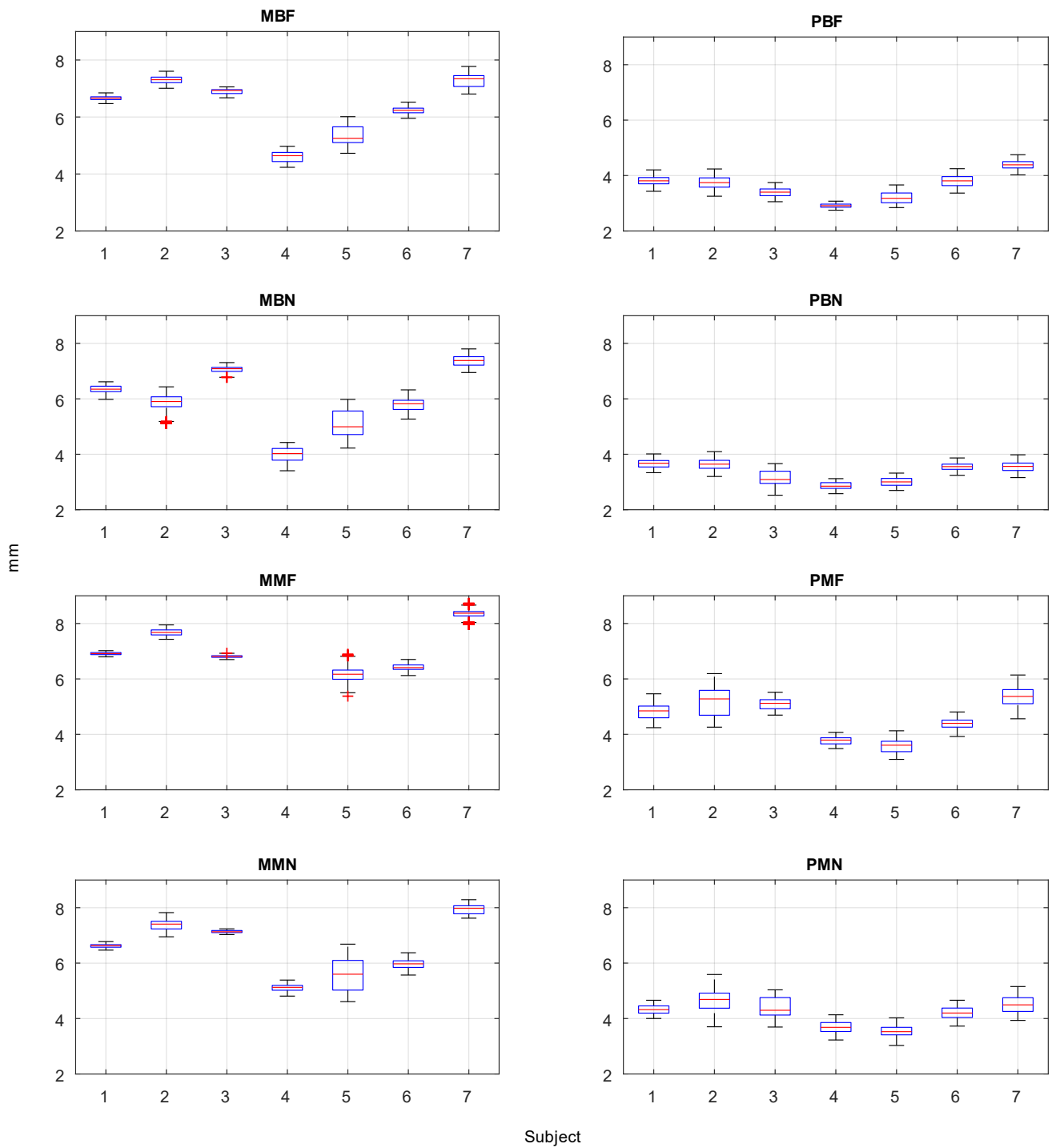


Figure 31 Boxplot of the pupil size per subject for each viewing condition.

Tables 16, 17 and 18 show the differences in mm between two conditions for each subject when fixing two of the three variables. A boxplot of the differences in the previous tables are represented in figure 32.

	Subject							Average	Standard Deviation
	1	2	3	4	5	6	7		
MBF – PBF	2.85	3.56	3.53	1.73	2.07	2.43	2.96	2.73	0.70
MBN – PBN	2.67	2.26	4.00	1.18	1.99	2.27	3.82	2.60	1.01
MMF – PMF	2.07	2.40	1.69	NaN	2.56	2.01	3.00	2.29	0.46
MMN – PMN	2.31	2.72	2.83	1.44	2.07	1.77	3.48	2.38	0.69

Table 16 Difference in pupil size generated by the illumination, all units are mm.

	Subject							Average	Standard Deviation
	1	2	3	4	5	6	7		
MBF – MBN	0.31	1.41	-0.16	0.62	0.26	0.42	-0.04	0.40	0.51
MMF – MMN	0.29	0.27	-0.32	NaN	0.57	0.44	0.39	0.27	0.31
PBF – PBN	0.13	0.10	0.31	0.06	0.18	0.25	0.82	0.27	0.26
PMF – PMN	0.53	0.59	0.82	0.11	0.08	0.20	0.87	0.46	0.33

Table 17 Difference in pupil size generated by the accommodation, all units are mm.

	Subject							Average	Standard Deviation
	1	2	3	4	5	6	7		
MBF – MMF	-0.25	-0.37	0.12	NaN	-0.92	-0.17	-1.03	-0.44	0.45
MBN – MMN	-0.28	-1.50	-0.04	-1.10	-0.61	-0.15	-0.59	-0.61	0.53
PBF – PMF	-1.04	-1.53	-1.72	-0.88	-0.43	-0.59	-0.98	-1.02	0.47
PBN – PMN	-0.64	-1.05	-1.21	-0.83	-0.53	-0.64	-0.93	-0.83	0.25

Table 18 Difference in pupil size generated by the binocularity, all units are mm.

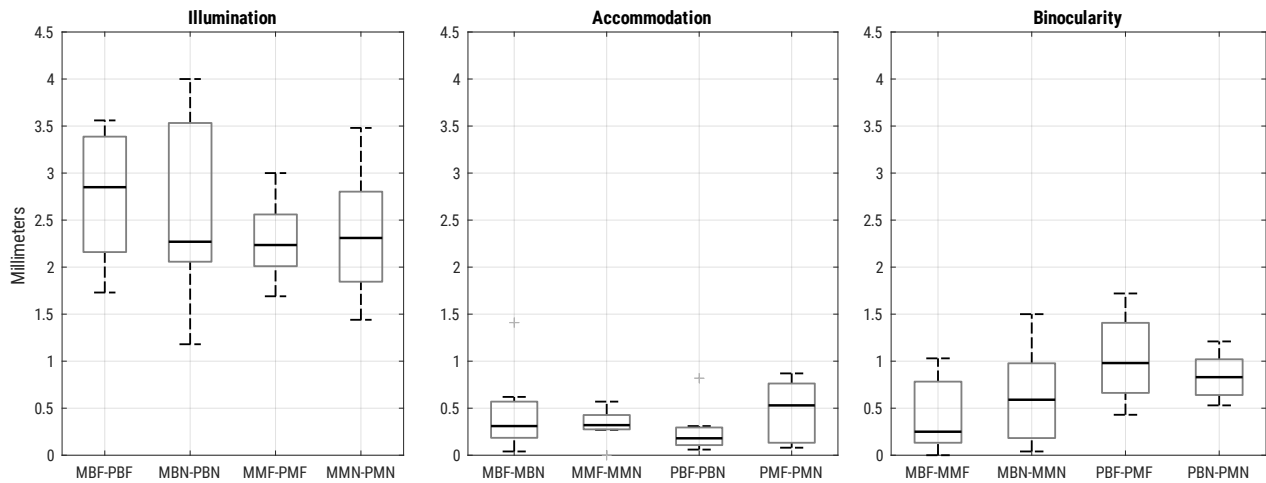


Figure 32 Boxplot of the differences per each variable.

The Anova analysis of the differences resulted in no statistical significant differences for all the combinations, so it makes sense to average the different combinations for each constant condition. The mean effect of the illumination on the pupil diameter was 2.50 ± 0.20 mm, the effect of the accommodation was 0.34 ± 0.15 mm and the effect of the binocularity was 0.71 ± 0.28 mm, figure 33.

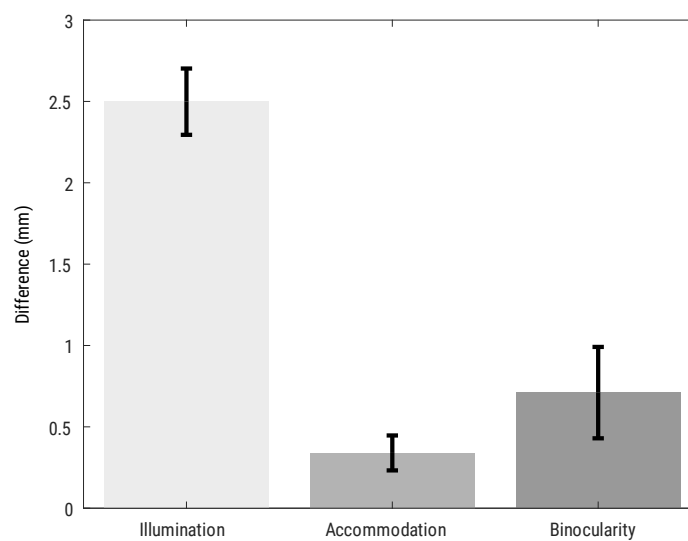


Figure 33 Mean change in the pupil size.

In order to relax the accommodation, disposable contact lenses with an increase of two positive dioptres were fitted and the experiment was repeated only for the near distance situation. The results are in table 19. These results are not normally distributed, the Kruskal Wallis test calculated p-values of zero for all subjects.

		Subject							Average	Standard Deviation
		1	2	3	4	5	6	7		
MBN2	median	6.63	7.23	7.52	3.53	5.77	6.36	7.89	6.42	1.46
	iqr	0.08	0.27	0.11	0.51	0.36	0.18	0.16	0.24	0.15
	max	6.81	7.57	7.68	4.16	6.31	6.61	8.13	6.75	1.31
	min	6.38	6.78	7.32	2.89	5.10	6.09	7.64	6.03	1.61
MMN2	median	6.70	7.84	7.79	3.96	6.08	6.74	8.53	6.80	1.51
	iqr	0.06	0.14	0.18	0.55	0.85	0.11	0.11	0.29	0.30
	max	6.83	8.05	7.96	4.53	7.04	6.94	8.72	7.15	1.35
	min	6.54	7.64	7.58	3.34	5.09	6.53	8.34	6.44	1.72
PBN2	median	3.32	3.53	4.29	3.07	3.38	3.46	4.37	3.63	0.50
	iqr	0.18	0.30	0.52	0.14	0.33	0.25	0.19	0.27	0.13
	max	3.65	4.05	5.13	3.33	3.94	3.84	4.69	4.09	0.62
	min	3.03	3.21	3.72	2.83	2.83	3.10	4.02	3.25	0.45
PMN2	median	4.10	4.73	5.45	4.60	3.74	4.18	5.20	4.57	0.61
	iqr	0.54	0.35	0.38	0.16	0.27	0.22	0.35	0.32	0.12
	max	4.71	5.21	5.95	4.81	4.35	4.51	5.64	5.03	0.60
	min	3.49	4.24	4.95	4.20	3.25	3.86	4.75	4.11	0.62

Table 19 Pupil diameter in mm when using a monofocal contact lens fitted for near distance vision.

Table 20 is the equivalent to the table 17 but replacing the data for the near condition with the new data.

	Subject							Average	Standard Deviation
	1	2	3	4	5	6	7		
MBF – MBN2	0.04	0.08	-0.59	1.12	-0.52	-0.12	-0.54	-0.08	0.60
MMF – MMN2	0.21	-0.17	-0.98	NaN	0.09	-0.33	-0.16	-0.22	0.42
PBF – PBN2	0.49	0.21	-0.88	-0.16	-0.20	0.35	0.02	-0.02	0.46
PMF – PMN2	0.75	0.55	-0.33	-0.80	-0.14	0.22	0.17	0.06	0.53

Table 20 Comparison between the monofocal contact lens for far distance and the lens for near distance.

The differences followed a normal distribution, an Anova was done to find statistically differences among the subjects. With a p-value of 0.7897 the null hypothesis was accepted. Averaging the results showed a mean of -0.07 ± 0.12 mm

5.4. Comparison with other systems

The illumination influence on the pupil diameter (2.50 ± 0.20 mm) is compatible with the different formulas proposed by Moon (Moon & Spencer) De Groot (De Groot & Gebhard 1952), Blackie (Blackie & Howland 1999) and the unified formula proposed by Watson (Watson & Yellott 2012) which estimates a change of 2.2 mm. The effect on the pupil size induced by the accommodation (0.34 ± 0.11) agrees with the results reported by Alpern (Alpern et al. 1961). They reported a change of 0.5 mm in the pupil diameter when changing the accommodative vergence from 0 to 2 dioptres.

The effect of the binocularity was reported at the beginning of the previous century by Reeves and Blanchard (Reeves 1918, Blanchard 1918) using

sophisticated photographic equipment reported a mean change of 0.92 ± 0.47 mm, this result was obtained from one subject with a completely different setup.

In comparison with other studies comparing monocular and binocular pupillometers the results reported in this thesis are really close to the study done by Wachler (Wachler 2003), 0.67 ± 0.27 mm. Kurz (Kurz et al. 2004) found different results in function of the order between the measurements, for the group “binocular first, then monocular” there were no differences in the scotopic condition while in the other group “monocular first, then binocular” the differences were significant (0.36 mm of change). Our results are slightly different, this could be because of the difference in the lightning level (0.3 versus 0.03 lux), the sample size and the age distribution (25 to 31 versus 13 to 44). In the photopic condition the mean difference was of 1.02 ± 0.47 mm, this difference is statistically significant (p-value < 0.0001). These results are virtually the same as those reported by Kawamorita (1.086 ± 1.1654 mm) (Kawamorita & Uozato 2014) and Kurz (1.14 mm for the “monocular first, then binocular” group, but only 0.29 mm for the “binocular first, then monocular” group).

Rosen (Rosen et al. 2002) reported similar values (1.12 ± 0.34 mm) for the influence of the binocularity under low mesopic illumination (0.15 lux). In their experiment both pupils were measured at the same time for a period of 2 seconds at a speed of 5 Hz. They suggest these values (times and number of measurements) as the best choice for determining the highest diameter of the pupil. To test this

affirmation with our data, every measurement was subdivided in intervals of 2 seconds (500 samples). On figure 34 is plotted an example of a single measurement. Figure 35 represents the boxplots of the different intervals.

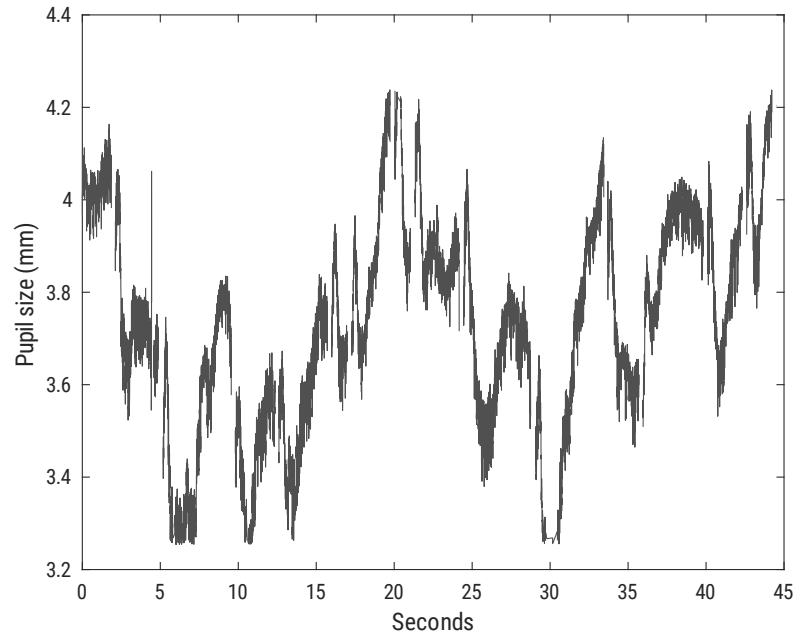


Figure 34 Example of pupil size VS time.

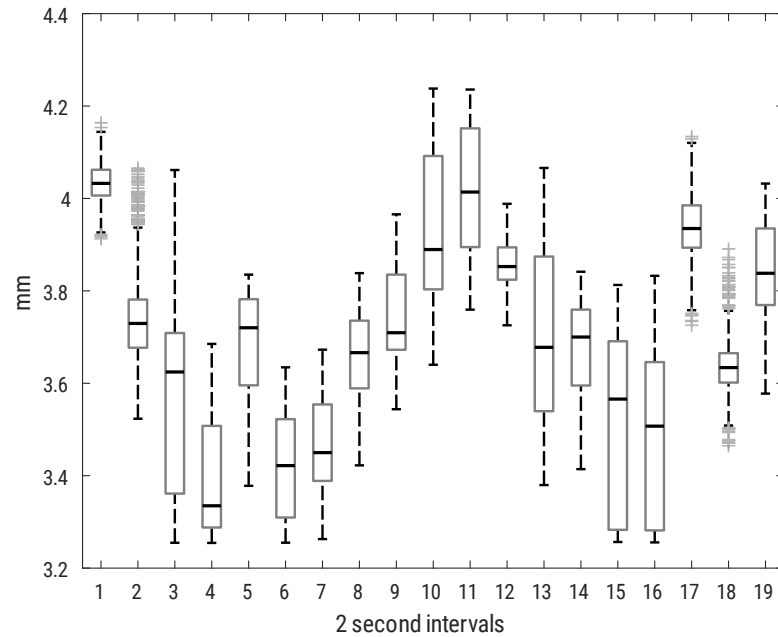


Figure 35 Boxplot of the 2-second subsamples.

From the viewing of the figure 35 it is evident that the differences are quite noticeable. When testing all the intervals with the Kruskal Wallis test, a p-value of 0 rejects the null hypothesis, so subdividing the measurements in intervals of 2 seconds is not equivalent to the 45 seconds measurement. When comparing the intervals among them in pairs, only 26 out of 171 possible combinations show a no significant p-value (>0.005). The results of this algorithm for all the measurements are in table 21. The highest number of equivalent matches is found for the subject 7 under MBN, this value, 61 is only the 35% of the possible combinations, so it is easy to figure out that a measurement of 2 seconds is not enough to characterise the pupil diameter under dynamic measurement.

Subject	Viewing Condition							
	MBF	MBN	MMF	MMN	PBF	PBN	PMF	PMN
1	32	27	35	27	34	36	29	36
2	26	24	31	26	26	22	26	22
3	32	23	19	27	27	25	32	32
4	24	16	NaN	23	36	27	30	23
5	29	23	23	20	23	34	18	23
6	27	30	37	30	27	33	26	28
7	32	61	33	44	35	23	34	28

Table 21 Number of significant matches per subject for each viewing condition.

A similar analysis can be done about the framerate. In this case, two alternative measurements were generated by taking values from the original vector, one every ten values and one every 50 values to simulate framerates of 25 and 5 Hz. In figures 36 and 37 the results of reducing the framerate to 25 Hz and

to 5 Hz can be seen. When applying the Kruskal Wallis test to the data the p-values are all close to 1, so there are no statistical differences in the results when reducing the framerate of the camera. The p-values can be consulted in table 22.

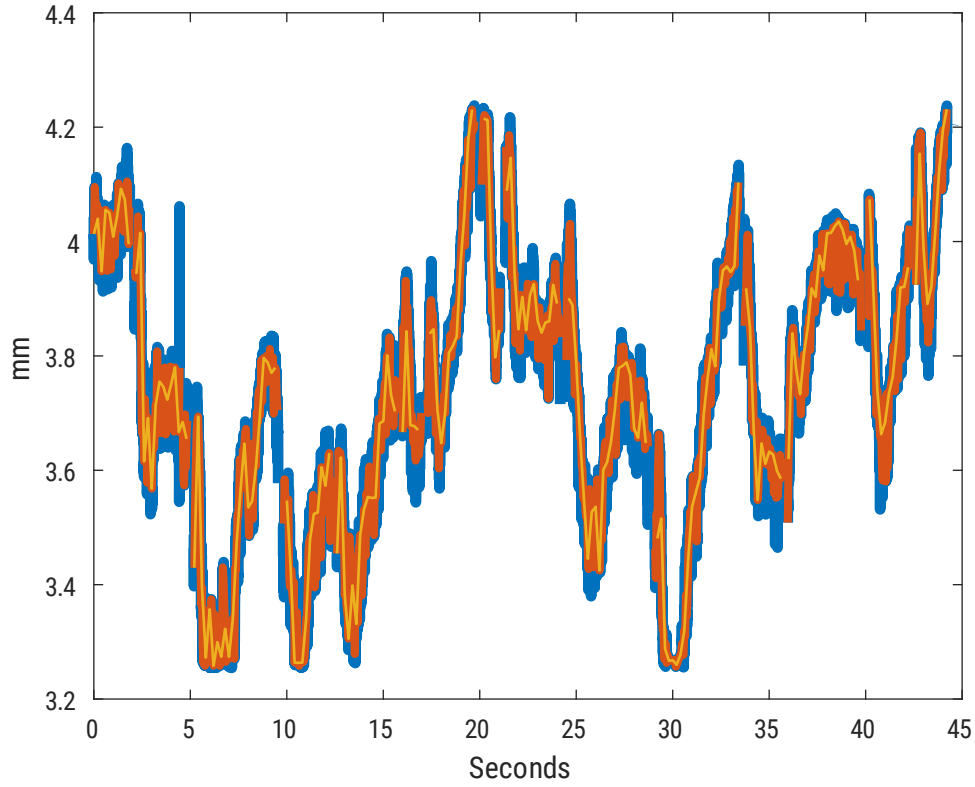


Figure 36 Pupil size VS time for different framerates: blue for 250 Hz, orange for 25 Hz and yellow for 5 Hz.

Subject	Viewing Condition							
	MBF	MBN	MMF	MMN	PBF	PBN	PMF	PMN
1	0.9445	0.9643	0.9168	0.8177	0.9990	0.8609	0.9980	0.9871
2	0.8152	0.9910	0.6111	0.9759	0.9957	0.9944	0.9775	0.9806
3	0.7523	0.9610	0.9044	0.7725	0.9883	0.9972	0.9744	0.9984
4	0.9754	0.9948	0.9044	0.9981	0.6431	0.9875	0.9905	0.9736
5	0.9363	0.9962	0.9842	0.9480	0.9526	0.9269	0.9440	0.9832
6	0.9860	0.9352	0.9059	0.8674	0.9692	0.9199	0.9618	0.9767
7	0.8165	0.9962	0.9100	0.7425	0.8023	0.9354	0.8104	0.9951

Table 22 p-values for the effect of the framerate value on the measurements.

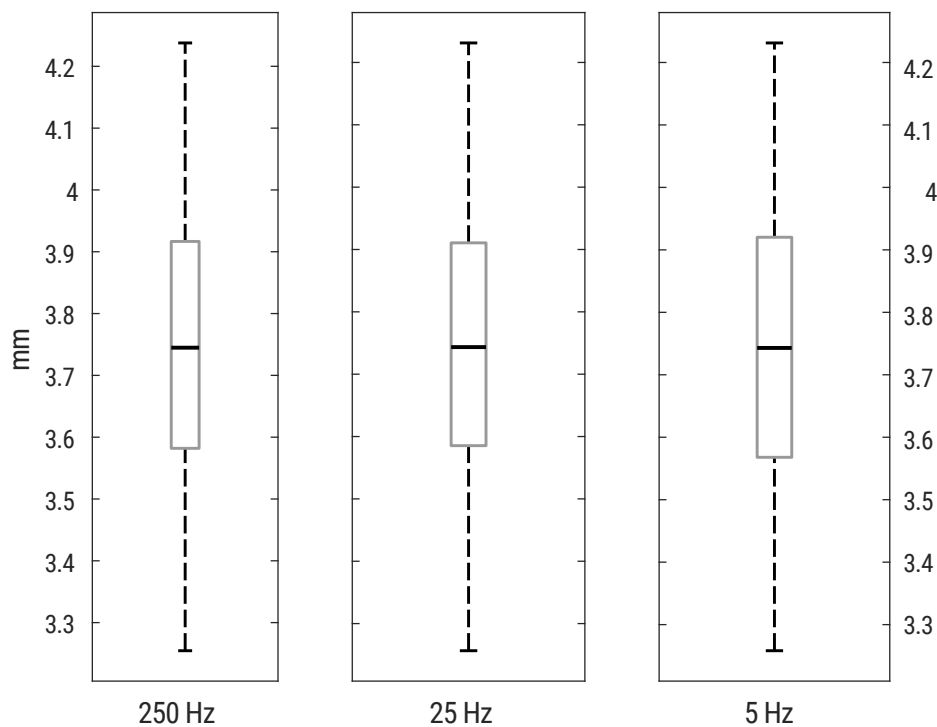


Figure 37 Boxplot of the measurement for different framerates.

5.5. Conclusions and future work

The conclusions of this experiment are that under constant viewing conditions of illumination, vergence of the stimulus and binocularity the pupil size cannot be considered constant. It fluctuates not following a normal distribution. The constant changes modify the retinal illumination, between 3318 and 5000 trolands under photopic far binocular viewing, these changes are supposed to not affect the contrast sensitivity (Westheimer 1960, van Ness & Bouma 1967).

Commercial devices such as autorefractometers and topographers usually include pupillometry as an extra feature. Considering our results, it is quite questionable the utility of the measurements taken under no natural conditions. But it would be possible to build a low-cost binocular pupillometer with common webcams without the infrared light filter because, as has been shown, it is not necessary a high-speed camera to characterise the pupil size if the measurement time is long enough under natural viewing conditions.

Nevertheless, pupil size is critical under some circumstances, especially related to the vision correction or compensation. The majority of the multifocal contact lenses show a design which relies on the pupil size to determine the dioptrical power of the lens, so the performance of these lenses and the satisfaction of the subject is directly related to the pupil size (Plainis et al. 2013). For refractive surgery, the best way to prevent complaints related to glare and halo perception under low light situations (Schummer et al. 2000) is to select candidates for the surgery based on the relation between the mesopic pupil size and the possible treatment area and also, to analyse the pupil fluctuations at different illumination levels because the magnitude of the fluctuations depends on the illuminance level (Howarth et al. 1993).

Final conclusions

- The objective measurement of the FD by means of the Web Cam Eye-Tracker is reliable.
- The results provided by our methodology cannot be compared directly with other studies because we have not found any data about the temporal evolution of the FD or the influence of the polarity of the stimulus.
- The use of bit-stealing for increasing the luminance resolution of common displays provides reliable results when measuring suprathreshold contrast discrimination and for the contrast sensitivity measurement for different retinal areas.
- The power law for contrast discrimination formulated by Legge may be not accurate for pedestal contrasts higher than 0.5 and for high spatial frequencies.
- When placing a fixation target in a contrast test the sensitivity for low frequencies diminishes.
- The use of Gabor patches for measuring the sensitivity for central vision is reliable for natural viewing conditions, the equivalent for peripheral areas are the ring patches.
- Pupil size cannot be considered constant under constant conditions of illumination, stimulus proximity and binocularity
- The variations of the pupil size do not follow a normal distribution

- When the pupil size is measured under not natural conditions the values differ from those obtained under natural vision
- The best strategy for determining the pupil size is to measure it under natural viewing conditions and taking measurements for a reasonable period of time even at a low capture speed

Annex I

Bit stealing

A digital image is equivalent to a bidimensional matrix. Each value inside the matrix represent a spatial unit known as pixel. The value of every pixel refers to the colour of that pixel. In 8-bit systems the possible values for each pixel is in the range from 0 to 255.

If we measure the luminance generated by each digital level for each colour component different curves are obtained. These curves can be fitted by exponential expressions (Berns 1996, Gibson & Fairchild 2000, Kwak & MacDonald 2000, Sharma 2002) characterised by the γ value.

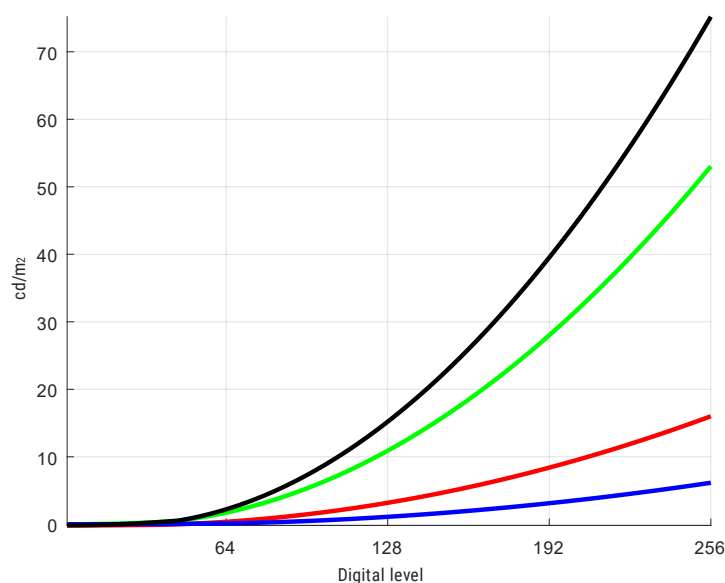


Figure 38 Luminance generated by each digital value for every channel and the grey-scale. Red for the red subpixel, green for the green subpixel, blue for the blue subpixel and black for the three subpixels at the same time

In figure 38 is easy to notice that the maximum luminance level for each colour channel differs greatly. The linear combination of the three channels determines the white channel luminance.

The colours of a digital image are determined by triplets of digital values. In particular, triplets of the same digital value generate grey colours. So the luminance steps of a grey-scale are 256 values, being $[0, 0, 0]$ the luminance level of the black and $[255, 255, 255]$ the luminance level of the white. These steps are too high for determining the contrast sensitivity threshold of the human visual system. For vision testing it is advisable to use appropriate hardware, a combination of a 12-bit graphic card with a 10-bit computer display but this is a really expensive solution. The options for using 8-bit hardware are based on external pieces of hardware, dithering, high temporal frequency noise and bit-stealing. An example of hardware solution is to use a system combining attenuators and amplifiers to increase the luminance resolution of the output from an 8-bit image (Li 2003), but with this kind of devices it is completely necessary to have detailed information on the kind of manipulation of the signal to generate a correct input image and cannot be used with tablets. The dithering, or halftoning method (Ulichney 1987, Ulichney 1988) is based in the method used by printers to generate a grey perception but sometimes a noise pattern can be perceived (Daly 2005). Another method is based on the high temporal resolution achieved by modern displays (Allard 2008), the idea is to generate a controlled noise so in average the mean luminance is the desired luminance.

The algorithm proposed by Tyler (Tyler 1992, Tyler 1997), based on Faubert (Faubert 1991) generates intermediate colours by appropriately modifying the grey triplets that will produce controlled luminance levels between the 256 real greys. This way we are generating greyish colours with a very low saturation.

For our system we chose to generate six intermediate luminance values following this procedure. First the combination of graphic card and display was characterised using a CL-200 Chroma Meter (Konica Minolta, Tokyo, Japan) photometer after 30 minutes of warm-up time for the display. Five full-screen colour samples were generated per each colour channel with these digital values: 0, 64, 128, 192 and 256. The luminance of each sample was measured in the centre of the screen. The grey luminance was calculated by adding the three-colour luminance. A second-degree polynomial was fitted for each channel. The luminance curves are shown in figure 1. Is easy to note that between two grey levels $[i, i, i]$ and $[i+1, i+1, i+1]$ the following greyish colours can be generated: $[i+1, i, i]$, $[i, i+1, i]$, $[i, i, i+1]$, which corresponds to a greyish red, a greyish green and a greyish blue respectively. Other three colours can be generated by modifying two digital levels at the same time: $[i+1, i+1, i]$, $[i+1, i, i+1]$, $[i, i+1, i+1]$, which corresponds respectively to a greyish yellow, a greyish purple and a greyish cyan. In table 22 the 8 triplets are sorted by ascending luminance. For example, for the grey triplets $[192, 192, 192]$, $[193, 193, 193]$ and $[194, 194, 194]$ the increasing in luminance is 0.4690 and 0.4718 cd/m^2 , using the bit-stealing technique the

contiguous triplets are [193, 193, 192], [193, 193, 193] and [193, 193, 194] and the increasing in luminance is 0.0395 and 0.0398 cd/m².

[i, i, i]
[i, i, i+1]
[i+1, i, i]
[i+1, i, i+1]
[i, i+1, i]
[i, i+1, i+1]
[i+1, i+1, i]
[i+1, i+1, i+1]

Table 22 Digital triplets corresponding to greyish colours which generates luminance levels between to grey steps in ascending order.

The result is that following this procedure we can generate $255 + 6 * 254$ possible luminance levels in a pseudo-grey scale, which is equivalent to a 10.8 bit-depth system. This increase in luminance resolution is more than enough to reach the contrast sensitivity threshold. All this procedure was coded in a Matlab© function to generate pseudo-grey images from luminance images.

From all the possible methods for increasing the luminance resolution, this is the best option for a low-cost setup.

Annex II

Web Cam Eye-Tracker

The WCE (Web Cam Eye-Tracker) is a low-cost eye-tracker built using a simple USB web cam and an own coded algorithm for Matlab©. Replacing the infrared filter on top of the sensor by a visible filter and adding an infrared illumination system the camera is able to capture infrared images.

The video based eye-trackers generally use infrared images for two reasons, the first one is that under infrared illumination the contrast between the pupil and the iris is independent of the iris colour and the second one is that the iris illumination cannot be perceived by the subject so it will not affect the pupil size.

A2.1. Pupil detection procedure

Once the image is acquired the histogram is adjusted to saturate the 1% of the data at lowest and highest intensities increasing the contrast of the whole image. The next step in the algorithm applies a threshold in order to segment the darkest pixels. This binarized image shows the pixels corresponding to the pupil and to other dark structures such as the eyelashes. Two morphological operations, first an erosion followed by a dilation using a circular structured element to

remove those black pixels not relating to the pupil. Once the binarized image of the pupil is treated to remove the noisy pixels a circular Hough transform implemented in Matlab© searches for the best matching circle to the pupil providing its centre and radius.

The Hough Transform (HT) is a feature extraction technique patented by Hough in 1962 (Hough 1962). This algorithm was originally designed for detecting straight lines. Duda and Hart perfected it and wrote the actual algorithm and generalised it to detect other shapes as circles (Duda & Hart 1972). Finally, thanks to Ballard (Ballard 1991) the Hough transform acquired its actual popularity as a feature extraction algorithm. There are different approaches for implementing the Hough transform with some notorious differences in their performance as analysed by Yuen (Yuen 1990). This algorithm is popular in many industrial applications such as the automatized quality control (Shafait et al. 2004), geology (Cross 1988), character recognition (Saitoh 1993), etc. Recently, new implementations related to the detection of the eye (Khairrosfaizal 2009), the pupil (Soltany 2011) or even pathological signs in the retina (Abdelazeem 2002) have appeared.

The procedure for detecting the dark pupil in the infrared image is as follows. From the original image (figure 39.a) and its reduced histogram (figure 39.b) the first treatment is to optimize its contrast through a histogram equalization to increase the contrast (figure 39.c) through a spreading of the

histogram (figure 39.d) all over the range of values of the 8-bit colour depth. After this optimization of the image, the pupil is segmented by thresholding the image by a low value (dark almost black pixels) as it is showed in figure 39.e. Sometimes, pixels not pertaining to the pupil appear in the binarized image because they have the same digital level than the pupil pixels so are included when thresholding the image (figure 39.f). Two morphological operations, erosion (figure 39.g) and dilation (figure 39.h) (van den Boomgard 1992) remove those small pixels. Finally, the circle HT algorithm finds the best fit circle for the shape in figure 39.h returning the circle centre and radius.

A2.2. Projection of the coordinates

This method provides the locations for the pupil centre in the video coordinates. A mapping procedure projects the positions in the video space into the stimulus space. For this is necessary to determine four corresponding points between both coordinate spaces.

The calibration points are placed around the target. The subject is asked to look for some seconds to each calibration point in a specific order. After the calibration the task for the experiment is done. When this task is finished a second calibration sequence is done to compensate possible head translations during the main task.

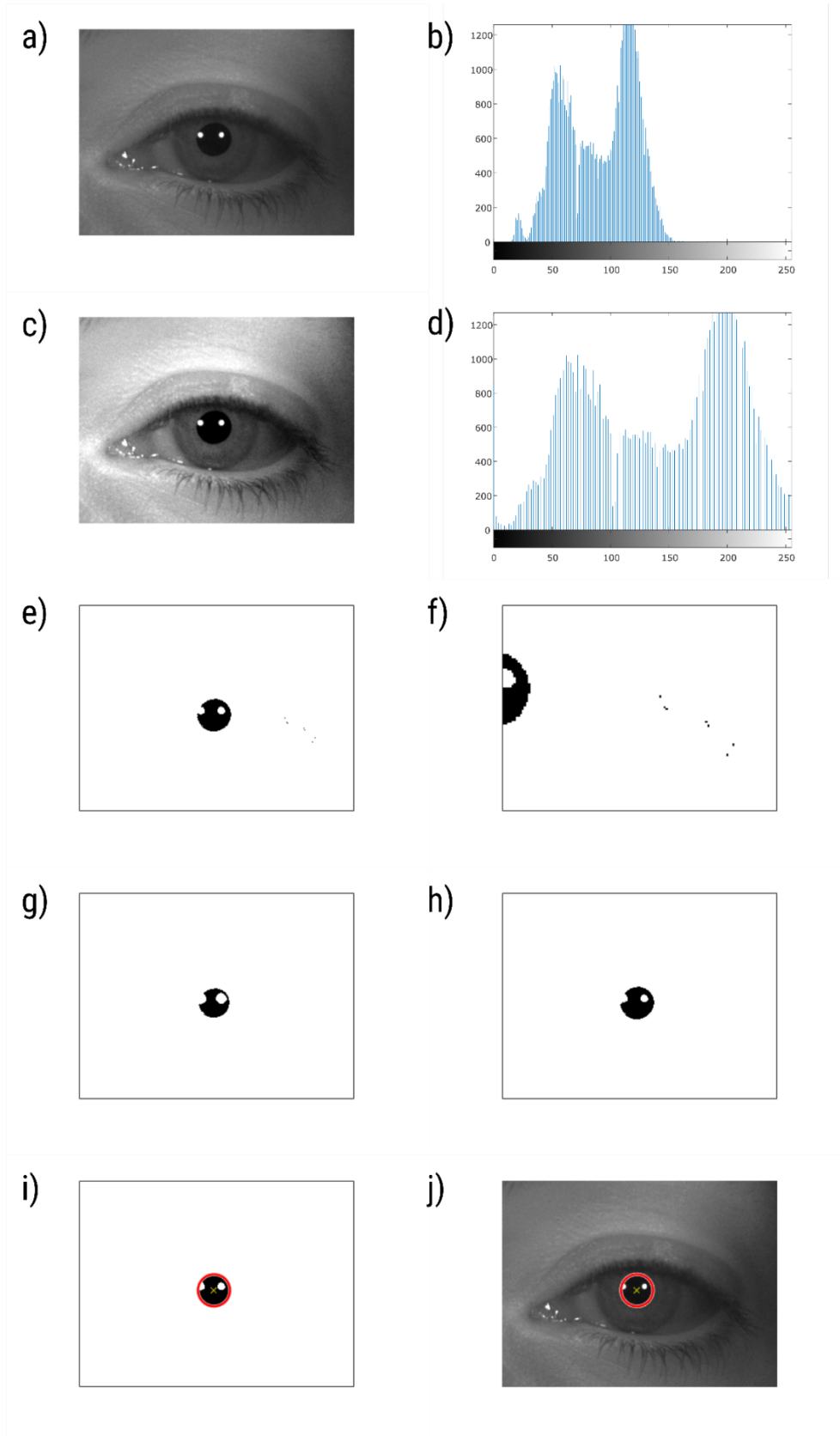


Figure 39 a) original image, b) original histogram, c) optimised image, d) optimised histogram, e) binarized image, f) noise included in the binarized image, g) eroded image, h) dilated image, i) best fit circle on top of the binarized image, j) best fit circle on top of the original image

Once the algorithm determines the pupil position for each frame, the researcher has to decide which coordinates correspond to the main task and which ones to both calibration sequences. After that, an own coded algorithm following the technique described by Volkov (Volkov 1999) maps all the points in the video space into the test space.

Due to different reasons: the noise in the sensor of the camera, illumination variations, Hough's transform sensitivity, fixational eye movements, breathing, heart beat and other body movements generate displacements of the detected pupil centre. This is why around each calibration point appears a cloud of positions for the gaze. The median of the cloud is chosen as the main gaze position corresponding to the calibration point.

A2.3. Possibilities of this device

This camera is able to record up to a HD ready resolution, 1280 per 720 pixels. The framerate depends on the spatial resolution, being lower, around 10 frames per second (fps) for the highest spatial resolution and 30 fps for the minimum resolution (320 per 240 pixels). An interesting property of the HT algorithm is that it works pretty good, providing accurate results with subpixel precision, even when parts of the desired shape are missing from the image (Du & Yang 2009). This makes the HT algorithm very appropriate for designing a low-cost pupil measurement portable device.

The different combinations for spatial and temporal resolution will be determined by the necessities of the researcher. It can be used to get low spatial resolution images at a normal framerate or to record high spatial resolution images at a lower framerate, for example, for using it as a binocular eye-tracker.

Our algorithm does not need exclusively a video recorded with the modified camera, it can also work with other video sources such as the High-Speed VET©.

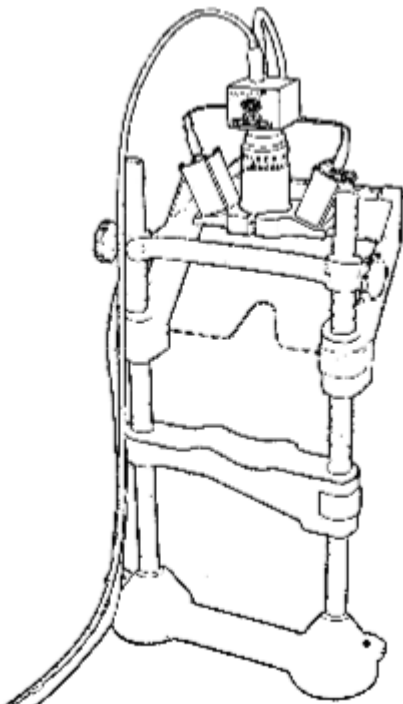
A2.4. Drawbacks

The main drawback is that the algorithm needs some human assistance to check if the image of the eye is well cropped, the pupil is well segmented, which data correspond to the calibration sequence and what points in the test are the calibration points. These factors make impossible to obtain the pupil position in real time.

Annex III

High Speed VET©

The High-Speed VET© (Cambridge Research Systems Ltd., Rochester, United Kingdom) is an infrared video eye-tracker device. Consists of a chin rest which holds the camera, the infrared illumination system and an infrared mirror. Once the subject is positioned the infrared mirror, which is transparent for the visible spectrum, reflects the infrared image of the eye to the camera. A scheme of the device can be seen in figure 40. This makes the system equivalent to a camera placed in front of the eye, but with this configuration the eye cannot perceive the camera and the illumination system, allowing binocular natural viewing.



The infrared camera has a spatial resolution of 320 per 240 pixels and a temporal frequency up to 250 Hz. The system detects in real time the dark pupil and the two bright Purkinje images of the illumination system and calculates the best fitting ellipse to the pupil shape this way determining its centre and its radius. The data is saved in a Matlab© file which

Figure 40 Scheme of the VET.

stores the pupil position and its radius for each frame. The recorded images can be exported to a series of BMP files.

References

Abdelazeem, S. (2002). Micro-aneurysm detection using vessels removal and circular Hough transform. In *Radio Science Conference, 2002.(NRSC 2002). Proceedings of the Nineteenth National* (pp. 421-426). IEEE.

Adams, A. J., Wong, L. S., Wong, L., & Gould, B. (1988). Visual acuity changes with age: some new perspectives. *Optometry & Vision Science*, 65(5), 403-406.

Allard, R., & Faubert, J. (2008). The noisy-bit method for digital displays: Converting a 256 luminance resolution into a continuous resolution. *Behavior Research Methods*, 40(3), 735-743.

Alpern, M., Mason, G. L., & Jardinico, R. E. (1961). Vergence and accommodation: V. Pupil size changes associated with changes in accommodative vergence. *American journal of ophthalmology*, 52(5), 762-767.

Apkarian, P., Tijssen, R., Spekreijse, H., & Regan, D. (1987). Origin of notches in CSF: optical or neural?. *Investigative ophthalmology & visual science*, 28(3), 607-612.

Arden, G. B. (1978). The importance of measuring contrast sensitivity in cases of visual disturbance. *British Journal of Ophthalmology*, 62(4), 198-209.

Arden, G. B. (1988). Testing contrast sensitivity in clinical-practice. *Clinical Vision Sciences*, 2(3), 213.

Arend, L. E. (1976). Temporal determinants of the form of the spatial contrast threshold MTF. *Vision research*, 16(10), 1035-IN1.

Artigas, J. M., Capilla, P., Felipe, A., & Pujol, J. (1995). Óptica Fisiológica: Psicofísica de la Visión. *Interamericana McGraw-Hill*.

Atick, J. J., & Redlich, A. N. (1992). What does the retina know about natural scenes?. *Neural computation*, 4(2), 196-210.

Bailey, I. L., & Lovie, J. E. (1976). New Design Principles for Visual Acuity Letter Charts*. *Optometry & Vision Science*, 53(11), 740-745.

Bailey, I. L., & Lovie, J. E. (1980). The design and use of a new near-vision chart. *Optometry & Vision Science*, 57(6), 378-387.

Ballard, D. H. (1991). Generalizing the Hough transform to detect arbitrary shapes. *Pattern Recognition*, 13(2), 183-194.

Barlow, H. B., Macleod, D. I. A., & Van Meeteren, A. (1976). Adaptation to gratings: no compensatory advantages found. *Vision research*, 16(10), 1043-1045.

Barlow, H. B. (1981). The ferrier lecture, 1980: Critical limiting factors in the design of the eye and visual cortex. *Proceedings of the Royal Society of London B: Biological Sciences*, 212(1186), 1-34.

Barten, P. G. (1992, August). Physical model for the contrast sensitivity of the human eye. In *SPIE/IS&T 1992 Symposium on Electronic Imaging: Science and Technology* (pp. 57-72). International Society for Optics and Photonics.

Barten, P. G. (1999). *Contrast sensitivity of the human eye and its effects on image quality* (Vol. 72). SPIE press.

Beatty, J., & Lucero-Wagoner, B. (2000). The pupillary system. *Handbook of psychophysiology*, 2, 142-162.

Bennett, A. G. (1965). Ophthalmic test types. A review of previous work and discussions on some controversial questions. *The British journal of physiological optics*, 22(4), 238-271.

Berkley, M. A., Kitterle, F., & Watkins, D. W. (1975). Grating visibility as a function of orientation and retinal eccentricity. *Vision research*, 15(2), 239-244.

Berns, R. S. (1996). Methods for characterizing CRT displays. *Displays*, 16(4), 173-182.

Blackie, C. A., & Howland, H. C. (1999). An extension of an accommodation and convergence model of emmetropization to include the effects of illumination intensity. *Ophthalmic and Physiological Optics*, 19(2), 112-125.

Blackwell, H. R. (1946). Contrast thresholds of the human eye. *JOSA*, 36(11), 624-643.

Blakemore, C. T., & Campbell, F. W. (1969). On the existence of neurones in the human visual system selectively sensitive to the orientation and size of retinal images. *The Journal of physiology*, 203(1), 237-260.

Blanchard, J. (1918). The brightness sensibility of the retina. *Physical Review*, 11(2), 81.

Bodis-Wollner, I. (1972). Visual acuity and contrast sensitivity in patients with cerebral lesions. *Science*, 178(4062), 769-771.

Bossomaier, T. R. J., Snyder, A. W., & Hughes, A. (1985). Irregularity and aliasing: solution?. *Vision research*, 25(1), 145-147.

Bour, L. J. (1980). MTF of the defocused optical system of the human eye for incoherent monochromatic light. *JOSA*, 70(3), 321-328.

Campbell, F. W., Cooper, G. F., & Enroth-Cugell, C. (1969). The spatial selectivity of the visual cells of the cat. *The Journal of Physiology*, 203(1), 223.

Campbell, F. W., & Green, D. G. (1965). Optical and retinal factors affecting visual resolution. *The Journal of Physiology*, 181(3), 576.

Campbell, F. W., & Gubisch, R. W. (1966). Optical quality of the human eye. *The Journal of Physiology*, 186(3), 558-578.

Campbell, F. W., & Kulikowski, J. J. (1966). Orientational selectivity of the human visual system. *The Journal of physiology*, 187(2), 437-445.

Campbell, F. W., & Robson, J. G. (1968). Application of Fourier analysis to the visibility of gratings. *The Journal of physiology*, 197(3), 551.

Chang DH. (2011). Determining ocular fixation for centering IOLs with Purkinje images. *Cataract & Refr. Surg. Today*, 11(7):32-34.

Chichilnisky, E. J. (2001). A simple white noise analysis of neuronal light responses. *Network: Computation in Neural Systems*, 12(2), 199-213.

Collewijn, H., & Kowler, E. (2008). The significance of microsaccades for vision and oculomotor control. *Journal of Vision*, 8(14), 20-20.

Corwin, T. R., & Richman, J. E. (1986). Three clinical tests of the spatial contrast sensitivity function: a comparison. *Optometry & Vision Science*, 63(6), 413-418.

Craik, K. J. W. (1939). The effect of adaptation upon visual acuity. *British Journal of Psychology. General Section*, 29(3), 252-266.

Cronly-Dillon, J. (1991). *Vision and visual dysfunction* (Vol. 16). CRC Press.

Cross, A. M. (1988). Detection of circular geological features using the Hough transform. *International Journal of Remote Sensing*, 9(9), 1519-1528.

Curcio, C. A., & Allen, K. A. (1990). Topography of ganglion cells in human retina. *Journal of comparative Neurology*, 300(1), 5-25.

Curcio, C. A., Millican, C. L., Allen, K. A., & Kalina, R. E. (1993). Aging of the human photoreceptor mosaic: evidence for selective vulnerability of rods in central retina. *Investigative ophthalmology & visual science*, 34(12), 3278-3296.

Daugman, J. G. (1980). Two-dimensional spectral analysis of cortical receptive field profiles. *Vision research*, 20(10), 847-856.

Daly, S. (2002). *U.S. Patent No. 6,441,867*. Washington, DC: U.S. Patent and Trademark Office.

De Groot, S. G., & Gebhard, J. W. (1952). Pupil size as determined by adapting luminance. *JOSA*, 42(7), 492-495.

de Lange Dzn, H. (1958). Research into the dynamic nature of the human fovea → cortex systems with intermittent and modulated light. I. Attenuation characteristics with white and colored light. *Josa*, 48(11), 777-784.

de Lange Dzn, H. (1958). Research into the dynamic nature of the human fovea-cortex systems with intermittent and modulated light. II. Phase shift in brightness and delay in color perception. *Josa*, 48(11).

De Luca, M., Spinelli, D., Zoccolotti, P., & Zeri, F. (2009). Measuring fixation disparity with infrared eye-trackers. *Journal of biomedical optics*, 14(1), 014013-014013.

De Valois, R. L., Albrecht, D. G., & Thorell, L. G. (1982). Spatial frequency selectivity of cells in macaque visual cortex. *Vision research*, 22(5), 545-559.

Dick, H. B., Krummenauer, F., Schwenn, O., Krist, R., & Pfeiffer, N. (1999). Objective and subjective evaluation of photic phenomena after monofocal and multifocal intraocular lens implantation. *Ophthalmology*, 106(10), 1878-1886.

Ditchburn, R. W., & Ginsborg, B. L. (1953). Involuntary eye movements during fixation. *The Journal of physiology*, 119(1), 1.

Dixon, W. J. (1988). Staircase Method (Up-And-Down). *Encyclopedia of Statistical Sciences*.

Drasdo, N. (1989). Receptive field densities of the ganglion cells of the human retina. *Vision Research*, 29(8), 985-988.

Du, W., & Yang, J. (2009). A robust Hough transform algorithm for determining the radiation centers of circular and rectangular fields with subpixel accuracy. *Physics in medicine and biology*, 54(3), 555.

Duda, R. O., & Hart, P. E. (1972). Use of the Hough transformation to detect lines and curves in pictures. *Communications of the ACM*, 15(1), 11-15.

Elliott, D. B., & Sheridan, M. (1988). The use of accurate visual acuity measurements in clinical anti-cataract formulation trials. *Ophthalmic and Physiological Optics*, 8(4), 397-401.

Ettinger, E. R., Wyatt, H. J., & London, R. (1991). Anisocoria. Variation and clinical observation with different conditions of illumination and accommodation. *Investigative ophthalmology & visual science*, 32(3), 501-509.

Fahle, M., & Edelman, S. (1993). Long-term learning in vernier acuity: Effects of stimulus orientation, range and of feedback. *Vision research*, 33(3), 397-412.

Faubert, J. (1990). Effect of target size, temporal frequency and luminance on temporal modulation visual fields. *Perimetry update*, 91, 381-390.

Ferris, F. L., Kassoff, A., Bresnick, G. H., & Bailey, I. (1982). New visual acuity charts for clinical research. *American journal of ophthalmology*, 94(1), 91-96.

Fleishman, J. A., Beck, R. W., Linares, O. A., & Klein, J. W. (1987). Deficits in visual function after resolution of optic neuritis. *Ophthalmology*, 94(8), 1029-1035.

Fogt, N., & Jones, R. (1998). Comparison of fixation disparities obtained by objective and subjective methods. *Vision research*, 38(3), 411-421.

Friendly, D. S., & Weiss, I. P. (1985). An automated visual acuity testing computer program using the Apple II system. *American journal of ophthalmology*, 99(2), 188-192.

Furlan, W. D., Corral, M. M., Martí, A. P., & Tortosa, G. S. (2011). *Instrumentos ópticos y optométricos: Teoría y prácticas*. Universitat de València.

Gibson, J. E., & Fairchild, M. D. (2000). Colorimetric characterization of three computer displays (LCD and CRT). *Munsell color science laboratory technical report*, 1-40.

Gilbert, D. S., & Fender, D. H. (1969). Contrast thresholds measured with stabilized and non-stabilized sine-wave gratings. *Optica acta*, 16, 191-204.

Ginsburg, A. P. (1984). A new contrast sensitivity vision test chart. *Optometry & Vision Science*, 61(6), 403-407.

Ginsburg, A. P., & Cannon, M. W. (1983). Comparison of three methods for rapid determination of threshold contrast sensitivity. *Investigative ophthalmology & visual science*, 24(6), 798-802.

González, E. G., Wong, A. M., Niechwiej-Szwedo, E., Tarita-Nistor, L., & Steinbach, M. J. (2012). Eye Position Stability in Amblyopia and in Normal Binocular Vision. *Investigative ophthalmology & visual science*, 53(9), 5386-5394.

Goodchild, A. K., Ghosh, K. K., & Martin, P. R. (1996). Comparison of photoreceptor spatial density and ganglion cell morphology in the retina of human, macaque monkey, cat, and the marmoset *Callithrix jacchus*. *Journal of Comparative Neurology*, 366(1), 55-75.

Graham, C. H., & Cook, C. (1937). Visual acuity as a function of intensity and exposure-time. *The American Journal of Psychology*, 49(4), 654-661.

Graham, N., & Nachmias, J. (1971). Detection of grating patterns containing two spatial frequencies: A comparison of single-channel and multiple-channels models. *Vision research*, 11(3), 251-IN4.

Green, D. G. (1970). Regional variations in the visual acuity for interference fringes on the retina. *The Journal of physiology*, 207(2), 351-356.

Green, D. M., & Swets, J. A. (1966). Signal detection theory and psychophysics. Wiley.

Guth, S. K., & Mcnelis, J. F. (1969). Threshold contrast as a function of target complexity. *Optometry & Vision Science*, 46(7), 491-498.

Hebbard, F. W. (1962). Comparison of Subjective and Objective Measurements of Fixation Disparity*. *JOSA*, 52(6), 706-712.

Heul, A. (1977). Time changes of contrast thresholds during automatic perimetry. *Acta ophthalmologica*, 55(4), 696-708.

Hess, R., & Woo, G. (1978). Vision through cataracts. *Investigative ophthalmology & visual science*, 17(5), 428-435.

Higgins, K. E., Jaffe, M. J., & Caruso, R. C. (1988). Spatial contrast sensitivity: Effects of age, test-retest, and psychophysical method. *JOSA A*, 5(12), 2173-2180.

Hofer, H., Carroll, J., Neitz, J., Neitz, M., & Williams, D. R. (2005). Organization of the human trichromatic cone mosaic. *Journal of Neuroscience*, 25(42), 9669-9679.

Hough, P. V. (1962). *Method and means for recognizing complex patterns* (No. US 3069654).

Howarth, P. A., Heron, G., Greenhouse, D. S., Bailey, I. L., & Berman, S. M. (1993). Discomfort from glare: the role of pupillary hippus. *International Journal of Lighting Research and Technology*, 25(1), 37-42.

Hubel, D. H., & Wiesel, T. N. (1959). Receptive fields of single neurones in the cat's striate cortex. *The Journal of physiology*, 148(3), 574-591.

Hubel, D. H., & Wiesel, T. N. (1962). Receptive fields, binocular interaction and functional architecture in the cat's visual cortex. *The Journal of physiology*, 160(1), 106-154.

Hubel, D. H., & Wiesel, T. N. (1972). Laminar and columnar distribution of geniculo-cortical fibers in the macaque monkey. *Journal of Comparative Neurology*, 146(4), 421-450.

Ikeda, M., & Saida, S. (1978). Span of recognition in reading. *Vision Research*, 18(1), 83-88.

Jacobs, R. J. (1979). Visual resolution and contour interaction in the fovea and periphery. *Vision research*, 19(11), 1187-1195.

Jaschinski, W., Jainta, S., & Kloke, W. B. (2010). Objective vs subjective measures of fixation disparity for short and long fixation periods. *Ophthalmic and Physiological Optics*, 30(4), 379-390.

Johnson, C. A. (1976). Effects of luminance and stimulus distance on accommodation and visual resolution. *JOSA*, 66(2), 138-142.

Johnson, C. A., Keltner, J. L., & Balestrery, F. (1978). Effects of target size and eccentricity on visual detection and resolution. *Vision Research*, 18(9), 1217-1222.

Johnston, A. (1987). Spatial scaling of central and peripheral contrast-sensitivity functions. *JOSA A*, 4(8), 1583-1593.

Khairrosfaizal, W. W. M., & Nor'aini, A. J. (2009, March). Eyes detection in facial images using circular hough transform. In *Signal Processing & Its Applications, 2009. CSPA 2009. 5th International Colloquium on* (pp. 238-242). IEEE.

Kawamorita, T., & Uozato, H. (2014). Natural pupil size and ocular aberration under binocular and monocular conditions. *Journal of Computer Science & Systems Biology*, 7(1), 15.

Kelly, D. H. (1984). Retinal inhomogeneity. I. Spatiotemporal contrast sensitivity. *JOSA A*, 1(1), 107-113.

Kertesz, A. E., & Lee, H. J. (1987). Comparison of simultaneously obtained objective and subjective measurements of fixation disparity. *Optometry & Vision Science*, 64(10), 734-738.

Kingdom, F. A., & Whittle, P. (1996). Contrast discrimination at high contrasts reveals the influence of local light adaptation on contrast processing. *Vision research*, 36(6), 817-829.

Kirkby, J. A., Blythe, H. I., Drieghe, D., Benson, V., & Liversedge, S. P. (2013). Investigating eye movement acquisition and analysis technologies as a causal factor in differential prevalence of crossed and uncrossed fixation disparity during reading and dot scanning. *Behavior research methods*, 45(3), 664-678.

Kline, D. W., Schieber, F., Abusamra, L. C., & Coyne, A. C. (1983). Age, the eye, and the visual channels: contrast sensitivity and response speed. *Journal of Gerontology*, 38(2), 211-216.

Kruk, R., Regan, D., Beverley, K. I., & Longridge, T. (1981). Correlations between visual test results and flying performance on the advanced simulator for pilot training (ASPT). *Aviation, space, and environmental medicine*.

Kruk, R., & Regan, D. (1983). Visual test results compared with flying performance in telemetry-tracked aircraft. *Aviation, space, and environmental medicine*, 54(10), 906-911.

Kulikowski, J. J. (1976). Effective contrast constancy and linearity of contrast sensation. *Vision research*, 16(12), 1419-1431.

Kulikowski, J. J., & Gorea, A. (1978). Complete adaptation to patterned stimuli: A necessary and sufficient condition for Weber's law for contrast. *Vision Research*, 18(9), 1223-1227.

Kulikowski, J. J., Marčelja, S., & Bishop, P. O. (1982). Theory of spatial position and spatial frequency relations in the receptive fields of simple cells in the visual cortex. *Biological cybernetics*, 43(3), 187-198.

Kulikowski, J. J., & Tolhurst, D. J. (1973). Psychophysical evidence for sustained and transient detectors in human vision. *The Journal of Physiology*, 232(1), 149.

Kurz, S., Krummenauer, F., Pfeiffer, N., & Dick, H. B. (2004). Monocular versus binocular pupillometry. *Journal of Cataract & Refractive Surgery*, 30(12), 2551-2556.

Kwak, Y., & MacDonald, L. (2000). Characterisation of a desktop LCD projector. *Displays*, 21(5), 179-194.

La Fleur, C. G., & Salthouse, T. A. (2014). Out of sight, out of mind? Relations between visual acuity and cognition. *Psychonomic bulletin & review*, 21(5), 1202-1208.

Lam, B. L., Thompson, H. S., & Corbett, J. J. (1987). The prevalence of simple anisocoria. *American journal of ophthalmology*, 104(1), 69-73.

Leek, M. R. (2001). Adaptive procedures in psychophysical research. *Attention, Perception, & Psychophysics*, 63(8), 1279-1292.

Legge, G. E. (1981). A power law for contrast discrimination. *Vision research*, 21(4), 457-467.

Legge, G. E. (1984). Binocular contrast summation—I. Detection and discrimination. *Vision research*, 24(4), 373-383.

Legge, G. E. (1984). Binocular contrast summation—II. Quadratic summation. *Vision research*, 24(4), 385-394.

Legge, G. E., & Campbell, F. W. (1981). Displacement detection in human vision. *Vision Research*, 21(2), 205-213.

Legge, G. E., & Foley, J. M. (1980). Contrast masking in human vision. *JOSA*, 70(12), 1458-1471.

Legge, G. E., Ross, J. A., Luebker, A., & Lamay, J. M. (1989). Psychophysics of reading. VIII. The Minnesota Low-Vision Reading Test. *Optometry & Vision Science*, 66(12), 843-853.

Legge, G. E., Rubin, G. S., & Luebker, A. (1987). Psychophysics of reading—V. The role of contrast in normal vision. *Vision research*, 27(7), 1165-1177.

Leibowitz, H. (1952). The effect of pupil size on visual acuity for photometrically equated test fields at various levels of luminance. *JOSA*, 42(6), 416-422.

Long, G. M., & Penn, D. L. (1987). Normative contrast sensitivity functions: the problem of comparison. *Optometry & Vision Science*, 64(2), 131-135.

Long, G. M., & Tuck, P. J. (1988). Reliabilities of alternate measures of contrast sensitivity functions. *Optometry & Vision Science*, 65(1), 37-48.

Loshin, D. S., & White, J. (1984). Contrast sensitivity: The visual rehabilitation of the patient with macular degeneration. *Archives of Ophthalmology*, 102(9), 1303-1306.

Lundström, M., Stenevi, U., & Thorburn, W. (1999). Outcome of cataract surgery considering the preoperative situation: a study of possible predictors of the functional outcome. *British journal of ophthalmology*, 83(11), 1272-1276.

Leek, M. R. (2001). Adaptive procedures in psychophysical research. *Attention, Perception, & Psychophysics*, 63(8), 1279-1292.

Li, X., Lu, Z. L., Xu, P., Jin, J., & Zhou, Y. (2003). Generating high gray-level resolution monochrome displays with conventional computer graphics cards and color monitors. *Journal of neuroscience methods*, 130(1), 9-18.

Maffei, L., & Fiorentini, A. (1973). The visual cortex as a spatial frequency analyser. *Vision research*, 13(7), 1255-1267.

Mansfield, R. J. W. (1974). Neural basis of orientation perception in primate vision. *Science*, 186(4169), 1133-1135.

Martinez-Conde, S., Macknik, S. L., & Hubel, D. H. (2004). The role of fixational eye movements in visual perception. *Nature Reviews Neuroscience*, 5(3), 229-240.

Marçelja, S. (1980). Mathematical description of the responses of simple cortical cells. *JOSA*, 70(11), 1297-1300.

Massof, R. W., & Rubin, G. S. (2001). Visual function assessment questionnaires. *Survey of ophthalmology*, 45(6), 531-548.

McCann, J. J., Savoy, R. L., & Hall, J. A. (1978). Visibility of low-frequency sine-wave targets: dependence on number of cycles and surround parameters. *Vision Research*, 18(7), 891-894.

McCarty, C. A., Keeffe, J. E., & Taylor, H. R. (1999). The need for cataract surgery: projections based on lens opacity, visual acuity, and personal concern. *British Journal of Ophthalmology*, 83(1), 62-65.

Meese, T. S., Georgeson, M. A., & Baker, D. H. (2006). Binocular contrast vision at and above threshold. *Journal of vision*, 6(11), 7-7.

Michelson, A. A. (1995). *Studies in optics*. Courier Corporation.

Miller, R. J. (1978). Temporal stability of the dark focus of accommodation. *Optometry & Vision Science*, 55(7), 447-450.

Mitchell, D. E. (1966). A review of the concept of "Panum's fusional areas". *Optometry & Vision Science*, 43(6), 387-401.

Montés-Micó, R. (2011). *Optometría: principios básicos y aplicación clínica*. Elsevier España.

Moon, P., & Spencer, D. E. (1944). On the stiles-crawford effect. *JOSA*, 34(6), 319-329.

Morrison, J. D., & McGrath, C. (1985). Assessment of the optical contributions to the age-related deterioration in vision. *Quarterly journal of experimental physiology*, 70(2), 249-269.

Nachmias, J. (1981). On the psychometric function for contrast detection. *Vision research*, 21(2), 215-223.

Nachmias, J., & Weber, A. (1975). Discrimination of simple and complex gratings. *Vision research*, 15(2), 217-223.

National Research Council. (1985). *Emergent techniques for assessment of visual performance*. National Academies.

Niven, J. I., & Brown, R. H. (1944). Visual resolution as a function of intensity and exposure time in the human fovea. *JOSA*, 34(12), 738-743.

Noorlander, C., Heuts, M. J., & Koenderink, J. J. (1980). Influence of the target size on the detection threshold for luminance and chromaticity contrast. *JOSA*, 70(9), 1116-1121.

Nyquist, H. (1928). Certain topics in telegraph transmission theory. *Transactions of the American Institute of Electrical Engineers*, 47(2), 617-644.

Ogle, K. N., Martens, T. G., & Dyer, J. A. (1968). Oculomotor imbalance in binocular vision and fixation disparity. *American Journal of Optometry and Archives of American Academy of Optometry*, 45(11), 783.

Olshausen, B. A., & Field, D. J. (1996). Natural image statistics and efficient coding. *Network: computation in neural systems*, 7(2), 333-339.

Olzak, L. A., & Thomas, J. P. (1981). Gratings: why frequency discrimination is sometimes better than detection. *JOSA*, 71(1), 64-70.

Olzak, L., & Thomas, J. (1986). Seeing spatial patterns. *Handbook of perception and human performance.*, 1, 7-1.

Osaka, N. (1987). Effect of peripheral visual field size upon eye movements during Japanese text processing. In *Eye Movements From Physiology to Cognition: Selected/Edited Proceedings of the Third European Conference on Eye Movements, Dourdan, France, September 1985* (pp. 421-429).

Osterberg, G. (1935). Topography of the layer of rods and cones in the human retina. *Acta Ophthalmologica Supplementum*, 6, 1-102.

Otero-Millan, J., Macknik, S. L., & Martinez-Conde, S. (2014). Fixational eye movements and binocular vision. *Frontiers in integrative neuroscience*, 8.

Owsley, C., Gardner, T., Sekuler, R., & Lieberman, H. (1985). Role of the crystalline lens in the spatial vision loss of the elderly. *Investigative ophthalmology & visual science*, 26(8), 1165-1170.

Owsley, C., Sekuler, R., & Siemsen, D. (1983). Contrast sensitivity throughout adulthood. *Vision research*, 23(7), 689-699.

Pantle, A. (1974). *Visual Information Processing of Complex Imagery*. Wright State Univ Dayton Ohio Dept Of Psychology.

Peli, E. (1990). Contrast in complex images. *JOSA A*, 7(10), 2032-2040.

Pelli, D. G. (1979, January). Effects of noise masking and contrast adaptation on contrast detection, contrast discrimination, and apparent contrast. In *Investigative Ophthalmology & Visual Science* (Pp. 59-60). 227 East Washington Sq, Philadelphia, Pa 19106: Lippincott-Raven Publ.

Pelli, D. G., & Bex, P. (2013). Measuring contrast sensitivity. *Vision research*, 90, 10-14.

Pelli, D. G., & Robson, J. G. (1988). The design of a new letter chart for measuring contrast sensitivity. In *Clinical Vision Sciences*.

Plainis, S., Atchison, D. A., & Charman, W. N. (2013). Power profiles of multifocal contact lenses and their interpretation. *Optometry & Vision Science*, 90(10), 1066-1077.

Pointer, J. S., & Hess, R. F. (1989). The contrast sensitivity gradient across the human visual field: With emphasis on the low spatial frequency range. *Vision research*, 29(9), 1133-1151.

Polyak, S. L. (1941). The retina.

Pollen, D. A., & Ronner, S. F. (1981). Phase relationships between adjacent simple cells in the visual cortex. *Science*, 212(4501), 1409-1411.

Pons, A. (1997). *Estudio de las funciones de respuesta al contraste del sistema visual* (Doctoral dissertation, Ph. D. dissertation, Dept. d'Òptica, Fac. Física, Univ. València, València, Spain).

Pons, A. M., Lorente, A., Illueca, C., Artigas, J. M., & Felipe, A. (2000). Influence of the gaze-stabilizing eye movements on the quality of the retinal image of the human eye. *Journal of Modern Optics*, 47(8), 1339-1345.

Ramrattan, R. S., Wolfs, R. C., Panda-Jonas, S., Jonas, J. B., Bakker, D., Pols, H. A., ... & de Jong, P. T. (2001). Prevalence and causes of visual field loss in the elderly and associations with impairment in daily functioning: the Rotterdam Study. *Archives of Ophthalmology*, 119(12), 1788-1794.

Rayner, K., & Bertera, J. H. (1979). Reading without a fovea. *Science*, 206(4417), 468-469.

Rayner, K. (1998). Eye movements in reading and information processing: 20 years of research. *Psychological bulletin*, 124(3), 372.

Reeves, P. (1918). Rate of pupillary dilation and contraction. *Psychological Review*, 25(4), 330.

Remole, A. (1985). Fixation disparity vs. binocular fixation misalignment. *Optometry & Vision Science*, 62(1), 25-34.

Robson, J. G. (1966). Spatial and temporal contrast sensitivity functions of the visual system. *Journal of the Optical Society of America*, 56(8), 1141-1142.

Robson, J. G., & Graham, N. (1981). Probability summation and regional variation in contrast sensitivity across the visual field. *Vision research*, 21(3), 409-418.

Rosen, E. S., Gore, C. L., Taylor, D., Chitkara, D., Howes, F., & Kowalewski, E. (2002). Use of a digital infrared pupillometer to assess patient suitability for refractive surgery. *Journal of Cataract & Refractive Surgery*, 28(8), 1433-1438.

Ross, J. E., Bron, A. J., & Clarke, D. D. (1984). Contrast sensitivity and visual disability in chronic simple glaucoma. *British journal of ophthalmology*, 68(11), 821-827.

Rózanowski, K., Bernat, M., & Kamińska, A. (2015). Estimation of operators' fatigue using optical methods for determination of pupil activity. *International journal of occupational medicine and environmental health*, 28(2), 263-281.

Rubin, G. S. (1988). Reliability and sensitivity of clinical contrast sensitivity tests. *Clin Vision Sci*, 2(3), 169-177.

Saitoh, F. (1993). *U.S. Patent No. 5,220,621*. Washington, DC: U.S. Patent and Trademark Office.

Shannon, C. E. (1949). Communication in the presence of noise. *Proceedings of the IRE*, 37(1), 10-21.

Schade, O. H. (1956). Optical and photoelectric analog of the eye. *JoSA*, 46(9), 721-739.

Schein, O. D., Steinberg, E. P., Cassard, S. D., Tielsch, J. M., Javitt, J. C., & Sommer, A. (1995). Predictors of outcome in patients who underwent cataract surgery. *Ophthalmology*, 102(5), 817-823.

Schroth, V., Joos, R., & Jaschinski, W. (2015). Effects of Prism Eyeglasses on Objective and Subjective Fixation Disparity. *PloS one*, 10(10), e0138871.

Schumer, D. J., Bains, H. S., & Brown, K. L. (2000). Dark-adapted pupil sizes in a prospective evaluation of laser in situ keratomileusis patients. *Journal of Refractive Surgery*, 16(2), S239-S241.

Shafait, F., Imran, S. M., & Klette-Matzat, S. (2004, July). Fault detection and localization in empty water bottles through machine vision. In *E-tech 2004* (pp. 30-34). IEEE.

Sharma, G. (2002). LCDs versus CRTs-color-calibration and gamut considerations. *Proceedings of the IEEE*, 90(4), 605-622.

Sheedy, J. E., Bailey, I. L., & Raasch, T. W. (1984). Visual acuity and chart luminance. *Optometry & Vision Science*, 61(9), 595-600.

Sheikh, H. R., Sabir, M. F., & Bovik, A. C. (2006). A statistical evaluation of recent full reference image quality assessment algorithms. *IEEE Transactions on image processing*, 15(11), 3440-3451.

Simoncelli, E. P., & Olshausen, B. A. (2001). Natural image statistics and neural representation. *Annual review of neuroscience*, 24(1), 1193-1216.

Sjöstrand, J. (1979). Contrast sensitivity in macular disease using a small-field and a large-field Tv-System. *Acta ophthalmologica*, 57(5), 832-846.

Sletteberg, O., Høvdig, G., & Bertelsen, T. (1995). Do we operate too many cataracts?. *Acta Ophthalmologica*, 73(1), 77-80.

Sloan, L. L. (1951). Measurement of visual acuity: a critical review. *AMA archives of ophthalmology*, 45(6), 704-725.

Sloan, L. L. (1959). New test charts for the measurement of visual acuity at far and near distances. *American journal of ophthalmology*, 48(6), 807-813.

Sloane, M. E., Owsley, C., & Alvarez, S. L. (1988). Aging, senile miosis and spatial contrast sensitivity at low luminance. *Vision research*, 28(11), 1235-1246.

Snellen, H. (1862). *Test-types for the determination of the acuteness of vision*. PW van de Weijer.

Soltany, M., Zadeh, S. T., & Pourreza, H. R. (2011). Fast and accurate pupil positioning algorithm using circular Hough transform and gray projection. In *International Conference on Computer Communication and Management* (pp. 556-561).

Spauschus, A., Marsden, J., Halliday, D. M., Rosenberg, J. R., & Brown, P. (1999). The origin of ocular microtremor in man. *Experimental Brain Research*, 126(4), 556-562.

Stark, L., Campbell, F. W., & Atwood, J. (1958). Pupil unrest: an example of noise in a biological servomechanism. *Nature*, 182(4639), 857-858.

Steinman, R. M. (1965). Effect of target size, luminance, and color on monocular fixation. *JOSA*, 55(9), 1158-1164.

Stone, J., & Fukuda, Y. (1974). Properties of cat retinal ganglion cells: a comparison of W-cells with X-and Y-cells. *Journal of Neurophysiology*, 37(4), 722-748.

Summers, R. J., & Meese, T. S. (2009). The influence of fixation points on contrast detection and discrimination of patches of grating: Masking and facilitation. *Vision Research*, 49(14), 1894-1900.

Swets, J. A., Tanner Jr, W. P., & Birdsall, T. G. (1961). Decision processes in perception. *Psychological review*, 68(5), 301.

Thibos, L. N., Still, D. L., & Bradley, A. (1996). Characterization of spatial aliasing and contrast sensitivity in peripheral vision. *Vision research*, 36(2), 249-258.

Thibos, L. N., Cheney, F. E., & Walsh, D. J. (1987). Retinal limits to the detection and resolution of gratings. *JOSA A*, 4(8), 1524-1529.

Thomas JP, Gille J, Barker RA. (1982). Simultaneous detection and identification: Theory and data. *J Opt Soc Am* 72:1642-1651.

Thomas, J. P., & Gille, J. (1979). Bandwidths of orientation channels in human vision. *JOSA*, 69(5), 652-660.

Thurstone, L. L. (1927). Psychophysical analysis. *The American journal of psychology*, 38(3), 368-389.

Torralba, A., & Oliva, A. (2003). Statistics of natural image categories. *Network: computation in neural systems*, 14(3), 391-412.

Triantaphillidou, S., Jarvis, J., & Gupta, G. (2013, January). Contrast sensitivity and discrimination of complex scenes. In *Proc. SPIE* (Vol. 8653).

Triantaphillidou, S., Jarvis, J., Gupta, G., & Rana, H. (2013, October). Defining human contrast sensitivity and discrimination from complex imagery. In *SPIE Security+ Defence* (pp. 89010C-89010C). International Society for Optics and Photonics.

Trick, G. L., Burde, R. M., Cordon, M. O., Santiago, J. V., & Kilo, C. (1988). The relationship between hue discrimination and contrast sensitivity deficits in patients with diabetes mellitus. *Ophthalmology*, 95(5), 693-698.

Tsotsos, J. K. (1988). A 'complexity level' analysis of immediate vision. *International Journal of Computer Vision*, 1(4), 303-320.

Tunnacliffe, A. H. (1993). 'Eye movements' in Introduction to visual optics. The Association of British Dispensing Opticians.

Turano, K. A., Rubin, G. S., & Quigley, H. A. (1999). Mobility performance in glaucoma. *Investigative Ophthalmology & Visual Science*, 40(12), 2803-2809.

Turano, K. A., Broman, A. T., Bandeen-roche, K., Munoz, B., Rubin, G. S., West, S. K., & See Project Team. (2004). Association of visual field loss and mobility performance in older adults: Salisbury Eye Evaluation Study. *Optometry & Vision Science*, 81(5), 298-307.

Tyler, C. W., Chan, H., Liu, L., McBride, B., & Kontsevich, L. L. (1992, August). Bit stealing: how to get 1786 or more gray levels from an 8-bit color monitor. In *SPIE/IS&T 1992 Symposium on Electronic Imaging: Science and Technology* (pp. 351-364). International Society for Optics and Photonics.

Tyler, C. W. (1997). Colour bit-stealing to enhance the luminance resolution of digital displays on a single pixel basis. *Spatial vision*, 10(4), 369-377.

Ukai, K., Tsuchiya, K., & Ishikawa, S. (1997). Induced pupillary hippus following near vision: increased occurrence in visual display unit workers. *Ergonomics*, 40(11), 1201-1211.

Ulichney, R. (1987). *Digital halftoning*. MIT press.

Ulichney, R. A. (1988). Dithering with blue noise. *Proceedings of the IEEE*, 76(1), 56-79.

Van Den Boomgaard, R., & Van Balen, R. (1992). Methods for fast morphological image transforms using bitmapped binary images. *CVGIP: Graphical Models and Image Processing*, 54(3), 252-258.

van Doorn, A. J., Koenderink, J. J., & Bouman, M. A. (1972). The influence of the retinal inhomogeneity on the perception of spatial patterns. *Biological Cybernetics*, 10(4), 223-230.

van Nes, F. L., & Bouman, M. A. (1967). Spatial modulation transfer in the human eye. *JOSA*, 57(3), 401-406.

van Nes, F. L. (1968). *Experimental studies in spatiotemporal contrast transfer by the human eye* (Doctoral dissertation, Bronder-Offset [Goudsesingel 260]).

Virsu, V., & Rovamo, J. (1979). Visual resolution, contrast sensitivity, and the cortical magnification factor. *Experimental Brain Research*, 37(3), 475-494.

Volkov, E. A., & Kornoukhov, A. K. (1999). An approximate conformal mapping of a trapezoid onto a rectangle and its inversion obtained by the block method. *Computational mathematics and mathematical physics*, 39(7), 1100-1108.

von Boehmer, H., & Kolling, G. H. (1998). Effect of exposure time using single Landolt-rings on visual acuity in normal individuals and in patients with nystagmus. *Der Ophthalmologe*, 95(10), 717-720.

Wachler, B. S. B. (2003). Effect of pupil size on visual function under monocular and binocular conditions in LASIK and non-LASIK patients. *Journal of Cataract & Refractive Surgery*, 29(2), 275-278.

Wang, Z., Bovik, A. C., & Lu, L. (2002, May). Why is image quality assessment so difficult?. In *Acoustics, Speech, and Signal Processing (ICASSP), 2002 IEEE International Conference on* (Vol. 4, pp. IV-3313). IEEE.

Wang, Z., Bovik, A. C., Sheikh, H. R., & Simoncelli, E. P. (2004). Image quality assessment: from error visibility to structural similarity. *IEEE transactions on image processing*, 13(4), 600-612.

Watson, A. B., & Robson, J. G. (1981). Discrimination at threshold: labelled detectors in human vision. *Vision research*, 21(7), 1115-1122.

Watson, A. B., & Yellott, J. I. (2012). A unified formula for light-adapted pupil size. *Journal of vision*, 12(10), 12-12.

Watson, A. B., Barlow, H. B., & Robson, J. G. (1983). What does the eye see best?. *Nature*, 302(5907), 419-422.

Watson, A. B., & Yellott, J. I. (2012). A unified formula for light-adapted pupil size. *Journal of vision*, 12(10), 12-12.

Werner, J. S., Peterzell, D. H., & Scheetz, A. J. (1990). Light, vision, and aging. *Optometry & Vision Science*, 67(3), 214-229.

Westheimer, G. (1960). Modulation thresholds for sinusoidal light distributions on the retina. *The Journal of physiology*, 152(1), 67.

Westheimer, G. (1975). Editorial: Visual acuity and hyperacuity. *Investigative Ophthalmology & Visual Science*, 14(8), 570-572.

Wichmann, F. A., & Hill, N. J. (2001). The psychometric function: I. Fitting, sampling, and goodness of fit. *Attention, Perception, & Psychophysics*, 63(8), 1293-1313.

Wick, B., & Schor, C. (1984). A comparison of crowding bar and linear optotype acuity in amblyopia. *Am J Optom Assoc*, 55, 359-361.

Wiesel, T. N. (1960). Receptive fields of ganglion cells in the cat's retina. *The Journal of Physiology*, 153(3), 583.

Wilhelm, B., Stüber, G., Lüdtke, H., & Wilhelm, H. (2014). The effect of caffeine on spontaneous pupillary oscillations. *Ophthalmic and Physiological Optics*, 34(1), 73-81.

Williams, D. R., & Collier, R. (1983). Consequences of spatial sampling by a human photoreceptor mosaic. *Science*, 221(4608), 385-387.

Williams, D. R., Hofer, H., Carroll, J., Neitz, M., & Neitz, J. (2003). Organization of the human trichromatic cone mosaic. *Investigative Ophthalmology & Visual Science*, 44(13), 1909-1909.

Wilson, H. R., McFarlane, D. K., & Phillips, G. C. (1983). Spatial frequency tuning of orientation selective units estimated by oblique masking. *Vision research*, 23(9), 873-882.

Yoss, R. E., Moyer, N. J., & Hollenhorst, R. W. (1970). Pupil size and spontaneous pupillary waves associated with alertness, drowsiness, and sleep. *Neurology*, 20(6), 545-545.

Yuen, H. K., Princen, J., Illingworth, J., & Kittler, J. (1990). Comparative study of Hough transform methods for circle finding. *Image and vision computing*, 8(1), 71-77.

